



**MISKOLCI**  
EGYETEM  
UNIVERSITY OF MISKOLC

# *Theoretical Study on Molecular Networks of Carbon Dioxide to Methanol Conversion*

**Ph.D. Dissertation**

***Rachid Hadjadj***

**Supervisor:  
Prof. Dr. Béla Viskolcz**

**Antal Kerpely Doctoral School of Materials Science & Technology**

**Institute of Chemistry  
University of Miskolc**

**Miskolc 2020**

*“But over all those endowed with knowledge is the All-Knowing”*

**The Noble Qur'an [Chapter 12-Yusuf, Verse 76]**

# Contents

Acknowledgments.....	5
List of figures.....	7
List of tables.....	9
Abbreviations.....	11
1 Introduction.....	13
1.1 Historical background.....	14
1.2 Trend of the energy sector.....	15
1.3 The energetic transition.....	16
1.3.1 Biofuels.....	16
1.3.2 Hydrogen based electricity.....	17
1.3.3 Nuclear-based electricity.....	18
1.3.4 Renewable energies.....	18
1.3.5 Energy storage problem.....	20
1.4 CO <sub>2</sub> management.....	21
1.4.1 CO <sub>2</sub> emission and climate change.....	21
1.4.2 CO <sub>2</sub> and economy.....	22
1.4.3 Carbon Capture and Storage (CCS).....	22
1.4.4 Carbon Capture and Usage (CCU) as potential energy storage methods.....	22
1.5 The methanol synthesis.....	24
1.5.1 Route of CO <sub>2</sub> reduction.....	24
1.5.2 Side reactions.....	25
1.5.3 Catalysts.....	26
1.5.4 Industrial processes for methanol production.....	27
1.6 Goal.....	28
2 Computational methods.....	29
2.1 Computational chemistry.....	30
2.2 Level of theory.....	30
2.2.1 Methods.....	30
2.2.2 Basis set.....	32

2.3	Composite methods .....	33
2.4	Solvent model.....	33
2.4.1	Implicit models .....	33
2.4.2	Explicit models .....	34
2.5	Potential energy surface and reaction mechanism .....	34
2.6	Gas phase calculations .....	36
2.6.1	Structure generation .....	36
2.6.2	Quantum chemical calculations .....	36
2.7	Aqueous phase calculations .....	37
2.7.1	Uncatalyzed mechanism .....	37
2.7.2	Catalyzed-like mechanism .....	38
2.8	Methods validation.....	38
2.8.1	Gas phase .....	38
2.8.2	Aqueous phase .....	40
2.8.3	Results comparability.....	41
3	Results and Discussion .....	42
3.1	Gas phase results .....	43
3.2	Aqueous phase results .....	51
3.3	Catalyzed-like aqueous phase mechanism for CO <sub>2</sub> conversion to methanol .....	60
3.4	Comparison between the uncatalyzed and the catalyzed-like water enhanced mechanism 73	
4	Summary.....	74
5	New scientific results.....	78
6	Scientific publications .....	81
7	References .....	85

# Acknowledgments

My doctorate would not have been possible without the help of many people whom I would like to thank here.

I deeply thank Prof. Dr. Viskolcz Béla, my thesis director, for his advices, for his indestructible confidence and optimism and for giving me the opportunity to work within his team on a topical subject.

I am very happy for having frequent meetings with a great Hungarian mind, a person that gave me the feeling of having a grandfather again! Prof. Imre G. Csizmadia, the most brilliant person I have talked to. Thank you for your help, your hospitality, and humour.

A big thank you to a person whom I consider as my older brother, Dr. Fiser Béla, not only for his daily scientific help, but for being the first person I think about knocking the door in all circumstances.

Thanks to Dr. Szóri Milan for everything he taught me during my thesis period.

Thanks to the administrative team, Vanczákné Jutka in particular, for all the help and for her smile.

Thanks to Edina Reizer for being such a good friend.

Merci à tous les membres de ma famille. Papa, merci pour ton soutien constant, j'ai toujours rêvé de porter le nom de Dr. Hadjadj après toi, voilà que ça se réalise enfin.

Mama, merci pour ton amour éternel et pour avoir enduré la douleur de mon éloignement.

Sid Ahmed et Amine, mes frères bien-aimés, de tout mon cœur, je vous souhaite un magnifique avenir ensemble.

Merci à mes trois meilleurs amis, Dr. Sid Ahmed Kessas, Dr. Mohamed El-Bachir Belaid et M. Yacine Sardi, d'avoir gardé cette amitié pendant près d'une décennie.

Merci aux amis que j'ai rencontré ici en Hongrie : Gacem Walid, Benchabane Mehdi, Mehdi Yacine et Dib Amine.

Je dédie ce travail à une personne très importante pour moi, une personne qui n'est plus en vie, le directeur de ma thèse de Master, le Prof. Rachid Kessas. Vous êtes probablement la personne que je voulais le plus me voir obtenir le titre de docteur. Je suis tellement fier d'être la dernière personne que vous avez encadré dans votre vie, vous êtes la personne qui m'a fait choisir la recherche scientifique, et j'espère que je suivrai votre chemin. Si seulement j'ai pu vous dire tout ça la dernière fois que nous nous sommes parlé...

Many thanks to the reviewers and jury members for agreeing to judge this work.

This research was supported by the European Union and the Hungarian State, co-financed by the European Regional Development Fund in the framework of the GINOP-2.3.4-15-2016-00004 project, aimed to promote the cooperation between the higher education and the industry.

# List of figures

<b>Figure 1:</b> Energy production types.....	14
<b>Figure 2</b> Global energy consumption trend.....	15
<b>Figure 3:</b> Biofuel production in different regions. ....	16
<b>Figure 4:</b> Hydrogen based electricity consumption. ....	17
<b>Figure 5:</b> Nuclear-based electricity consumption. ....	18
<b>Figure 6:</b> Renewable energy consumption.....	19
<b>Figure 7:</b> Characteristics of different energy storage types. ....	20
<b>Figure 8:</b> World CO <sub>2</sub> emission in the 2008-2018 time period. ....	21
<b>Figure 9:</b> CO <sub>2</sub> emission in Hungary between 2008-2018.....	22
<b>Figure 10:</b> CO <sub>2</sub> valorisation by chemical reactions. ....	23
<b>Figure 11:</b> Stepwise reaction of carbon dioxide hydrogenation to achieve methanol and methane. .....	24
<b>Figure 12:</b> Proposed reaction mechanism for the synthesis of methanol from CO <sub>2</sub> on Cu. ....	25
<b>Figure 13:</b> Schematic representation of a potential energy surface. ....	34
<b>Figure 14:</b> Reaction steps of CO <sub>2</sub> hydrogenation to methane. ....	40
<b>Figure 15:</b> Thermodynamic properties of the CH <sub>8</sub> O <sub>2</sub> stoichiometry which could be involved in CO <sub>2</sub> reduction. Relative Gibbs free energy ( $\Delta G_r^0$ ) and entropy ( $\Delta S_r^0$ ) computed using the WIBD method for the molecular composition obtained by combinatorial tools. The triplet states are signed by tr. The red line defines the highest energy level of the stable section (>300kJ/mol). The oxidation state of the most stable structures is shown in green. CO <sub>2</sub> + 4H <sub>2</sub> considered as a reference level and highlighted with a red dot.....	44
<b>Figure 16:</b> Methanol and methane formation network through CO <sub>2</sub> hydrogenation. Letters are assigned to every structure, and each transition state is named as TS followed respectively with the letter referring to the reactant and then the product ( <i>e.g.</i> TS <sub>AB</sub> ). The preferred pathway is highlighted with red lines.....	46
<b>Figure 17:</b> Gibbs free energy profile of the uncatalyzed hydrogenation of CO <sub>2</sub> to methanol and methane calculated at the WIBD level of theory plotted against the reaction coordinates with a highlighted energetically favoured route in red. ....	48

**Figure 18:** Reaction pathways of the envisaged water enhanced CO<sub>2</sub> – methanol conversion. Letters are assigned to every structure, and each transition state is named as TS followed respectively with the letter referring to the reactant and then the product (*e.g.* TS<sub>AB</sub>). The preferred pathway is highlighted by dashed lines. .... 51

**Figure 19:** Gibbs free energy change ( $\Delta G_r^0$ , kJ/mol) of the water enhanced conversion of CO<sub>2</sub> to methanol calculated at the W1U level of theory. The transition states are named as TS followed by the reactant and the product, where the hydrogenation steps are highlighted with the (H<sub>2</sub>) sign close to the barrier. **(B)**, **(K)**, **(E)** and **(L)** could have more than one conformer. \*Morse potential - barrierless elementary reaction step **JK**. \*\*Double Morse potential - barrierless elementary reaction step **HI**..... 53

**Figure 20:** Total energy change ( $\Delta E_{tot}$ ) of the two types of barrierless reactions (**JK**) (Morse potential, hydration) and (**HI**) (Double Morse potential, protonation)..... 55

**Figure 21:** Total energy change ( $\Delta E_{tot}$ ) of the (**DE**) reaction step (double Morse potential). ... 56

**Figure 22:** Cross-sectional diagram of an electrolytic CO<sub>2</sub> reduction flow cell<sup>110</sup>..... 60

**Figure 23:** CO<sub>2</sub> - formic acid conversion cell configuration showing reactions and ion transport<sup>112</sup>. .... 61

**Figure 24:** Step-by-step water enhanced CO<sub>2</sub> hydrogenation reaction considering hydrogen atoms as reaction partners. .... 62

**Figure 25:** Reaction pathways of the envisaged CO<sub>2</sub> – methanol conversion mechanism using atomic hydrogenations. Letters are assigned to every structure, and each transition state is named as TS followed with the letter referring to the reactant and then the product (*e.g.* TS<sub>AB</sub>), respectively. The +H<sup>•</sup> refers to a hydrogen atom addition..... 63

**Figure 26:** Gibbs free energy change ( $\Delta G_r^0$ , kJ/mol) of the water enhanced conversion of CO<sub>2</sub> to methanol calculated at the W1U level of theory. The transition states are named as TS followed by the reactant and the product, where the hydrogen addition steps are highlighted with the (+H) sign close to the barrier. **(B)**, **(K)**, **(E)** and **(L)** could have more than one conformer. .... 66

**Figure 27:** Total energy change ( $\Delta E_{tot}$ ) of the (**E\*F**) barrierless reaction step (Morse potential). .... 68

**Figure 1:** Gibbs free energy change of the preferred pathways of the gas phase and aqueous phase uncatalyzed mechanism, and catalyzed-like process. .... 76

# List of tables

<b>Table 1:</b> The performance of Cu-based catalysts in CO <sub>2</sub> -methanol conversion. ....	26
<b>Table 2</b> The performance of Au, Pd, NiIn and NiGa catalysts in CO <sub>2</sub> -methanol conversion .....	27
<b>Table 3:</b> Heat of formation ( $\Delta_f H^0$ ) of 10 optimized structures have been calculated using the Feller-Helgaker (F.H.) extrapolation and the W1BD method and compared to experimental values from the literature. All values are in kJ/mol. ....	39
<b>Table 4:</b> Enthalpy calculated results at W1U level of theory and experimental heat of formation values of the involved species in the CO <sub>2</sub> conversion. ....	<b>Error! Bookmark not defined.</b>
<b>Table 5:</b> Comparison of the computed enthalpy changes ( $\Delta H_r^0$ ) of each molecule produced through elementary reaction steps and their respective experimental gas phase enthalpy of formation ( $\Delta \Delta_f H_{exp}^0$ ) differences. The calculated and experimental values have also been compared and listed in the table (Calc-Exp). ....	40
<b>Table 6:</b> Comparison of the computed results of the two arbitrarily chosen molecules formaldehyde and methanol using the W1BD and W1U protocols .....	41
<b>Table 7:</b> Thermodynamic properties of the CH <sub>8</sub> O <sub>2</sub> species calculated at the W1BD level of theory. ....	45
<b>Table 8:</b> Thermodynamic properties ( $\Delta H_r^0$ , $\Delta G_r^0$ in kJ/mol and $S$ in J/mol*K) of the stable structures and the transition states involved in the reaction network calculated at the W1BD level of theory. The highlighted red values belong to the preferred pathway of the mechanism. ....	49
<b>Table 9:</b> Thermodynamic properties ( $\Delta H_r^0$ , $\Delta G_r^0$ in kJ/mol and $S$ in J/mol*K) of the studied carbon dioxide – methanol conversion reaction mechanism have been calculated at the W1U level of theory. The transition states of each elementary reaction steps are named as TS followed with the letter of the reactant and then the product ( <i>e.g.</i> <b>TS<sub>AB</sub></b> ). The barrierless reactions are noted by giving a letter of the reactant followed by the product ( <i>e.g.</i> <b>AJ</b> ). The structures corresponding to the preferred pathway are highlighted in red. ....	57
<b>Table 10:</b> The comparison of the preferred carbon dioxide-methanol conversion pathways in gas and aqueous phase. ....	59
<b>Table 11:</b> Thermodynamic properties ( $\Delta H_r^0$ , $\Delta G_r^0$ in kJ/mol and $S$ in J/mol*K) of the studied water enhanced carbon dioxide – methanol conversion reaction mechanism have been calculated at the W1U level of theory. The complexes formed during barrierless reactions and corresponds to	

double Morse potentials are noted as M followed by the letter of the reactant and then the product (e.g.  $M_{AJ}$ ). The species labelled with an (\*) and highlighted in red are involved in the atomic hydrogenations..... 70

**Table 12:** Comparison of the preferred carbon dioxide-methanol conversion pathways of the uncatalyzed and catalyzed-like aqueous phase mechanisms. .... 73

# Abbreviations

$\Delta G_r^\circ$ : Gibbs free energy of a reaction.

$\Delta H_r^\circ$ : Heat of a reaction.

$\Delta H_f^\circ$ : Heat of Formation of species.

$\Delta G^\circ$ : Relative Gibbs free energy.

$\Delta H^\circ$ : Relative enthalpy.

$\Delta S^\circ$ : Relative entropy.

$\Delta E_{\text{tot}}$ : Total energy change.

$\eta$ : Efficiency.

**B3LYP**: Becke, 3-parameter, Lee-Yang-Parr method.

**CC**: Coupled cluster methods.

**CCS**: Carbon Capture and Storage.

**CCU**: Carbon Capture and Usage.

**CI**: Configuration interaction method.

**CPCM**: Conduction-like Polarizable Continuum Model.

**DFT**: Density functional theory.

$G_{\text{ref}}$ : Gibbs free energy of the reference species.

$G_{\text{(X)}}$ : Gibbs free energy of structure X.

**GTO**: Gaussian-type orbitals

**HF**: Hartree-Fock method.

**MD**: Molecular Dynamics.

**MEA**: Monoethanolamine.

**MM**: molecular mechanics.

**MP**: Møller–Plesset perturbation.

**MPa**: Mega pascal.

**Mtoe**: Million tonnes oil equivalent.

**Mt**: Million tonnes.

**MW:** Megawatt.

**PES:** Potential energy surface.

**pKa:** Acid dissociation constant.

**PCM:** Polarizable Continuum Model.

**RMSD:** Root Mean Square deviation

**RWGS:** Reverse-Water Gas Shift.

**S:** Entropy.

**SCRf:** Self Consistent Reaction Field.

**SNG:** Substitute Natural Gas.

**TS:** Transition State.

**TWh:** Terawatt hour.

**QCISD:** Quadratic Configuration Interaction including Single and Double substitutions.

**Wn:** Weizmann-n method.

**W1BD:** Brueckner Doubles variation of the Weizmann 1 method (W1).

**W1U:** Unrestricted variation of the Weizmann 1 method.

**WHSV:** Weight hourly space velocity.

# 1 Introduction

*“Two things are infinite: the universe and human stupidity; and I'm not sure about the universe.”*

**Albert Einstein**

# 1.Introduction

## 1.1 Historical background

People who are interested in human history are usually classified into two groups, the ones who are interested in the history of past, are called *historians*, and the other group which is interested in the future are called *futurologists*. In this dissertation, we are concerned about the energy production, which was started about four centuries ago with the invention of the steam engine and that *historical background* influenced climate change. In contrast to that there is the *futuristic aspect* of energy production, which could be based on atomic nuclear fusion. Such device could be operational in the second half of the twenty first century, perhaps as early as 2050. By then, several European countries are trying to reach carbon neutrality (net zero carbon dioxide emissions)<sup>1</sup>. Between the *historic aspect* of the past and the *futuristic aspect* which will last about another 5 centuries there must have a *transition period*. In this case the most important challenge during the *transition* is the reduction of CO<sub>2</sub> to chemically useful compounds (**Figure 1**).

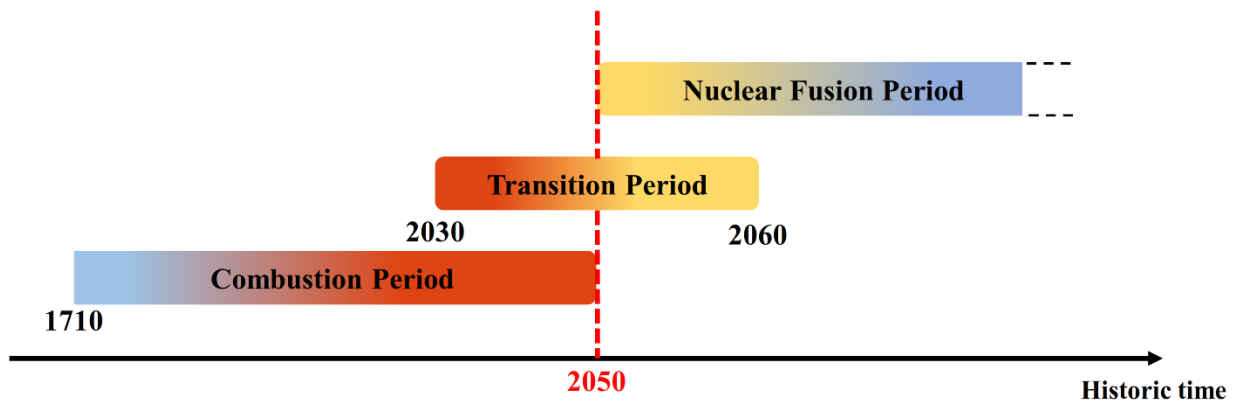


**Figure 1:** Energy production types.

During the past industrial phase of the global civilization, the energy production was mainly based on combustion (**Figure 1**, left). Sooner or later, this type of energy production will be replaced by nuclear fusion (**Figure 1**, right), but till that, we have to get through a transition period (**Figure 1**, middle) in the near future, within which the world has to focus on CO<sub>2</sub> management.

1. Introduction

1.2 Trend of the energy sector

According to the 68<sup>th</sup> edition of the statistical review of world energy consumption created by the British Petroleum company<sup>2</sup>, the growth of the world population is reflected in an increasing energy demand of all the economic branches. Consequently, the annual consumption of primary energy in the world is constantly increasing (**Figure 2**).

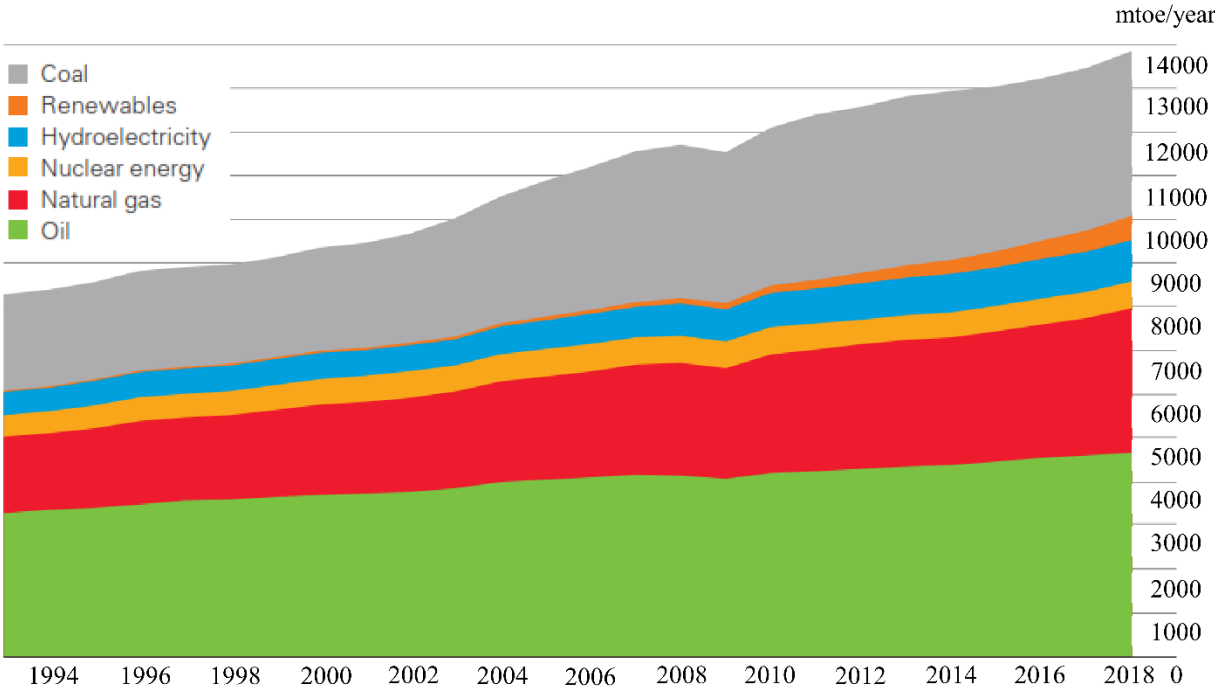


**Figure 2** Global energy consumption trend<sup>2</sup>.

The primary global energy consumption in the world do not stop increasing (**Figure 2**). The total energy consumed in the year 2018 is equal to **13864.9** million tonnes oil equivalent (**mtoe**), where North America and Europe are the most energy intensive continents (**2832.0 mtoe, 2050.7 mtoe**). The growth rate of the global energy consumption is **2.9%**. It is the double of the “10-year growth increasing average” of **1.5%** which makes it the fastest since 2010. Oil, natural gas, and coal are the most widely used fuels in the world (**Figure 2**). Natural gas is leading in the consumption growth by **40%** of the increase. Of course, the consumptions of each fuel grew, and renewables and hydroelectricity are not making exception<sup>2</sup>.

With limited fossil resources, asking the question of new sources of energy for the future is unavoidable. It is certain that the growth in energy demand will continue especially in emerging

1. Introduction

countries and eliminating carbon dioxide from the equation of the power sector is perhaps the most important challenge facing the global energy system over the next 30 years.

1.3 The energetic transition

Energy, the basic element that every nation need, is now a debated subject pushing the scientific world to look for sustainable forms<sup>3</sup>. The declining resources combined with the increasing demand as well as the environmental impact led to what is called “Energetic Transition”. It is nothing but the progressive replacement of fossil fuels (oil, natural gas, coal) by renewable energies (solar energy, wind energy, water energy, biomass).

1.3.1 Biofuels

As an alternative of fossil fuels, biofuels are produced from biomass through contemporary processes. They can be produced from plants, or from agricultural, commercial, domestic, and/or industrial wastes (if the waste has a biological origin)<sup>4</sup>.

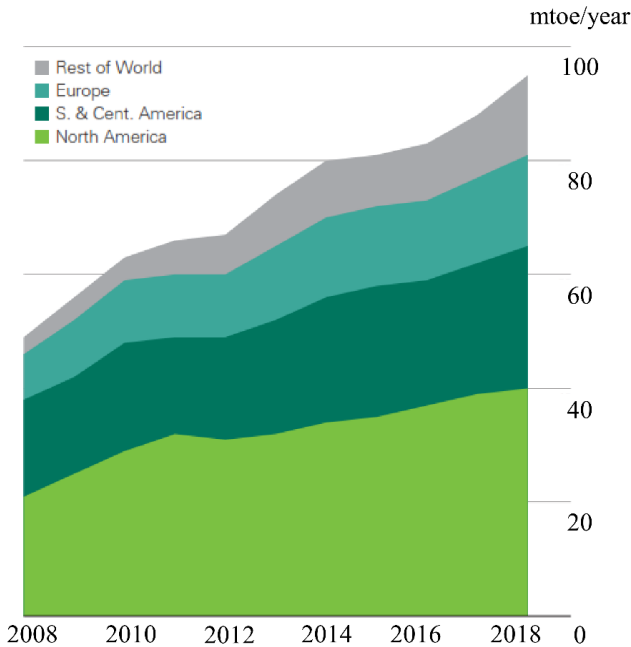


Figure 3: Biofuel production in different regions<sup>2</sup>.

From 2012, more and more biofuels are produced each year (Figure 3). The total world production reached 95371 mtoe in 2018. This amount is shared between North America (39.5 mtoe) which is the largest producer in the world, South and Central America (25.5 mtoe), and Europe (15.9 mtoe), and the rest of the world shares the rest of the production.

## 1. Introduction

The average growth of biofuel production reached **9.7%** in 2018, which is the highest growth since 2010 and slightly above the 10-year average<sup>2</sup>. Though biofuels have a number of advantages over fossil fuels, their integration into the fuel supply chain have some limitations. In fact, the production of biofuels requires growing crops, which means that an excessive use of water will be needed, and the use of fertilizers. In addition to that, crops cannot grow in every region of the globe. Also, the amounts produced in the world are almost neglectable compared to the total energy needed.

### 1.3.2 Hydrogen based electricity

Hydrogen fuel is considered as a zero CO<sub>2</sub> emission fuel while it reacts with oxygen. It is mainly used in fuel cells and internal combustion engines. It has been adapted to function in vehicles such as cars and buses for many years. It is also used as a fuel for spacecraft propulsion<sup>5</sup>.

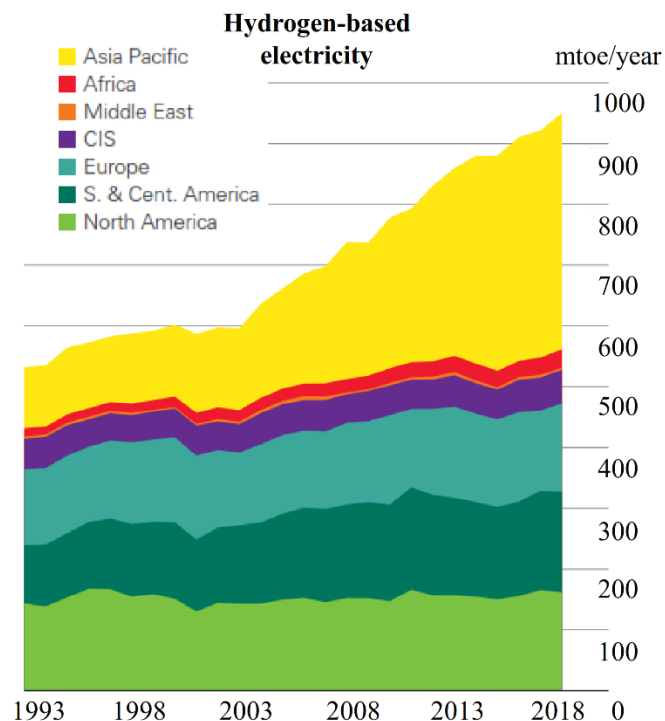


**Figure 4:** Hydrogen based electricity consumption<sup>2</sup>.

Electricity produced from hydrogen-based processes is also growing (**Figure 4**). The world has consumed **948.8 mtoe** in 2018 and the curve does not seem to stop increasing in the near future.

## 1. Introduction

### 1.3.3 Nuclear-based electricity

To generate nuclear power, nuclear reactions have to be used for the release of nuclear heat energy, which is used in steam turbines to produce electricity in a nuclear power plant. In addition to all the risks of disastrous nuclear explosions, the nuclear plants generate radioactive nuclear waste, which might have a detrimental effect on the human race for generations. Thus, scientists are turning into developing the nuclear fusion instead of the actual fission of uranium and plutonium<sup>6</sup>.

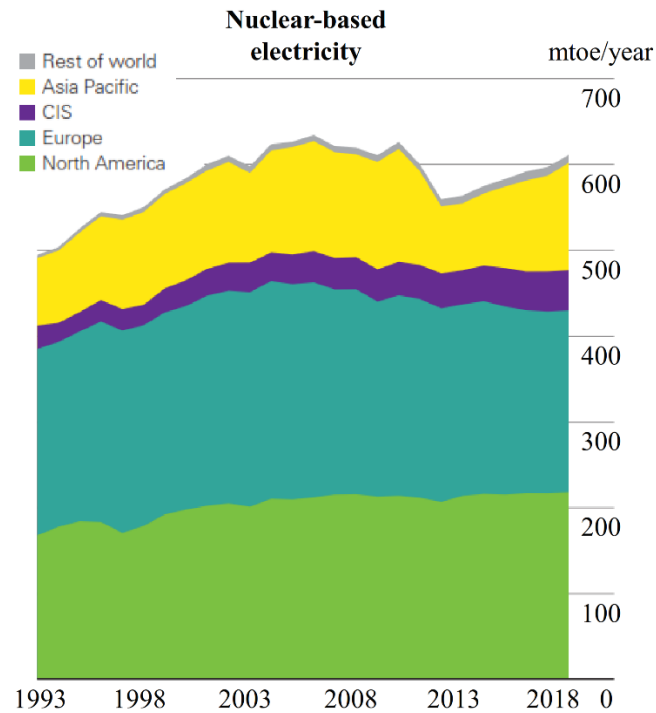


**Figure 5:** Nuclear-based electricity consumption<sup>2</sup>.

Global nuclear-based energy consumption is increasing with a rate of **2.4%** starting from 2013 and reached **611.3 mtoe** in 2018. But comparing the last 25 years, it has been continuously fluctuating, and the amount used in 2018 is lower than the one used in 2006 for example (**Figure 5**).

### 1.3.4 Renewable energies

Renewable energy has a vital role to play in meeting the challenge of eliminating CO<sub>2</sub> emissions. Nevertheless, its production is not stable, and highly depends on the weather and other factors, and the energy consumption fluctuates as well, which means that the development of various energy storage procedures is necessary<sup>7</sup>.

1. Introduction

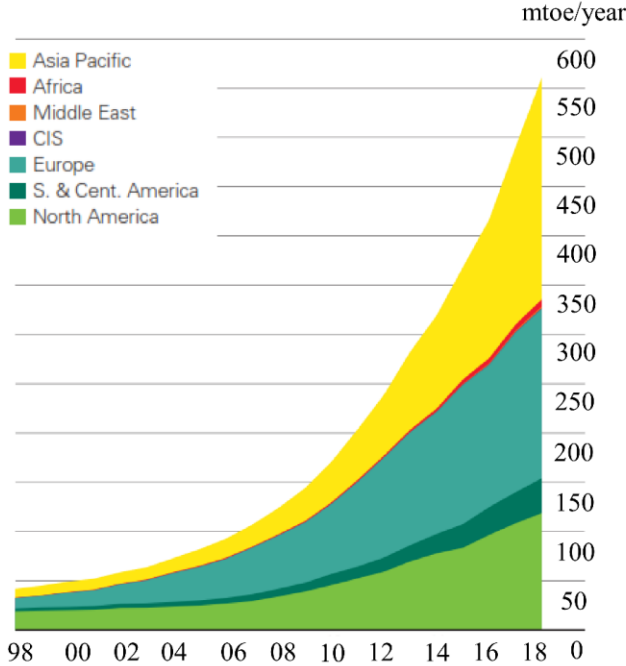


Figure 6: Renewable energy consumption<sup>2</sup>.

Renewable energy consumption exponentially increases in different locations of the world (Figure 6). It means that the renewables are promoted to be the most favorable substitute of the fossil fuels. Asia Pacific seem to lead in terms of the renewable energy amounts consumed (225.4 mtoe) followed by Europe (172.2 mtoe) and North America (118.8 mtoe). It is necessary to mention that the largest concentrated solar farm located in Morocco, which is called Noor (meaning light in Arabic).

In 2018, renewable energy in power generation (excluding hydro) increased by 14%, slightly below the 10-year average growth (16%). China alone, contributed in 45% of the global growth. Compared to solar energy (131 TWh), wind contributed more to the growth of renewable energy (142 TWh), and it has accounted for around 50% generated in the last few years. Solar has constantly increased its share and now represents 24%.

1. Introduction

1.3.5 Energy storage problem

Although there are several ways of energy storage, not all of them have the same storage capacity and duration (**Figure 7**).

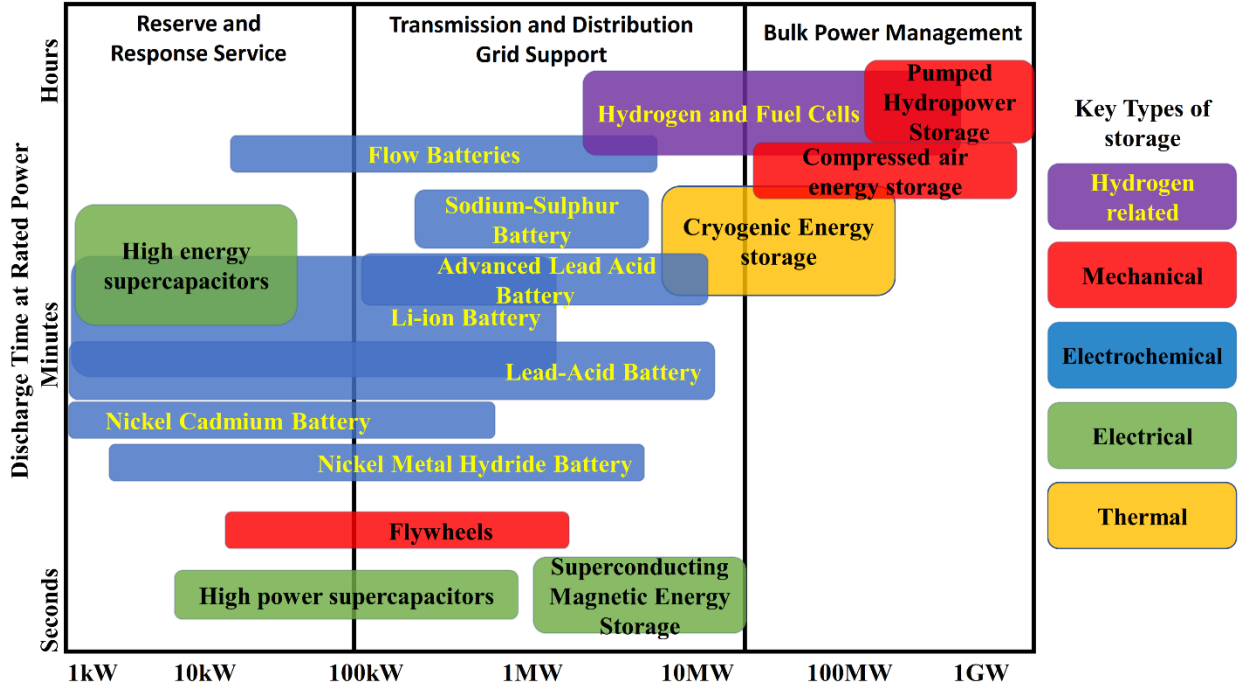


Figure 7: Characteristics of different energy storage types<sup>8</sup>.

Batteries are the most used devices for energy storage. The storage power and the discharge time can vary according to their type. The flywheels, high power superconductors and the magnetic energy storage methods have the lowest potential for energy storage. The best energy storage methods are the compressed energy storage systems, the pumped hydrogen power systems and the hydrogen fuel cells.

It is important to note that large capacity energy storage methods are badly needed for the extensive use of renewable electricity. The renewable electricity production highly depends on the weather, and thus, its production is fluctuating. Unfortunately, the electricity consumption is also fluctuating, but in a different frequency. Therefore, the storage problem of renewable electricity should be solved<sup>7</sup>. The high capacity of energy storage can be completed with Substitute Natural Gas (SNG). Storing energy in chemical bonds by recycling of carbon dioxide via hydrogenative reductions can be the most convenient way of storage for the renewable electrical energy<sup>9</sup>.

## 1. Introduction

### 1.4 CO<sub>2</sub> management

The energy transition aims to reduce CO<sub>2</sub> emissions. The valorization of this molecule presents an additional opportunity to achieve this goal. Instead of letting it escape to the atmosphere, it has to be captured where it is generated. It can be collected from several sources such as the industrial or biochemical processes<sup>10</sup>. By chemical transformations, added value molecules can be created allowing it to be recycled. This process is called Carbon Capture and Usage (CCU)<sup>11</sup>.

#### 1.4.1 CO<sub>2</sub> emission and climate change

The harmful effect of carbon dioxide emitted into the atmosphere is a well-known issue, and research in environmental protection is a challenge nowadays<sup>12</sup>. CO<sub>2</sub> emissions do not stop increasing as shown in **Figure 8**, as a result of the consumption of fossil fuels<sup>13</sup>, which is one of the factors behind global warming and the acidification of the oceans<sup>14</sup>.

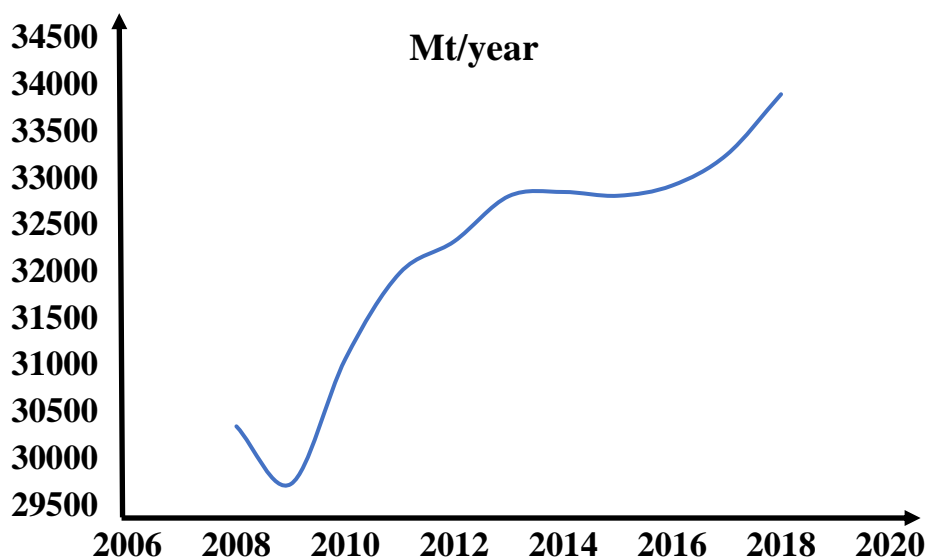


**Figure 8:** World CO<sub>2</sub> emission in the 2008-2018 time period<sup>2</sup>.

From the **Figure 8** we notice that since 2009 the amount of global CO<sub>2</sub> emissions is continuously increasing and it reached **33890.8 Mt** in 2018 with a growth rate of **2.0%**, which is the fastest in the last seven years.

## 1. Introduction

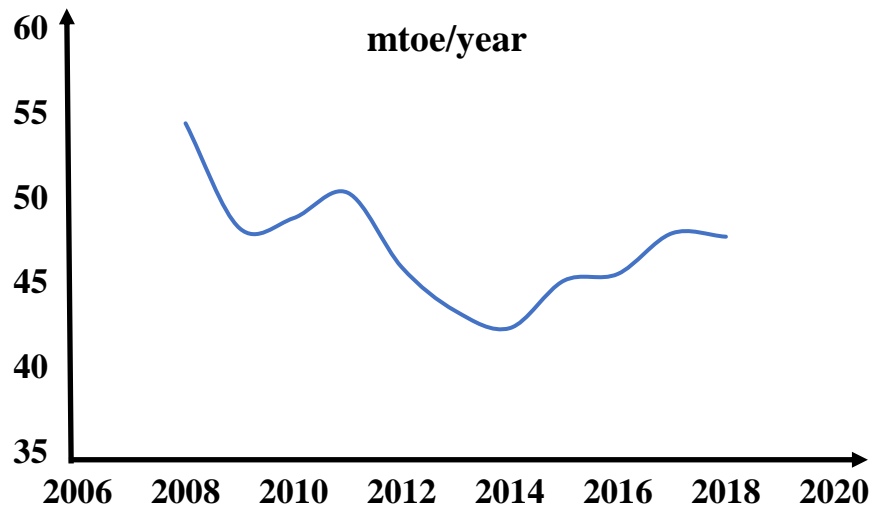


**Figure 9:** CO<sub>2</sub> emission in Hungary between 2008-2018<sup>2</sup>.

In Hungary, the CO<sub>2</sub> emission seems to be fluctuating between **50.3 Mt** and **42.3Mt** except for the year 2008 where the emissions reached the highest value **54.4 Mt** as shown in the **Figure 9**.

### 1.4.2 CO<sub>2</sub> and economy

An increasing and successful economy requires an increasing amount of energy production, which nowadays means increasing production of CO<sub>2</sub>. Reducing the present production rate would lead to an economic collapse unless different energy production methods are introduced. In the meantime, serious efforts must be made to reduce CO<sub>2</sub> emission and its concentration in the atmosphere.

### 1.4.3 Carbon Capture and Storage (CCS)

Most of the solutions proposed till now are mainly Carbon Capture and Storage (CCS) methods<sup>15</sup> which are not definitive solutions to eradicate the excess of CO<sub>2</sub> from the atmosphere<sup>16</sup>. For example, some ocean scientists think that ocean storage of CO<sub>2</sub> might be a good idea. In this case, the gas would be injected and trapped into the deep ocean<sup>17</sup>, but will it stay there forever?

### 1.4.4 Carbon Capture and Usage (CCU) as potential energy storage methods

From a chemical point of view, the best solution would be the total transformation of carbon dioxide into added value products<sup>18,19</sup>, and in this way the produced renewable energy can also be stored<sup>20</sup>. It could be used to carry out the reactions and convert carbon dioxide chemically into different molecules for the sake of energy storage<sup>21</sup>. These molecules can be used not only for the

## 1. Introduction

storage and production of energy, but to produce other chemicals in a renewable basis<sup>22</sup>. The necessary hydrogen could be obtained from the electrolysis of water using renewable electrical energy<sup>23</sup>, or steam reforming of natural gas<sup>24</sup> which ideally will contribute to the decrease of CO<sub>2</sub> emission<sup>9</sup>.

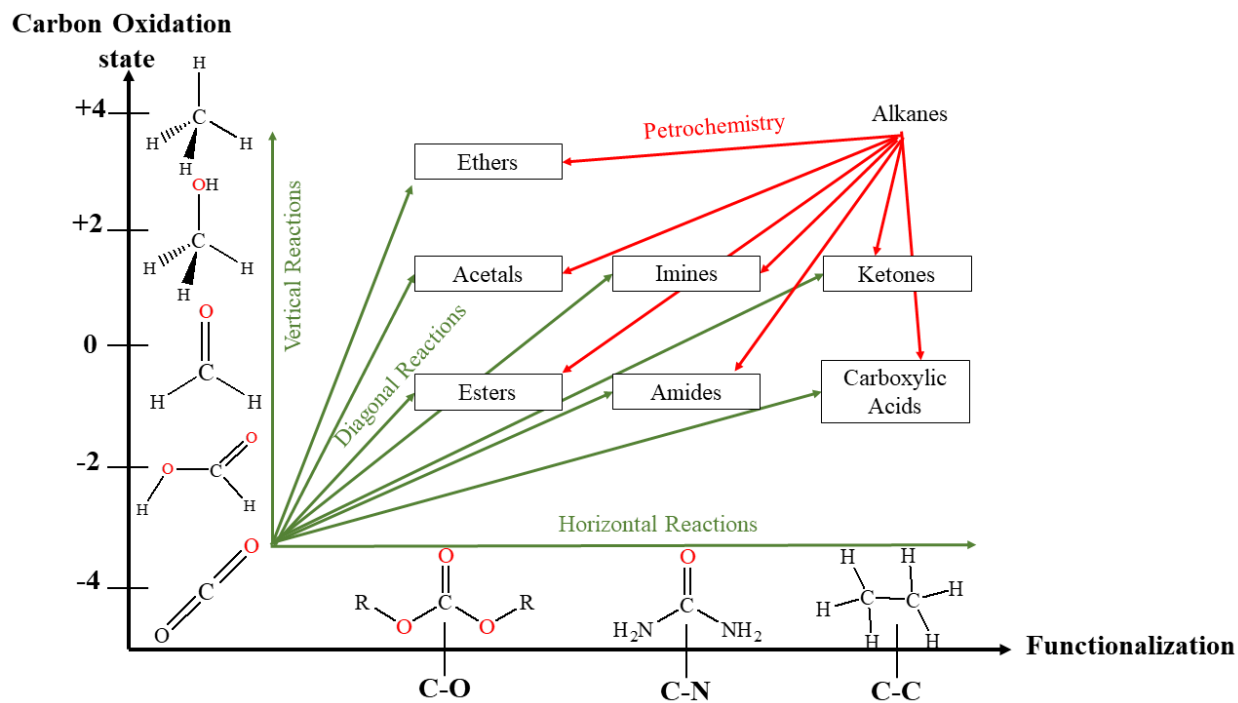


**Figure 10:** CO<sub>2</sub> valorisation by chemical reactions.

A more feasible option to handle CO<sub>2</sub> could be using it as a reactant and by the formation of new C-O and C-N bonds, more complex molecules such as polycarbonates, urea and alkenes can be created with new functions and with a high added value (**Figure 10**).

Furthermore, by the hydrogenation of CO<sub>2</sub> energy can be stored in chemical bonds (**Figure 10**). The reduction of carbon dioxide could lead to formic acid, formaldehyde, methanol and methane by decreasing the oxidation state of carbon.

Extensive research efforts are made to find novel methods for CO<sub>2</sub> recycling. In order to get hydrocarbons, which are used as fuels and basic reagents to access other chemicals, in a competitive manner to petrochemistry, reduction and the formation of new C-C, C-O and C-N bonds were combined. It is expected that methanol will play a growing role in future non-fossil fuels and getting it from the valorization of carbon dioxide is very promising.

## 1. Introduction

Methanol has a high energy density and its ability to be reintroduced into other chemical processes as feedstock to produce more advanced chemical compounds<sup>19</sup>.

### 1.5 The methanol synthesis

Between the different methanol production processes, CO<sub>2</sub> can be reduced directly, or introduced first in a reverse water-gas shift reaction (RWGS) as a fraction of synthesis gas<sup>25</sup>. In the last decades CO<sub>2</sub> hydrogenation to methanol has been a widespread subject of interest, large variety of solid catalysts have been designed and tested<sup>26</sup>. However, the reduction mechanism is still a debated subject and new processes are proposed<sup>27</sup>.

#### 1.5.1 Route of CO<sub>2</sub> reduction

The reduction involves the uptake of a hydrogen atom, a process which may be achieved by electrochemical reaction or by catalytic hydrogenation (**Figure 11**).

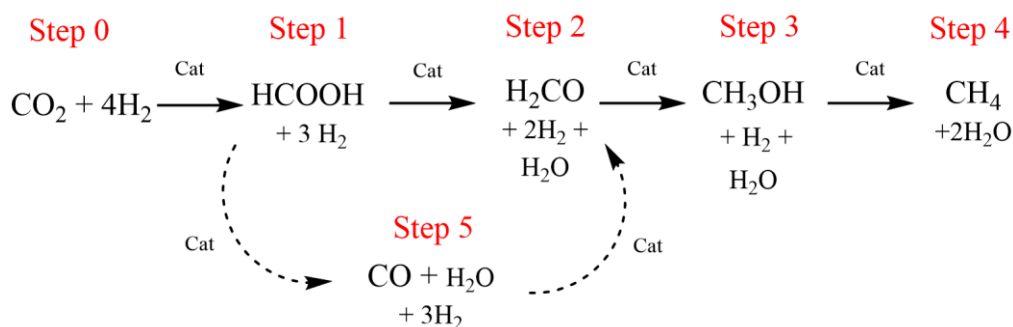


**Figure 11:** Stepwise reaction of carbon dioxide hydrogenation to achieve methanol and methane.

The reduction stages of CO<sub>2</sub> can be described by four isolable products, such as HCOOH, H<sub>2</sub>CO, CH<sub>3</sub>OH and CH<sub>4</sub><sup>28</sup>. Step 5 can be considered as a stepwise reaction, where through two steps carbon monoxide is formed as an extra intermediate.

## 1. Introduction

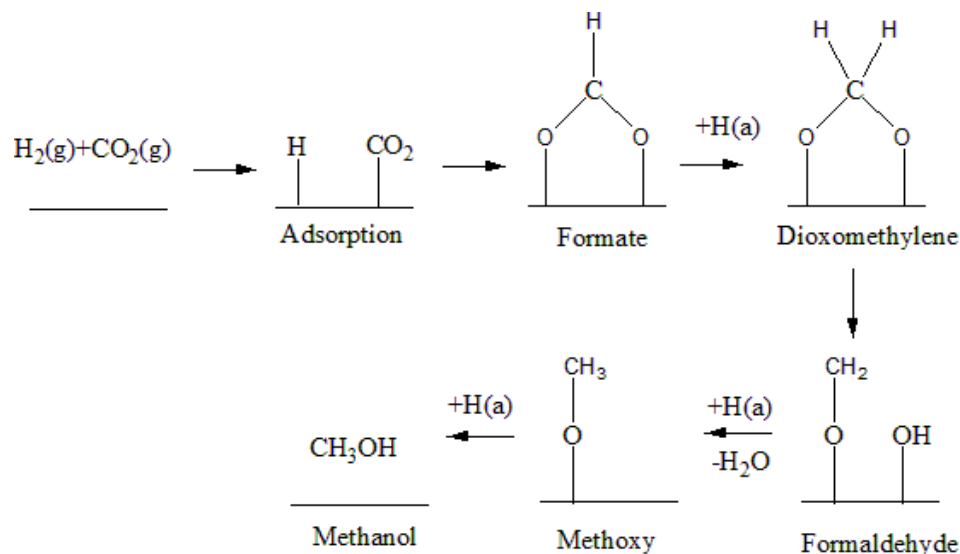


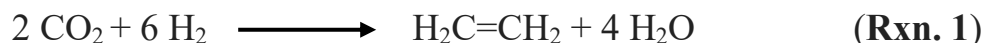
**Figure 12:** Proposed reaction mechanism for the synthesis of methanol from  $\text{CO}_2$  on  $\text{Cu}^{29}$ .

Most of the mechanisms proposed for the synthesis of methanol on the surface of Cu catalysts only consider the metallic phase (**Figure 12**). After the adsorption of  $\text{CO}_2$  and hydrogen, formate is formed. It is generally considered to be the most stable intermediate. Then, by a series of elementary steps involving the successive hydrogenation of intermediates, the formate is transformed into methoxy species, before undergoing a final hydrogenation into methanol.

### 1.5.2 Side reactions

Besides the main steps discussed above (**Figure 11**), several side reactions (*e.g.* leading to hydrocarbons) could also occur during the hydrogenation of  $\text{CO}_2$ .  $\text{CO}_2$  and  $\text{H}_2$  are considered as synthesis gas that can produce higher hydrocarbons. The simplest hydrocarbons in this case are expected to be ethylene and ethane.

At this stage it might be reasonable to point out that the following possible side reaction:



will lead to a valuable product (ethylene) which is a monomer for polyethylene formation, and it is very useful for other purposes in the chemical industry.

## 1. Introduction

### 1.5.3 Catalysts

The nature of the catalyst is a key question both in terms of its effectiveness and in terms of how many of the 4 main steps (**Figure 11**) can be catalyzed with it (formation of the targeted product and avoiding side products). In the following section, we have focused mainly on these two questions.

The catalysts used for CO<sub>2</sub> transformation are mostly metal-based systems. These systems can be divided into two groups, copper-based catalysts, and catalysts based on Au, Pd, NiIn or NiGa (**Table 1** and **Table 2**).

**Table 1:** The performance of Cu-based catalysts in CO<sub>2</sub>-methanol conversion.

Catalyst	T (°C)	P (Mpa)	H <sub>2</sub> :CO <sub>2</sub>	WHSV (mL.g <sup>-1</sup> .h <sup>-1</sup> )	CO <sub>2</sub> Conversion (%)	CH <sub>3</sub> OH selectivity (%)	Ref.
Cu/ZnO	250	3.0	3:1	18000	11.0	-	30
Cu/ZrO <sub>2</sub>	260	8.0	3:1	3600	15.0	86.0	31
CuO/ZnO	250	2.0	3:1	3750	8.6	45.0	32
Cu/ZnO/Al <sub>2</sub> O <sub>3</sub>	270	5.0	3:1	4000	23.7	43.7	33
Cu/ZnO/Al <sub>2</sub> O <sub>3</sub> /ZrO <sub>2</sub>	190	5.0	3:1	4000	10.7	81.8	34
Cu/ZnO/Al <sub>2</sub> O <sub>3</sub> /Y <sub>2</sub> O <sub>3</sub>	230	9.0	3:1	10000	29.9	89.7	35
Cu/ZnO/ZrO <sub>2</sub> /AlO <sub>3</sub> /SiO <sub>2</sub>	250	5.0	2.8:1	10000	-	89.7	36
Cu/ZnO/Ga <sub>2</sub> O <sub>3</sub> /	240	4.5	2.8:1	18000	27.0	50.0	37
Cu/TiO <sub>2</sub>	260	3.0	3:1	3600	-	64.7	38
Cu/ZrO <sub>2</sub> /CNTs	260	3.0	-	3600	16.3	43.5	39
CuZnO/Ui-bpy	250	4.0	3:1	18000	3.3	100.0	40

A wide variety of copper-based catalysts have been used to convert CO<sub>2</sub> to methanol (**Table 1**). The operating conditions are varied, but the temperature (T) and the ratio of the reactants was in most cases around to 250 °C and 3:1 (H<sub>2</sub>:CO<sub>2</sub>), respectively. The pressure (P) varied between 3-9 MPa, and there was no special value applied for the Weight Hourly Space Velocity (WHSV). The results of the experiments focused mainly on conversion and selectivity. In five of the cases the selectivity got over 80%, and in the case of (CuZnO/Ui-bpy) it even reached 100%. However, the conversion was the lowest in this case (3.3%). In the case of the conversion parameter among all the catalysts, the highest measured value is 29.9%, and it belongs to the Cu/ZnO/Al<sub>2</sub>O<sub>3</sub>/Y<sub>2</sub>O<sub>3</sub> system where the selectivity was equal to 89.7%.

## 1. Introduction

**Table 2:** The performance of Au, Pd, NiIn and NiGa catalysts in CO<sub>2</sub>-methanol conversion.

Catalyst	T (°C)	P (Mpa)	H <sub>2</sub> :CO <sub>2</sub>	WHSV (mL.g <sup>-1</sup> .h <sup>-1</sup> )	CO <sub>2</sub> Conversion (%)	CH <sub>3</sub> OH selectivity (%)	Ref.
Au/ZnO	240	0.5	3:1	-	0.4	49.0	41
Au/ZnO	240	5.0	3:1	-	1.0	70.0	41
Pd/ZnO	250	2.0	3:1	3600	11.1	59.0	42
Pd/ZnO/TiO <sub>2</sub>	250	2.0	3:1	3600	10.1	40.0	43
PdZnO/CNFs	275	0.1	9:1	7500	3.3	12.1	44
PdCuZnO/SiC	200	0.1	9:1	7500	-	80.9	45
Pd/Plate Ga <sub>2</sub> O <sub>3</sub>	250	5.0	3:1	6000	17.3	51.6	46
Ni <sub>3.5</sub> In <sub>5.3</sub> Al/SiO <sub>2</sub>	260	0.1	3:1	12000	3.8	2.3	47
NiGa/SiO <sub>2</sub>	250	0.1	3:1	-	-	98.3	48
Pd/Mo <sub>2</sub> C	135	-	3:1	-	-	95.0	49
Pd/In	190	-	3:1	-	-	94.0	50

In the case of the non-Cu-based catalysts (**Table 2**), the pressure and temperature varied between 0.1 to 5 MPa, and 200 to 275 °C, while and the ratio was kept in most of the cases to 3:1. The conversion in these cases was not excellent, the highest value was achieved in the case of the Pd/plate Ga<sub>2</sub>O<sub>3</sub> system (17.3%). The highest selectivity is 98.3% and it was achieved with the NiGa/SiO<sub>2</sub> catalyst, but in this case the conversion rate is not mentioned.

The industrially used catalysts nowadays are copper-based thermally stable materials due to the support structure of alumina and mainly optimized for mixtures of synthesis gas (H<sub>2</sub>, CO and CO<sub>2</sub>) and generally issued from natural gas reforming process.

### 1.5.4 Industrial processes for methanol production

The worldwide methanol production is mainly dominated by processes from only a few companies. The Imperial Chemical Industries (ICI) is accounting for 61% of the installed capacity with the Syntex process, and the Lurgi process for 27%<sup>9</sup>. Other processes exist such as the Mitsubishi Gas Company (MGC) process, but the main differences between all them remain in the type of the reactor design and the catalyst disposure (fixed bed reactor, fluidized bed reactor, tubular reactor...)<sup>9</sup>. Nowadays, most methanol productions are using methane as feed stock. Trough hydrocracking, methane is transformed to syngas (mainly CO<sub>2</sub>, H<sub>2</sub>, CO) which is routed directly to a reactor where the catalytic methanol reaction takes place<sup>51</sup>.

## 1. Introduction

### 1.6 Goal

The chemical hydrogenation of CO<sub>2</sub> to methanol by using renewable energies can be the key to solve the problem of renewable energy storage as well as reduce CO<sub>2</sub> emissions. However, carbon dioxide hydrogenation is a mechanistically complicated multistep process. Therefore, it is indispensable to understand the mechanism. To do that, computational chemistry tools can be used.

This thesis is an assembly of three major computational chemistry studies:

- A gas phase study: where all the molecular complexes that might be formed from the (CO<sub>2</sub>+4H<sub>2</sub>) reaction mixture are investigated and the most stable ones will be selected to be part of a newly designed network for the uncatalyzed carbon dioxide hydrogenation to methanol and methane. The network will be energetically studied, and the efficiency of the most favourable pathway will be calculated.
- An aqueous phase study: knowing that carbon dioxide can be absorbed by water as it happens in the oceans, an uncatalyzed water enhanced hydrogenation mechanism for CO<sub>2</sub> conversion to methanol will be designed and thermodynamically studied. The efficiency of the preferred pathway will be calculated and compared to the gas phase results.
- An aqueous phase catalyzed-like study: the major mechanistical role of a solid catalyst in the methanol synthesis is the conversion of hydrogen molecules to hydrogen atoms (bond dissociation). To mimic this special property of the catalysts, a catalyzed-like mechanism will be constructed involving hydrogen atoms instead of hydrogen molecules and studied energetically. After that the efficiency will be calculated taking into account the hydrogen bond dissociation energy.

These studies aim to provide a better understanding of this difficult process, and to identify the rate limiting steps, targeting their reduction and/or avoidance, in different conditions. The findings can be applied in the near future to design and develop new special purpose catalysts.

## 2 Computational methods

*“The history of science shows that theories are perishable. With every new truth that is revealed we get a better understanding of nature and our conceptions and views are modified”*

**Nicolas Tesla (1856 – 1943)**

## 2. Computational methods

### 2.1 Computational chemistry

Computational chemistry uses the basics of quantum chemistry to predict molecular properties for a better understanding of nature from a chemical point of view. It describes a system's physical properties using the wave function through the action of operators and determines through the Schrödinger equation (1) its energetic state.

$$H \Psi = E \Psi \quad (1)$$

Here  $H$  is the Hamiltonian operator which describes the kinetics and potential energies of the system.  $\Psi$  is the electronic wave function and  $E$  is the total electron energy.

Because of the vast computational demands, many approximations are necessary. In most of the cases, quantum chemists assume that the motion of electrons is separated from that of the nuclei. In the Born-Oppenheimer approximation<sup>52</sup>, only the electronic part is solved and the nuclear one is only approximated.

The most important properties (such as  $\Delta_r G$ ,  $\Delta_r H$ ,  $S$ ,  $\Delta_f H^\circ$ ,  $pK_a$ ) of short-lived molecules, unstable intermediates, and transition states, can be calculated using computational chemistry methods. Thus, the reaction mechanisms can be examined in a detailed manner, and appropriate catalysts can be designed to avoid the potential by-products and side reactions.

### 2.2 Level of theory

The different theoretical approaches which corresponds to various approximations of the electronic Schrödinger equation with a certain accuracy are called the levels of theory. It has two degrees of freedom: one is the treatment of electron correlation, and the other is the basis set.

#### 2.2.1 Methods

##### 2.2.1.1 Ab initio molecular orbital theory

Ab initio molecular orbital theory is used to predict the properties of atomic and molecular systems. It is based upon the fundamental laws of quantum mechanics and uses a variety of mathematical transformation and approximation techniques to solve the fundamental equations. The only inputs into an ab initio calculation are physical constants<sup>53</sup>.

The most widely used approximation in quantum chemistry is the Hartree-Fock (HF) method<sup>54</sup> which is the basis of the molecular orbital theory. It assumes that the Slater determinant wave function of an electron cloud can be constructed from the corresponding spin-orbital product<sup>55</sup>

## 2. Computational methods

and this can be extended to any number of electrons and thus, can be used to approximate the multielectron wave function of the system.

The HF *ab initio* method does not handle the electron correlation, which leads to a low computational time, but a lower accuracy as well.

To achieve higher accuracy, post-Hartree-Fock *ab initio* methods have been developed within which the treatment of electron correlation have been included. The Møller–Plesset perturbation theory (MP)<sup>56</sup> is one of those which has a relatively low computational cost, but it is ideal only if the electron correlation level is relatively low. Higher order perturbation methods can be derived from the Møller-Plesset expansion when it is truncated at second (MP2)<sup>57</sup>, third (MP3) or fourth (MP4) order.

Another type of post-Hartree-Fock methods is the configuration interaction (CI). A special correction of this is called quadratic configuration interaction including single and double substitutions or QCISD<sup>58</sup>. Coupled cluster methods (CC)<sup>59</sup> are used to describe multibody systems constructing multielectron wave functions and employing the exponential cluster operator to account for electron correlation. These methods apply series expansion which resulted in the formation of determinants from the reference Slater determinant like wave function where one or more electrons are transferred to the unoccupied orbitals in the reference. A drawback of the method is that it is not variational. The CCSD<sup>60</sup> (coupled cluster singles and doubles) method contains single and double excitations, while the CCSD(T) additionally includes the perturbative approximation of triple excitations. Currently, the CCSD(T) is the most precise electronic structure method still applicable for small systems.

### 2.2.1.2 Density functional theory (DFT)

The hybrid density functional theories (DFT)<sup>61</sup> are the most popular quantum chemical approaches used to determine the electronic structure of the molecules. Also derives from quantum mechanics but instead of using the wave function to determine the properties of multi-electron systems as it is done in *ab initio* methods, these methods uses the electron density function to calculate the energy using an exchange-correlation functional.

A large number of different functionals are parameterized by using experimental or highly accurate *ab initio* data. The B3LYP (Becke, 3-parameter, Lee-Yang-Parr)<sup>62,63</sup> is one of the most well-known DFT and tested methods in computational chemistry. This functional<sup>64</sup> employs three empirical parameters<sup>65,66</sup>. Originally, it has been tested on 56 atomization energies, 42 ionization potentials,

## 2. Computational methods

8 proton affinities, and 10 total atomic energies of first and second-row systems and it was found that this functional fit experimental atomization energies with an impressively small average absolute deviation of 2.4 kcal/mol<sup>67</sup>. In terms of calculation time, the B3LYP is generally faster than most of the post-Hartree-Fock methods and usually provides comparable results, which is especially hold for geometry.

The *ab initio* methods discussed so far provides accurate geometry, but to get more precise energy calculations results, higher-level methods such as CCSD, QCISD, CCSD(T), QCISD(T) are recommended. However, it has to be noted that using high level of theory methods costs a longer calculation time.

### 2.2.2 Basis set

A basis set is a collection of mathematical functions used to build up the quantum mechanical wave function for a molecular system. All of the previously mentioned electronic structure methods require a basis set to describe the electronic wave function. In principle, if the number of the mathematical functions used is high, the description of the electronic structure would be more accurate, and again, the drawback is the higher computing time. Minimal basis sets contain the minimal number of basis functions needed for each atom. The most common minimal basis set is STO-nG, where n is an integer. This n value represents the number of Gaussian primitive functions comprising a single basis function. The STO-3G for example uses three Gaussian primitives per basis function, it is referred by “3G”, “STO” stands for “Slater Types Orbitals”<sup>68</sup>. However, the computation of the integrals is greatly simplified by using Gaussian-type orbitals (GTO)<sup>69</sup> for basis functions. The basis set can be made larger by increasing the number of basis functions per atom. Split valence basis sets such as People basis sets<sup>70</sup>, are defined as X-YZg. X is the number of Gaussian primitives comprising each core atomic orbital basis function. The Y and Z indicate that the valence orbitals are composed of two basis functions each, composed of a linear combination of Y and Z primitive Gaussian functions, respectively. In this case, the presence of two numbers after the hyphens implies that this basis set is a split-valence double-zeta basis set. Split-valence triple- and quadruple-zeta basis sets are denoted as X-YZWg, X-YZWWg, etc. There is one basis function for the core electrons and two or more for the valence. When the core orbital is made of 6 Gaussians and the valence is described by 2 orbitals (first is derived from 3 Gaussians and the second from 1) the basis set is called: 6-31G. Polarization can also be added to the non-hydrogen (d) and the hydrogen atoms as well (p)<sup>71</sup>.

## 2. Computational methods

One of the most widely used basis sets are those developed by Dunning and coworkers<sup>72</sup> abbreviated as (aug-)cc-pVNZ, where the size of the basis grows with  $N$ . The term VNZ refers to “valence  $X$ -tuple zeta” where  $N=D,T,Q,5\dots$ (Double, Triple, Quadruple, etc.). The “cc-p”, stands for “correlation-consistent polarized” indicating that more functions with higher angular momentum quantum numbers are involved, and the “aug-” means “augmented” and indicates the inclusion of diffuse functions. For period-3 atoms (Al-Ar), additional functions have turned out to be necessary; these are the cc-pV(N+d)Z basis sets.

### 2.3 Composite methods

Quantum chemistry composite methods are a combination of several computational chemistry methods aiming high accuracy. They are also called thermochemical recipes and commonly used to calculate thermodynamic properties. These are essentially a combination of higher and lower levels of theory. Various families of these exist, including Gaussian (Gn)<sup>73</sup>, CBS<sup>74</sup>, and also Weizmann (Wn)<sup>75</sup>. The W1 protocol is based on the B3LYP density functional theory (DFT) method<sup>63</sup> for geometry optimization<sup>76</sup> and frequency calculation<sup>77</sup>, coupled with the cc-pV(T+d)Z basis set, and steps further with coupled cluster calculations for the thermochemistry part. This protocol will be used for the calculations of this work.

### 2.4 Solvent model

To compute reactions in an aqueous phase, the solvent effect on the reaction has to be taken into account. To do this, different solvent models can be used. Neglecting this can significantly affect the energetics of the studied system.

#### 2.4.1 Implicit models

Implicit solvents or continuum solvents, are models in which one accepts the assumption that implicit solvent molecules can be replaced by a homogeneously polarizable medium as long as this medium, gives equivalent properties to a good approximation<sup>78</sup>. Generally, for implicit solvents, a calculation proceeds by encapsulating the solute in a cavity. The cavity containing the solute is embedded in homogeneously polarizable continuum describing the solvent. The dielectric constant is the value responsible for defining the degree of polarizability of the solvent. The charge of the solute distribution meets the continuous dielectric field at the surface of the cavity and polarizes the surrounding medium, which causes a change in the polarization on the solute. This defines the reaction potential, a response to the change in polarization.

## 2. Computational methods

Several standard models exist and have all been used successfully in a number of situations. The Polarizable Continuum Model (PCM) is a commonly used implicit model and has seeded the birth of several variants<sup>79</sup>.

### 2.4.2 Explicit models

Explicit solvent models treat explicitly the solvent molecules. This is a more intuitively realistic picture in which there are direct, specific solvent interactions with a solute, in contrast to continuum models. These models generally occur in the application of molecular mechanics (MM) and dynamics (MD).

### 2.5 Potential energy surface and reaction mechanism

A potential energy surface (PES) is a multi-dimensional mathematical representation of the energy variations happening during chemical reactions.

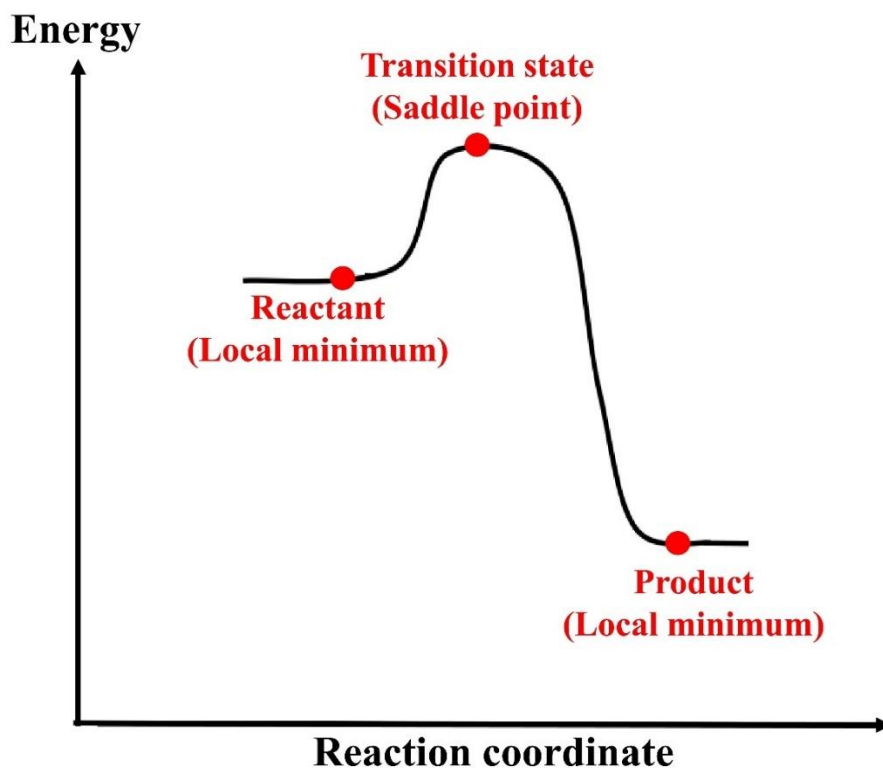


**Figure 13:** Schematic representation of a potential energy surface.

In order to explore the steps of a reaction (reaction mechanism), the initial reactants, the final products and the intermediate structures as well as the transition structures of a reaction pathway have to be determined (**Figure 13**).

## 2. Computational methods

Geometry optimization generally attempt to locate minimum on the potential energy surface, thereby predicting equilibrium structures of molecular systems. Optimizations can also locate transition structures. At both minima and saddle points, the first derivative of the energy with respect to all internal coordinates, known as the gradient, is zero. The structure at these points may correspond to a minimum (Reactant, intermediate structure, or product), or to a saddle point which is a minimum in some direction of the PES, and a maximum in one or more directions. First order saddle points, which are a maximum in one direction and a minimum in all others correspond to transition state structures. This is determined by calculating the Hess matrix

The first critical step that has to be made before any quantum chemical calculation is to build the initial structure which is close enough to the sought structure. The Gaussian 09 program<sup>80</sup> can determine optimized structures by changing the structural parameters and calculating the corresponding electronic energy and the nuclei-nuclei repulsion energy (their sum is the so-called total energy,  $E_{\text{tot}}$ ) at the selected level of theory. The minimum energy structure is formed when all the convergence criteria are fulfilled. The optimization is done as the following, in each iteration of the geometry optimization, the maximum remaining force on an atom in the system as well as the average mass weighted force constant on all atoms together has to be checked, and their values must be smaller than the corresponding threshold value. Furthermore, two other criteria also have to converge (maximum displacements). The maximum structural change of one coordinate, and the average standard deviation (RMS) change over all structural parameters in the last two iterations. Once the values of all four criteria fall below the given threshold, the optimization is considered as complete. After optimization, frequency calculation at the optimized geometry of the predicted structure will confirm if that is in fact a minimum. Frequency calculations consider the nuclear vibration in the molecular systems as if they are in their equilibrium states. If the geometry is optimized into a minimum, the gradient is zero, and the force constant matrix determines the behavior of the system under small displacements.

## 2. Computational methods

To carry out the calculations discussed along our work, the Gaussian 09 program package<sup>80</sup> have been used. Detailed mechanisms of the uncatalyzed CO<sub>2</sub> hydrogenation to achieve methanol in gas phase and in aqueous phase have been studied thermodynamically. After that, a catalyzed-like aqueous phase mechanism has also been described. The W1 protocol has been chosen to carry out all the calculations.

### 2.6 Gas phase calculations

As the hydrogenation of carbon dioxide is a complicated procedure, various computational chemical tools (combinatorial chemistry<sup>83</sup> in combination with *ab initio* calculations followed by thermodynamic calculations using the W1 protocol) have been applied to understand the mechanistic details of the process. The molecular complexes were generated using the MOLGEN 5.0 software<sup>84</sup>, and after that, all the generated structures were optimized.

#### 2.6.1 Structure generation

If the nuclei and chemical bonds are considered as the nodes and the edges of a graph, respectively, The enumeration of all the molecules corresponding to our stoichiometry (CH<sub>8</sub>O<sub>2</sub>) from a graph theory<sup>84</sup> is possible. A certain number of atoms with a limited number of different valences defines the number of constitutional isomers<sup>85</sup>. All possible stoichiometric isomers of CH<sub>8</sub>O<sub>2</sub> are generated by allowing carbon to form 2 or 4 chemical bonds, while hydrogen and oxygen to form 1 and 2 chemical bonds, respectively. This graph representation is extended to three dimensions by the means of the atom type specific geometric parameter set obtained from the simplified MM2 force field. By using this procedure, in this case 27 three dimensional molecular configurations can be generated by the Molgen 5.0 program<sup>84</sup>. These configurations are used as initial structures in the search for local minima on the multidimensional potential energy surface for all the species.

#### 2.6.2 Quantum chemical calculations

Additionally, the W1BD composite method<sup>75</sup> has been selected to calculate all of the species. The W1BD method is the Brueckner doubles variation of the Weizmann-1 (W1)<sup>86</sup> calculation scheme. The BD algorithm which is employed in the method involves macro iterations to update the orbitals<sup>75</sup>. A network involving the optimized species for the uncatalyzed hydrogenation of CO<sub>2</sub> to methanol and methane is proposed. Beside the stable species all transition states (TS) were also characterized by using the W1BD level of theory. The transitions states have also been verified by

## 2. Computational methods

normal mode analysis and IRC (Internal Reaction Coordinates)<sup>87</sup> calculations. All the calculations were carried out by using the Gaussian 09 software package<sup>80</sup>. The overall potential energy surface (PES) was constructed from the individual relative energies of the obtained structures.

### 2.7 Aqueous phase calculations

#### 2.7.1 Uncatalyzed mechanism

The option of CO<sub>2</sub> reduction in aqueous phase had to be considered as well. A reaction network involving a water molecule and protonation steps has been constructed starting with an initial reactant mixture of CO<sub>2</sub>+3H<sub>2</sub>+H<sub>2</sub>O+H<sub>3</sub>O<sup>+</sup>. All the thermodynamic properties of the involved species and transition states have been computed at standard conditions by using the Gaussian 09 program package<sup>80</sup>. The Potential Energy Surface (PES) of the studied reaction has been analyzed and the important points (minima, TS, etc.) have been located. IRC calculations have been used to verify the transition states are located between the corresponding minima. Initially, the calculations have been carried out by using the B3LYP density functional theory (DFT) method<sup>88,89</sup> in combination with the 6-31G(d) basis set<sup>69</sup>. To further improve the accuracy of the analysis, the structures have been recalculated by using the W1U (Unrestricted Weizmann-1) composite method<sup>75,86,90</sup>. In our previous work (gas phase)<sup>91</sup>, the W1BD<sup>75</sup> protocol was applied for gas phase calculations, but it is not applicable in this case. The BD algorithm is not compatible with the SCRF implicit solvation model<sup>92</sup>. Thus, the W1U method has been selected instead and the solvent effect have been mimicked by using the conductor-like polarizable continuum model (CPCM)<sup>93,94</sup>. To validate the choice of W1U, it was compared to W1BD in gas phase calculations and they gave almost identical results within less than 1 kJ/mol deviation (see section **2.8.3**).

## 2. Computational methods

### 2.7.2 Catalyzed-like mechanism

At this stage, we have decided to imitate the role of solid catalysts in the aqueous phase mechanism. In catalytic hydrogenation reactions, the hydrogen molecules split into atoms. Thus, the hydrogen addition reactions will be then replaced by atomic hydrogenations ( $H^{\bullet}$ ). For a system with the  $CO_2+6H^{\bullet}+H_2O+H_3O^+$  reactants mixture, the thermodynamic properties of the intermediate species and transition states have been computed at standard conditions using the Gaussian 09 program package<sup>80</sup>. The new reactions were calculated as a first step by the B3LYP density functional theory (DFT) method<sup>88,89</sup> in combination with the 6-31G(d) basis set<sup>69</sup>. Then, to reach higher accuracy, all of these reactions have been recalculated by using the WIU (Unrestricted Weizmann-1)<sup>75,86,90</sup> composite method. IRC (Internal Reaction Coordinates)<sup>87</sup> calculations have been carried out to verify that the transition states are located between the corresponding minima. Relaxed energy scans have been carried out to verify the barrierless reactions. In one case, a rigid energy scan was performed by freezing an inter atomic angle to avoid some undesirable interactions. Since an aqueous phase process is envisaged, the solvent effect have also been mimicked by using the conductor-like polarizable continuum model (CPCM)<sup>93,94</sup>.

## 2.8 Methods validation

### 2.8.1 Gas phase

To estimate the accuracy of the theoretical level and to select appropriate method for our system, the heat of formation of 10 optimized structures have been calculated using the Feller-Helgaker extrapolation procedure<sup>81,82</sup> and the WIBD composite method and compared to experimental values (**Table 3**). All structures generated by graph theory are optimized with the MP2 method<sup>95</sup> in combination with the aug-cc-pVTZ<sup>96</sup> basis set. Then, the outputs are submitted for single point calculations using the CCSD(T)<sup>97</sup> method combined with the cc-pVTZ, cc-pVQZ, and cc-pV5Z<sup>72</sup> basis sets.

## 2. Computational methods

**Table 3:** Heat of formation ( $\Delta_f H^0$ ) of 10 optimized structures have been calculated by using the Feller-Helgaker (F.H.) extrapolation and the W1BD method and compared to experimental values from the literature. All values are in kJ/mol.

Species	$\Delta_f H^0$		Experiment	Ref.	$\Delta\Delta_f H^0$	
	F.H.	W1BD			F.H.	W1BD
<b>HCOOH</b>	-373.62	-381.11	-378.80	<sup>98</sup>	5.18	2.31
<b>CO</b>	-106.81	-110.17	-110.53	<sup>99</sup>	3.72	0.36
<b>CH<sub>2</sub></b>	430.42	428.76	428.80	<sup>100</sup>	1.62	0.04
<b>CO<sub>2</sub></b>	-388.14	-394.67	-393.51	<sup>99</sup>	5.37	1.16
<b>H<sub>2</sub>CO</b>	-107.25	-110.59	-108.70	<sup>98</sup>	1.45	1.89
<b>CH<sub>3</sub>OH</b>	-202.04	-205.11	-201.00	<sup>98</sup>	1.04	4.11
<b>CH<sub>4</sub></b>	-72.65	-76.43	-74.60	<sup>98</sup>	1.95	1.83
<b>H<sub>2</sub>O</b>	-244.70	-244.31	-241.81	<sup>101</sup>	2.89	2.50
<b>H<sub>2</sub>O<sub>2</sub></b>	-137.69	-134.38	-135.77	<sup>101</sup>	1.92	1.39
<b>H<sub>3</sub>COOH</b>	-128.07	-130.50	-131.00	<sup>102</sup>	2.93	0.50
			<b>Average</b>		2.81 ± 1.53	1.61 ± 1.21
			<b>Max. dev.</b>		5.37	4.10

Both methods are highly accurate compared to the experimental heat of formations. However, the average deviation as well as the maximum deviation are smaller in the case of the W1BD method. Thus, it was selected for further calculations.

## 2. Computational methods

### 2.8.2 Aqueous phase

In the aqueous phase calculations, the unrestricted version of the W1 method has been chosen. To estimate the accuracy of the level of theory used in this case (W1U), calculations have been carried out for the elementary reaction steps. The reaction enthalpies of a simple mechanism which is close to our system (converts CO<sub>2</sub> and hydrogen to methanol and methane, **Figure 14**) have been computed and compared to experimental values by using the heat of formations of the species available in the literature<sup>102</sup>.

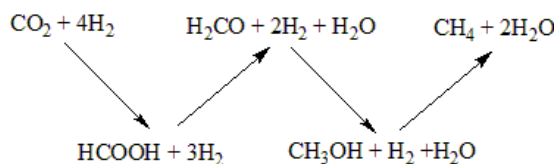


**Figure 14:** Reaction steps of CO<sub>2</sub> hydrogenation to methane.

The envisaged test reaction includes successive H<sub>2</sub> addition steps, where the formic acid, formaldehyde and methanol are formed, leading to the formation of methane (**Figure 14**).

**Table 4:** Comparison of the computed enthalpy changes ( $\Delta H_r^o$ ) of each molecule produced through elementary reaction steps and their respective experimental gas phase enthalpy of formation ( $\Delta\Delta_f H_{exp}^0$ ) differences. The calculated and experimental values have also been compared and listed in the table (Calc-Exp).

	$\Delta H_r^o$	$\Delta\Delta_f H_{exp}^0$	Abs. dev. (kJ/mol)
	(kJ/mol) Calc	(kJ/mol) Exp	
CO <sub>2</sub> + 4H <sub>2</sub>	0.00	0.00	0.00
HCOOH + 3H <sub>2</sub>	13.93	14.91	0.98
H <sub>2</sub> CO + 2H <sub>2</sub> + H <sub>2</sub> O	40.08	35.78	4.30
H <sub>3</sub> COH + H <sub>2</sub> + H <sub>2</sub> O	-53.78	-49.81	3.97
CH <sub>4</sub> + 2 H <sub>2</sub> O	-169.16	-165.02	4.14

The highest absolute deviation between the computed and the experimental values belongs to (H<sub>2</sub>CO + 2H<sub>2</sub> + H<sub>2</sub>O) which is equal to 4.30 kJ/mol. All in all, it can be considered that our computed results are precise and applicable to study CO<sub>2</sub> hydrogenation reactions.

## 2. Computational methods

### 2.8.3 Results comparability

In order to be able to compare the results calculated using two W1 sub-protocols (W1BD and W1U), we have to prove that they have very similar results for the same calculations (**Table 6**).

**Table 5:** Comparison of the computed results of the two arbitrarily chosen molecules formaldehyde and methanol using the W1BD and W1U protocols

Energies (kJ/mol)	Abs. Dev. of the results from W1BD and W1U	
	Formaldehyde	Methanol
ZPE	0.000	0.000
Thermal Energy	0.000	0.000
Tot. Energy	0.985	0.396

The highest deviation we got between the two methods is less than 1kJ/mol. Thus, it can be concluded that the W1U method is applicable and the two methods can be compared.

## 3 Results and Discussion

*“The world is a book, and those who do not travel read only a page”*

**Saint Augustin**

**Born and died in Algeria**

**(354-430)**

### 3. Results and discussion

This chapter is an assembly of the results of three major computational chemistry studies:

The first part of the results section is dedicated to the gas phase results. The results of the combinatorial chemistry calculations used to select the most stable molecular complexes from the (CO<sub>2</sub>+4H<sub>2</sub>) reaction mixture will be shown. The selected molecules will be used to design a network for the uncatalyzed carbon dioxide hydrogenation to methanol and methane. The results of the energetically studied network will be presented, and the efficiency of the most favorable pathway will be calculated.

After that, the aqueous phase results will be listed. It is a mechanistically studied water enhanced hydrogenation mechanism for CO<sub>2</sub> conversion to methanol. The efficiency of the preferred pathway will be calculated and compared to the gas phase results.

In the end, the results of the aqueous phase catalyzed-like study will be shown. This study has been made to mimic this special property of the solid catalysts to split the hydrogen molecules to hydrogen atoms. A catalyzed-like mechanism will be constructed and studied energetically, and the efficiency will be calculated taking into account the hydrogen bond dissociation energy.

#### 3.1 Gas phase results

All the possible molecules and molecular complexes that can be described by the CH<sub>8</sub>O<sub>2</sub> stoichiometry and involved in the gas phase uncatalyzed CO<sub>2</sub> hydrogenation to methanol and methane (*e.g.* CO<sub>2</sub> + 4H<sub>2</sub>, CH<sub>4</sub> + 2H<sub>2</sub>O) have been investigated<sup>91</sup>. By selecting the most stable intermediate molecules, a network of the hydrogenation process has been constructed. The thermodynamics of stable species and all the energy barriers were calculated using computational chemistry tools<sup>103</sup>, and the most favorable pathway leading to methanol and methane has been selected. The structures have been generated by using the MOLGEN 5.0 software<sup>84</sup> and optimized by using the Gaussian 09<sup>80</sup> program package. The corresponding relative Gibbs free energy values were plotted against the relative entropies (**Figure 15**) to compare the stability of the species. Since the reactant mixture is CO<sub>2</sub> + 4H<sub>2</sub>, we have decided to consider it as a reference level.

The relative Gibbs free energy of every (X) structure will be calculated as follows:

$$\Delta G_r^o = \Delta G_{(X)} - \Delta G_{ref} \quad (2)$$

The relative enthalpy and entropy were derived analogically.

### 3. Results and discussion

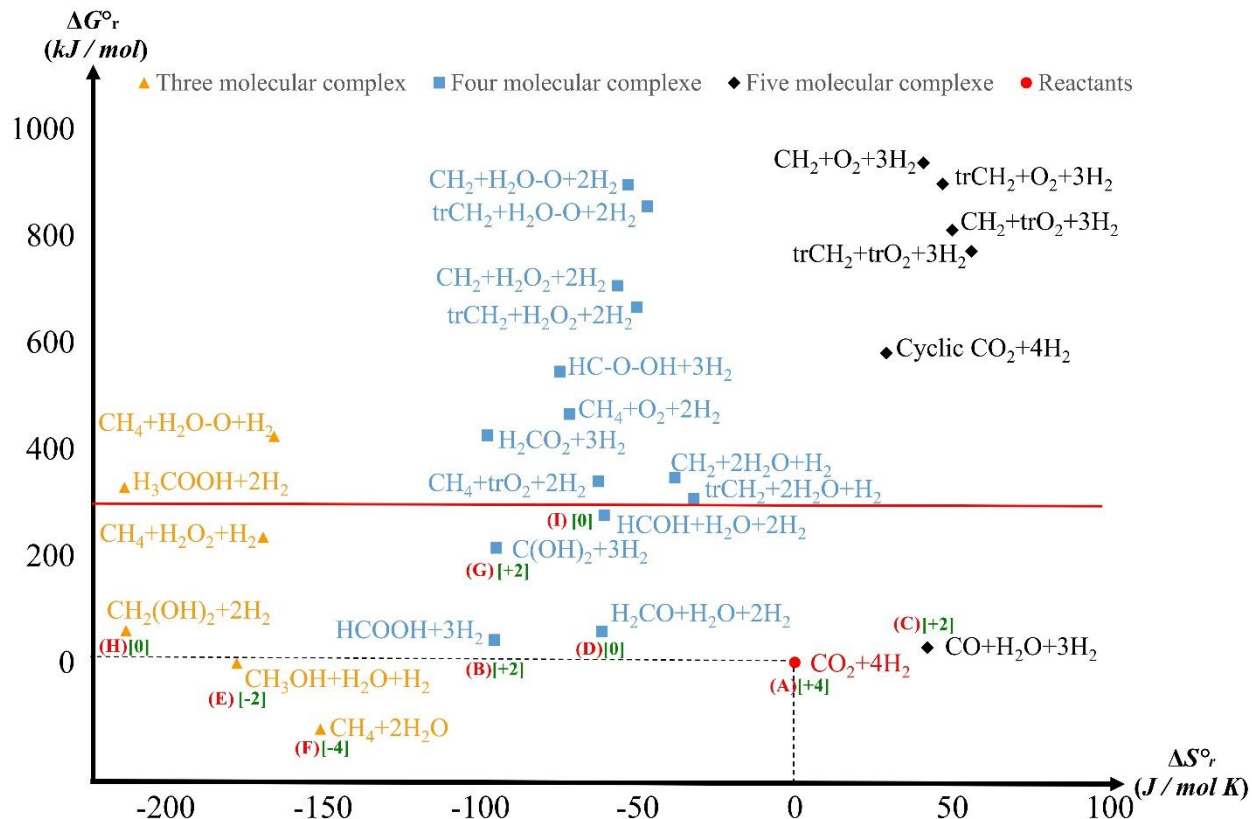


**Figure 15:** Thermodynamic properties of the  $\text{CH}_8\text{O}_2$  stoichiometry which could be involved in  $\text{CO}_2$  reduction. Relative Gibbs free energy ( $\Delta G_r^0$ ) and entropy ( $\Delta S_r^0$ ) computed using the WIBD method for the molecular composition obtained by combinatorial tools. The triplet states are signed by tr. The red line defines the highest energy level of the stable section ( $>300\text{kJ/mol}$ ). The oxidation state of the most stable structures is shown in green.  $\text{CO}_2 + 4\text{H}_2$  considered as a reference level and highlighted with a red dot.

Considering the number of molecules constituting a complex with  $\text{CH}_8\text{O}_2$  stoichiometry, the **Figure 15** shows well separated groups of species in a function of the entropy. The yellow triangles represent the three-, the blue squares the four-, while the black diamonds the five-membered complexes (**Table 7**). Only the methanol and methane complexes have lower free energy compared to the reference and both complexes have significantly lower entropy compared to the reference. This total entropy lowering could be hindered by the positive influence of the temperature on the equilibrium. We have considered the complexes having a relative Gibbs free energy lower than  $300\text{ kJ/mol}$  as relatively stable.

### 3. Results and discussion

**Table 6:** Thermodynamic properties of the CH<sub>8</sub>O<sub>2</sub> species calculated at the W1BD level of theory.

	Species	$\Delta G_r^{\circ}$ (kJ/mol)	$\Delta H_r^{\circ}$ (kJ/mol)	$\Delta S^{\circ}$ (J/mol K)
<b>5 Species</b>	<b>CO+H<sub>2</sub>O+3H<sub>2</sub></b>	40.27	27.70	42.15
	<b>CH<sub>2</sub>+O<sub>2</sub>+3H<sub>2</sub></b>	948.93	936.73	40.90
	<b>trCH<sub>2</sub>+O<sub>2</sub>+3H<sub>2</sub></b>	910.53	896.52	47.00
	<b>CH<sub>2</sub>+trO<sub>2</sub>+3H<sub>2</sub></b>	825.63	810.72	50.03
	<b>trCH<sub>2</sub>+trO<sub>2</sub>+3H<sub>2</sub></b>	787.24	770.51	56.12
	<b>Cycle_CO<sub>2</sub>+4H<sub>2</sub></b>	588.46	579.78	29.11
<b>4 Species</b>	<b>HCOOH+3H<sub>2</sub></b>	13.65	42.14	-95.56
	<b>H<sub>2</sub>CO+H<sub>2</sub>O+2H<sub>2</sub></b>	39.94	58.22	-61.32
	<b>C(OH)<sub>2</sub>+3H<sub>2</sub></b>	186.34	214.61	-94.84
	<b>HCOH+H<sub>2</sub>O+2H<sub>2</sub></b>	257.86	275.93	-60.61
	<b>HC-O-OH+3H<sub>2</sub></b>	522.99	545.24	-74.62
	<b>CH<sub>2</sub>+H<sub>2</sub>O<sub>2</sub>+2H<sub>2</sub></b>	689.22	706.02	-56.34
	<b>trCH<sub>2</sub>+H<sub>2</sub>O<sub>2</sub>+2H<sub>2</sub></b>	650.83	665.81	-50.25
	<b>CH<sub>2</sub>+2H<sub>2</sub>O+H<sub>2</sub></b>	335.07	346.44	-38.15
	<b>trCH<sub>2</sub>+2H<sub>2</sub>O+H<sub>2</sub></b>	296.67	306.23	-32.05
	<b>H<sub>2</sub>CO<sub>2</sub>+3H<sub>2</sub></b>	396.79	425.92	-97.68
	<b>CH<sub>4</sub>+O<sub>2</sub>+2H<sub>2</sub></b>	443.82	465.19	-71.69
	<b>CH<sub>4</sub>+trO<sub>2</sub>+2H<sub>2</sub></b>	320.52	339.18	-62.57
	<b>CH<sub>2</sub>+H<sub>2</sub>O-O+2H<sub>2</sub></b>	879.74	895.52	-52.91
	<b>trCH<sub>2</sub>+H<sub>2</sub>O-O+2H<sub>2</sub></b>	841.35	855.31	-46.81
<b>3 Species</b>	<b>CH<sub>3</sub>OH+H<sub>2</sub>O+H<sub>2</sub></b>	-54.49	-1.62	-177.33
	<b>CH<sub>4</sub>+2H<sub>2</sub>O</b>	-170.04	-125.10	-150.74
	<b>CH<sub>2</sub>(OH)<sub>2</sub>+2H<sub>2</sub></b>	-3.47	59.90	-212.51
	<b>H<sub>3</sub>COOH+2H<sub>2</sub></b>	264.34	327.85	-213.03
	<b>CH<sub>4</sub>+H<sub>2</sub>O<sub>2</sub>+H<sub>2</sub></b>	184.11	234.48	-168.93
	<b>CH<sub>4</sub>+H<sub>2</sub>O-O+H<sub>2</sub></b>	374.64	423.98	-165.50

It is important to note that CO formation (third most stable complex) has an entropy increasing by 40 kJ/mol\*K. It would be a preferred way of reduction by increasing the temperature. This complex without water could be referred to the classical syngas and can open different catalytic reduction pathways. Complexes of all other stable oxidation state of carbon atom can be found within a 60 kJ/mol relative Gibbs free energy range.

The structures were divided into three clusters:

- High energy cluster (above the red line;  $\Delta G_r^{\circ} > 300$  kJ/mol).

### 3. Results and discussion

- Energetically favoured cluster (below the reference;  $\Delta G_r^\circ < 0$  kJ/mol).
- Energetically available cluster (between the red line and the reference,  $0$  kJ/mol  $< \Delta G_r^\circ < 300$  kJ/mol).

To construct the molecular network which could lead to the desired product, we considered the molecules within the energetically favored and available clusters.

The  $[\text{CH}_4+\text{H}_2\text{O}_2+\text{H}_2]$  molecular complex was not included in the reaction network. Methane is already a part of the  $[\text{CH}_4+2\text{H}_2\text{O}]$  complex which is energetically the lowest of all the clusters  $\Delta G_r^\circ[\text{CH}_4+2\text{H}_2\text{O}]= -170.04$  kJ/mol.

The proposed reaction network (**Figure 16**) summarizes various routes leading to methanol and methane considering the molecular complexes which have a relative Gibbs free energy less than 300 kJ/mol.

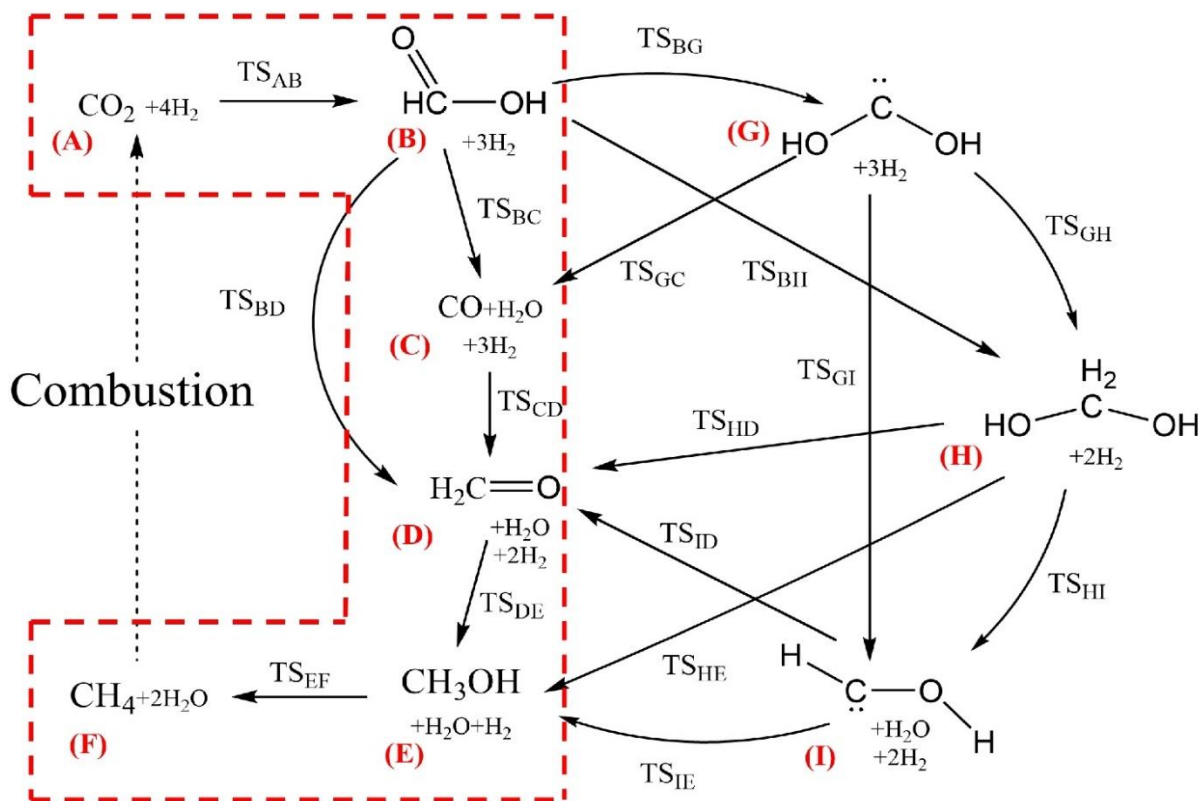


**Figure 16:** Methanol and methane formation network through CO<sub>2</sub> hydrogenation. Letters are assigned to every structure, and each transition state is named as TS followed respectively with the letter referring to the reactant and then the product (*e.g.* TS<sub>AB</sub>). The preferred pathway is highlighted with red lines.

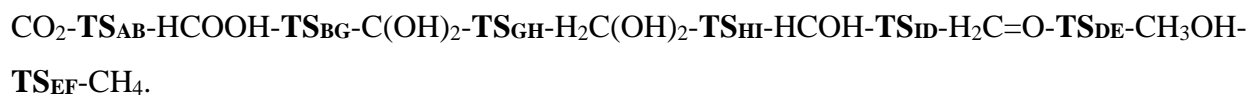
### 3. Results and discussion

The first intermediate of CO<sub>2</sub> hydrogenation is the formic acid (**B**). After that, several routes are possible:

- a) **The ABDEF route:** three successive direct hydrogenations of formic acid (**B**) (**TS<sub>BD</sub>**, **TS<sub>DE</sub>**, **TS<sub>EF</sub>** respectively) could lead to the formation of methane (**F**) through formaldehyde (**D**), and methanol (**E**) along with the formation of two water molecules. If the reaction **BD** can be replaced by two elementary reactions (**TS<sub>BC</sub>**, **TS<sub>CD</sub>**) than carbon monoxide (**C**) can be formed.
- b) **The ABGHIE route:** a hydrogen shift in formic acid (**TS<sub>BG</sub>**) could lead to (**G**) which is a relatively stable triplet state structure. From this point, methanediol CH<sub>2</sub>(OH)<sub>2</sub> (**H**) can be achieved by H<sub>2</sub> addition. These two reaction steps can be replaced by a direct hydrogenation (**TS<sub>BH</sub>**). After that, with a water elimination (**TS<sub>HI</sub>**) followed by a hydrogenation, methanol is formed. A shortcut getting around the reactions (**TS<sub>HI</sub>** and **TS<sub>IE</sub>**) is also possible, with a hydrogenation and a water elimination occurring at the same time (**TS<sub>HE</sub>**) and methanol can be reached.
- c) The above described routes can also be connected as follows:
  - A water elimination from (**G**) could lead to CO (**C**) through **TS<sub>GC</sub>**.
  - Formaldehyde can be reached by a water elimination from methanediol (**H**) and by a hydrogen shift in (**I**).

The classical combustion of methane can close the thermodynamic cycle.

The longest route to reach methanol and then methane is the following:



It contains 7 steps.

In contrast to that, the shortest route to reach methanol and then methane contains 4 steps only:



### 3. Results and discussion

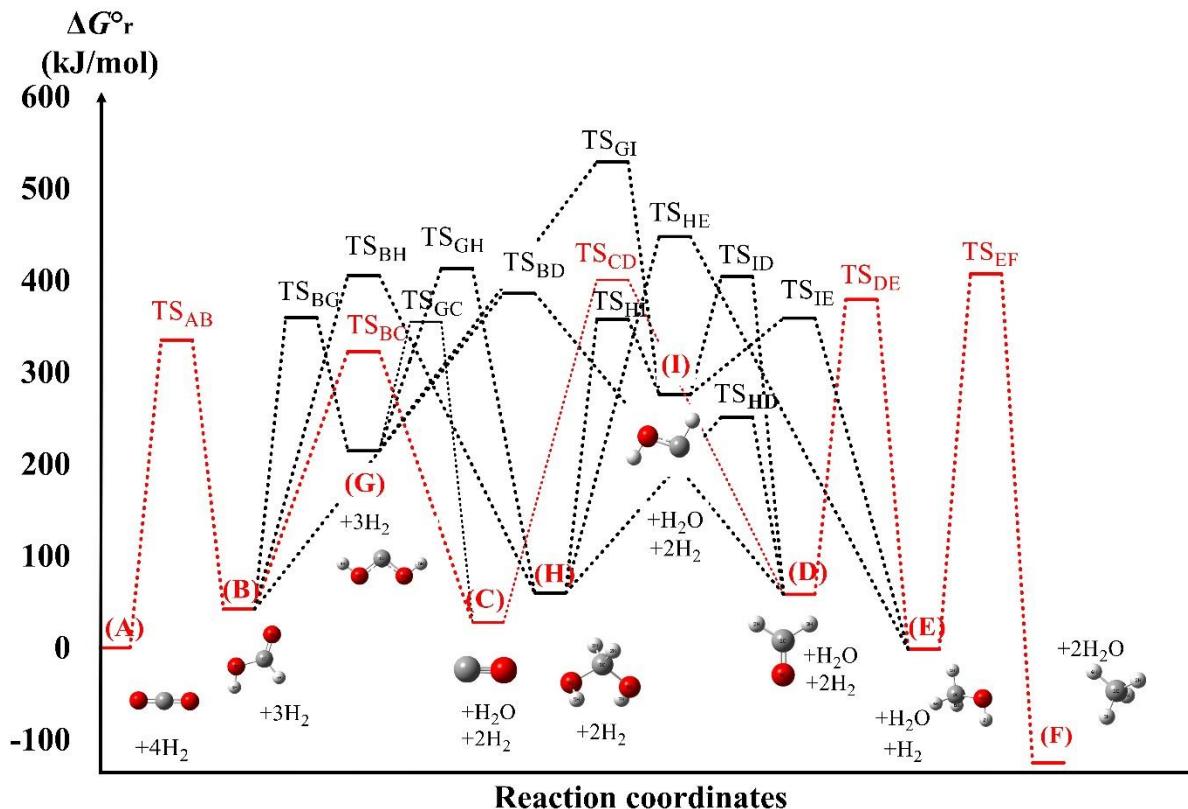


**Figure 17:** Gibbs free energy profile of the uncatalyzed hydrogenation of CO<sub>2</sub> to methanol and methane calculated at the W1BD level of theory plotted against the reaction coordinates with a highlighted energetically favoured route in red.

All Gibbs free energy values of the transition states are in the range of [250-530] kJ/mol (**Table 8**). The lowest energy reaction path leading to the products has been selected (**Figure 17**, red). The highest energy barrier, which corresponds to the rate limiting step ( $\Delta G_{\text{TS}_{\text{CD}}}^{\circ} = 400.66$  kJ/mol), is the energy needed to cross over all the barriers and reach methanol. In order to produce methane, another even higher barrier has to be overcome ( $\Delta G_{\text{TS}_{\text{EF}}}^{\circ} = 407.18$  kJ/mol).

Thus, the most feasible reaction pathway for methanol and methane production is:

Carbon dioxide (**A**) – **TS<sub>AB</sub>** – formic acid (**B**) – **TS<sub>BC</sub>** – carbon monoxide (**C**) – **TS<sub>CD</sub>** – formaldehyde (**D**) – **TS<sub>DE</sub>** – methanol (**E**) – **TS<sub>EF</sub>** – methane (**F**).

Another pathway which has to be mentioned, is the **ABHDEF**. This pathway involves the lowest transition state of the overall network (**TS<sub>HD</sub>** = 251.20 kJ/mol). Unfortunately, the rate limiting step ( $\Delta G_{\text{TS}_{\text{BH}}}^{\circ} = 405.60$  kJ/mol) is slightly higher (4.94 kJ/mol) than the rate limiting step of the preferred pathway **ABCDEF**. Otherwise, this route would have been more preferable.

### 3. Results and discussion

The CO (C) can be a key intermediate, as its formation can be influenced (slightly increased) with temperature. It allows a different entrance to the network, the classical syngas reaction<sup>104</sup>.

**Table 7:** Thermodynamic properties ( $\Delta H_r^\circ$ ,  $\Delta G_r^\circ$  in kJ/mol and  $S$  in J/mol\*K) of the stable structures and the transition states involved in the reaction network calculated at the WIBD level of theory. The highlighted red values belong to the preferred pathway of the mechanism.

Code	Particules	$\Delta G_r^\circ$ kJ/mol	$\Delta H_r^\circ$ kJ/mol	$S$ J/mol K
A	CO <sub>2</sub> +4H <sub>2</sub>	0	0	734.73
B	HCOOH+3H <sub>2</sub>	42.14	13.65	639.16
C	CO+H <sub>2</sub> O+3H <sub>2</sub>	27.7	40.27	776.88
D	H <sub>2</sub> CO+H <sub>2</sub> O+2H <sub>2</sub>	58.22	39.94	673.41
E	CH <sub>3</sub> OH+H <sub>2</sub> O+H <sub>2</sub>	-1.62	-54.49	557.40
F	CH <sub>4</sub> +2H <sub>2</sub> O	-125.1	-170.04	583.99
G	C(OH) <sub>2</sub> +3H <sub>2</sub>	214.61	186.34	639.89
H	CH <sub>2</sub> (OH) <sub>2</sub> +2H <sub>2</sub>	59.9	-3.47	522.21
I	HCOH+H <sub>2</sub> O+2H <sub>2</sub>	275.93	257.86	674.11
TS <sub>AB</sub>	A → B	334.82	306.20	638.74
TS <sub>BC</sub>	B → C	322.64	297.84	651.54
TS <sub>CD</sub>	C → D	400.66	383.07	675.73
TS <sub>DE</sub>	D → E	379.21	324.86	552.42
TS <sub>EF</sub>	E → F	407.18	321.41	447.05
TS <sub>BH</sub>	B → H	405.60	341.09	518.38
TS <sub>BG</sub>	B → G	359.65	331.98	641.89
TS <sub>GH</sub>	G → H	413.22	350.92	525.75
TS <sub>HD</sub>	H → D	251.20	186.88	519.00
TS <sub>HI</sub>	H → I	357.97	297.89	533.21
TS <sub>ID</sub>	I → D	404.19	386.36	674.92
TS <sub>IE</sub>	I → E	359.06	305.89	556.41
TS <sub>HE</sub>	H → E	447.74	353.81	419.67
TS <sub>GI</sub>	G → I	529.02	468.55	531.92
TS <sub>BD</sub>	B → D	385.91	322.70	522.72
TS <sub>GC</sub>	G → C	355.00	327.66	643.04

The thermodynamic properties of the generated structures are divided into two sections in **Table 8**. The first part shows the properties of the stable intermediate molecular complexes involved in the network. The second part contains the activation Gibbs free energy, enthalpies as well as the

### 3. Results and discussion

absolute entropy of the transition states ( $TS_{\alpha\beta}$ ), where  $\alpha$  and  $\beta$  refers to the reactants and the products.

Storing energy would be possible only in exothermic reactions. In other words, it can happen only in the case of products having a negative reaction enthalpy. Although the methanediol (**H**) corresponds to a local minimum in the potential energy surface (**Figure 17**) with a negative relative enthalpy ( $\Delta H_{\text{CH}_2(\text{OH})_2}^0$ ), it is a non-isolable product and almost thermoneutral. Thus, only two products are available for energy storage: methanol (**E**) and methane (**F**), with a relative enthalpy equal to -55 and -170 kJ/mol, respectively.

The  $\text{CO}_2$  reduction can be achieved in different routes to form (**E**) and (**F**) (**Figure 16**, **Figure 17**). To store energy, the reactants should reach the highest energy point of the most energy efficient route. This is corresponding to the highest activation energy of the reaction path  $\Delta H_{\text{TS}}^{\text{max}}$ ; and the system needs to achieve this energy to reach the product site. It can be assumed, that the theoretical efficiency of the energy storage can be estimated based on the computed thermodynamic functions. The theoretical efficiency can be defined by the ratio of the stored enthalpy  $|\Delta H_{\text{r}}^0|$  and the invested enthalpy ( $\Delta H_{\text{TS}}^{\text{max}}$ ), the highest enthalpy of the corresponding reaction path (**eq. 3**):

$$\eta = \frac{|\Delta H_{\text{r}}^0|}{\Delta H_{\text{TS}}^{\text{max}}} \quad (3)$$

It can be concluded that the theoretical efficiencies of methanol (**E**) and methane (**F**) formation are  $\eta_{(\text{E})} = 14.4 \%$  and  $\eta_{(\text{F})} = 44.4 \%$ , respectively ( $\Delta H_{\text{TS}}^{\text{max}} = \Delta H(\text{TS}_{\text{CD}})$  in both cases).

After analyzing the available results, it is obvious that in order to increase the efficiency of the energy storage, catalytic reactions are needed. Nevertheless, we have noticed a special molecule appearing as a constituent of several intermediate molecular complexes. This molecule is water ( $\text{H}_2\text{O}$ ). As a consequence, since the hydrated version of  $\text{CO}_2$  is the well-known carbonic acid ( $\text{CO}(\text{OH})_2$ ), the effect of a water molecule and protonation reactions on the reaction mechanism has been studied.

### 3. Results and discussion

#### 3.2 Aqueous phase results

In the gas phase network, the first and only elementary reaction was a hydrogenation, and the relative Gibbs free energy was quite high ( $\Delta G_{TS\_AB}^0=334.82\text{kJ/mol}$ ). In the aqueous phase network, to avoid some of the hydrogenation, hydration and protonation steps have been included. The mechanism has been compared energetically with the previously studied gas phase process.

A newly designed  $\text{CO}_2$  – methanol conversion mechanism is presented here<sup>105</sup>, which involves several intermediates and transition states and applies  $3\text{H}_2$ ,  $\text{H}_2\text{O}$  and  $\text{H}_3\text{O}^+$  as additional reactants.

The reaction pathways leading to methanol are starting either with a hydration or a protonation step (**Figure 18**).

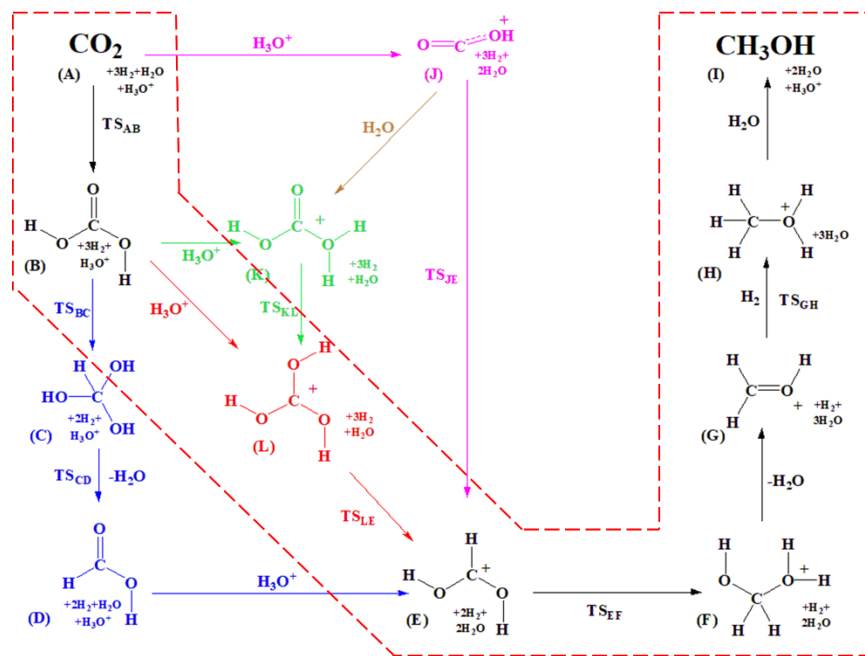


**Figure 18:** Reaction pathways of the envisaged water enhanced  $\text{CO}_2$  – methanol conversion.

Letters are assigned to every structure, and each transition state is named as TS followed respectively with the letter referring to the reactant and then the product (*e.g.*  $\text{TS}_{AB}$ ). The preferred pathway is highlighted by dashed lines.

As a first step  $\text{CO}_2$  (**A**) can be either hydrated to form carbonic acid (**B**), or protonated (**J**). The center element of the mechanism is the protonation of formic acid (**DE**). To reach this point, four alternative pathways can be followed:

### 3. Results and discussion

- a) **ABCDE route** (blue): by the hydration of CO<sub>2</sub> (**A**) carbonic acid (**B**) will form (there are three conformations, the one considered here is higher in energy by 3.14 kJ/mol than the most stable conformation). This will be hydrogenated to reach methanetriol (**C**) which could go further towards formic acid (**D**) by a water elimination (**TS<sub>CD</sub>**). Then, formic acid can be protonated to form (**E**).
- b) **ABLE route** (red): (**L**) can be achieved by the protonation of carbonic acid (**B**) which is the product of CO<sub>2</sub> hydration. The hydrogenation of (**L**) will lead directly through (**TS<sub>LE</sub>**) to the protonated formic acid (**E**) and the formation of an extra water molecule.
- c) **AJE route** (pink): The protonation of CO<sub>2</sub> followed by a hydrogenation (**TS<sub>JE</sub>**) leads directly to the protonated formic acid (**E**) through only two elementary steps.
- d) **AJKLE route** (green): In this route additional elementary steps and one intermediate molecule links the *red* and the *pink* routes mentioned above. The molecule (**K**) is a protonated carbonic acid, which can be formed through a hydration of the protonated carbon dioxide (**JK**) or by the protonation of carbonic acid (**BK**). Then, a hydrogen shift could occur (**TS<sub>KL</sub>**) to produce (**L**).

Then, the protonated formic acid (**E**) is hydrogenated to form (**F**), from where a water elimination will lead to (**G**), which is a protonated formaldehyde. After this point, another hydrogenation (**TS<sub>GH</sub>**) will occur to reach the protonated methanol (**H**) and the final step will be the release of the proton to a water molecule forming methanol (**I**) and hydronium ion.

The thermodynamic properties of the pathways have been computed (**Table 9**) and compared (**Figure 19**). CO<sub>2</sub> + 3H<sub>2</sub> + H<sub>2</sub>O + H<sub>3</sub>O<sup>+</sup> was selected as a reference to compute the relative thermodynamic properties of the individual steps (*e.g.*  $\Delta G_r^0 = G_{(X)} - G_{ref}$ , where  $G_{(X)}$  and  $G_{ref}$  are the Gibbs free energy of structure X and the reference species, respectively).

### 3. Results and discussion

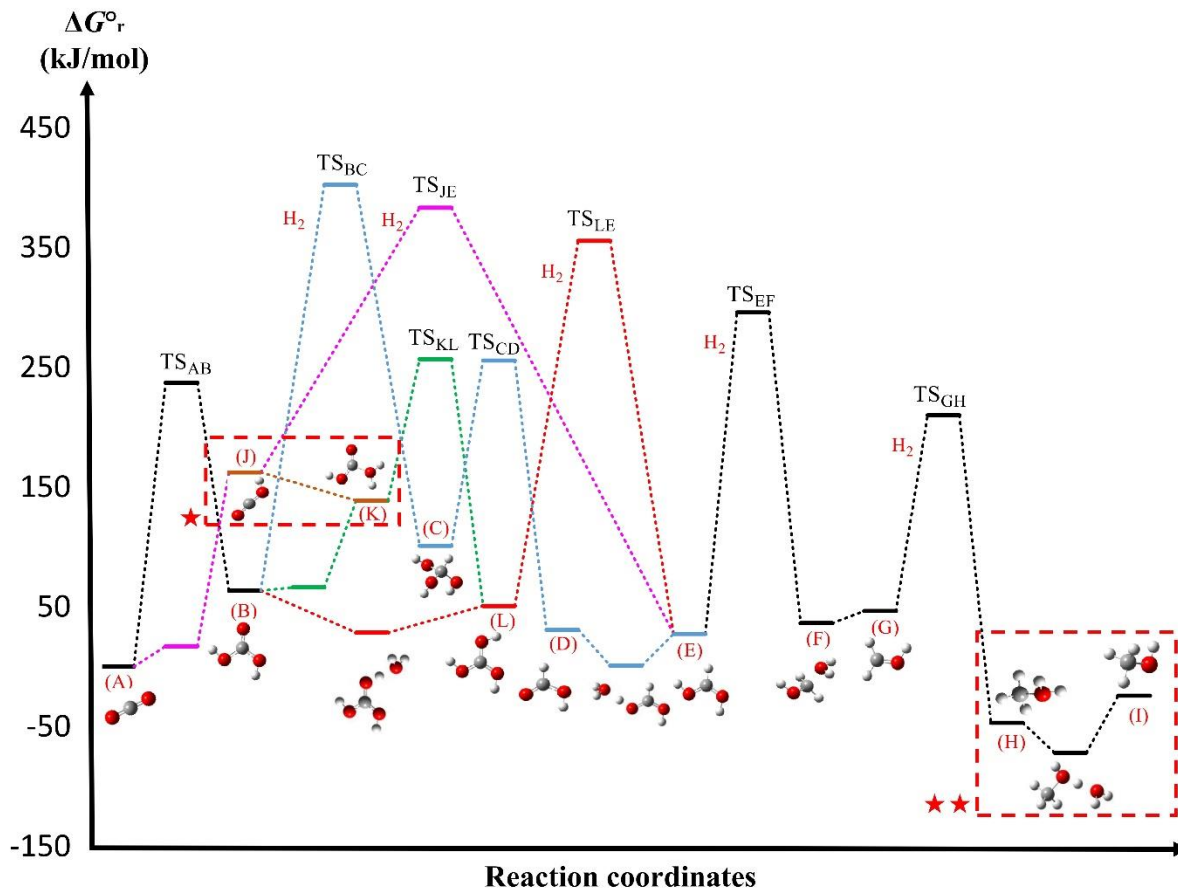


**Figure 19:** Gibbs free energy change ( $\Delta G_r^0$ , kJ/mol) of the water enhanced conversion of CO<sub>2</sub> to methanol calculated at the WIU level of theory. The transition states are named as TS followed by the reactant and the product, where the hydrogenation steps are highlighted with the (H<sub>2</sub>) sign close to the barrier. (B), (K), (E) and (L) could have more than one conformer. \*Morse potential - barrierless elementary reaction step JK. \*\*Double Morse potential - barrierless elementary reaction step HI.

The studied mechanism can be divided into two parts: [A-E] and [E-I] (Figure 19). In the case of [A-E] the conversion of CO<sub>2</sub> (A) to protonated formic acid (E) occurs through several different pathways, while [E-I] is one single route where (E) will be converted to methanol (I) after 4 consecutive reaction steps.

In the [A-E] part of the mechanism, all the routes starts with a hydration of CO<sub>2</sub> (A) to carbonic acid (B), except for the *pink* pathway which goes directly from CO<sub>2</sub> (A) through a protonation followed by a hydrogenation to the protonated formic acid (E) with one single barrier ( $\Delta G_{TS_{JE}}^0 = 383.18$  kJ/mol) which is the second highest energy barrier in the system. The *blue* pathway shows the possibility to reach (E) through three reaction steps, within which there are two

### 3. Results and discussion

transition states (TS) and one of which (**TS<sub>BC</sub>**) corresponds to the highest barrier height in the system with a value of 402.34 kJ/mol. The other two steps are (**TS<sub>CD</sub>**) ( $\Delta G_{\text{TS}_{\text{CD}}}^{\circ}=255.58$  kJ/mol) and (**DE**) which is a barrierless reaction step. Through the *red* pathway, the protonated formic acid (**E**) can be reached from carbonic acid with only two reaction steps where one is a barrierless process (**BL**) while the other is a hydrogenation ( $\Delta G_{\text{TS}_{\text{LE}}}^{\circ}=355.52$  kJ/mol). The hydrogenation (**TS<sub>LE</sub>**) has the lowest energy barrier in the [**A-E**] section, and which makes this part of the preferred pathway. The overall preferred pathway is [**A-TS<sub>AB</sub>-B-BL-L-TS<sub>LE</sub>-E-TS<sub>EF</sub>-F-G-TS<sub>GH</sub>-H-HI-I**].

It is possible to link the *pink* and *red* pathways through the hydration reaction (**JK**) highlighted with the frame (\*, **Figure 19**), followed by the hydrogen shift ( $\Delta G_{\text{TS}_{\text{KL}}}^{\circ}=256.78$ kJ/mol) which is a part of the *green* reaction channel.

The two highlighted steps (**JK**) (\*) and (**HI**) (\*\*\*) are representing the two types of barrierless reactions (Morse potential) in the system (**Figure 19**). All the possible pathways involve protonation steps. It is important to note that, in these cases, the reaction is barrierless and goes through a minimum instead of a transition state, and these are double Morse potentials (association + dissociation). (**HI**) (\*\*\*, **Figure 20**) was used as an example to describe these cases (**AJ**, **BK**, **BL**, **DE** and **HI**). The second type of barrierless step is a simple Morse potential reaction of a (de)hydration, where (**JK**) (\*, **Figure 20**) was used as an example. This type can also be observed in the reaction **FG**.

### 3. Results and discussion

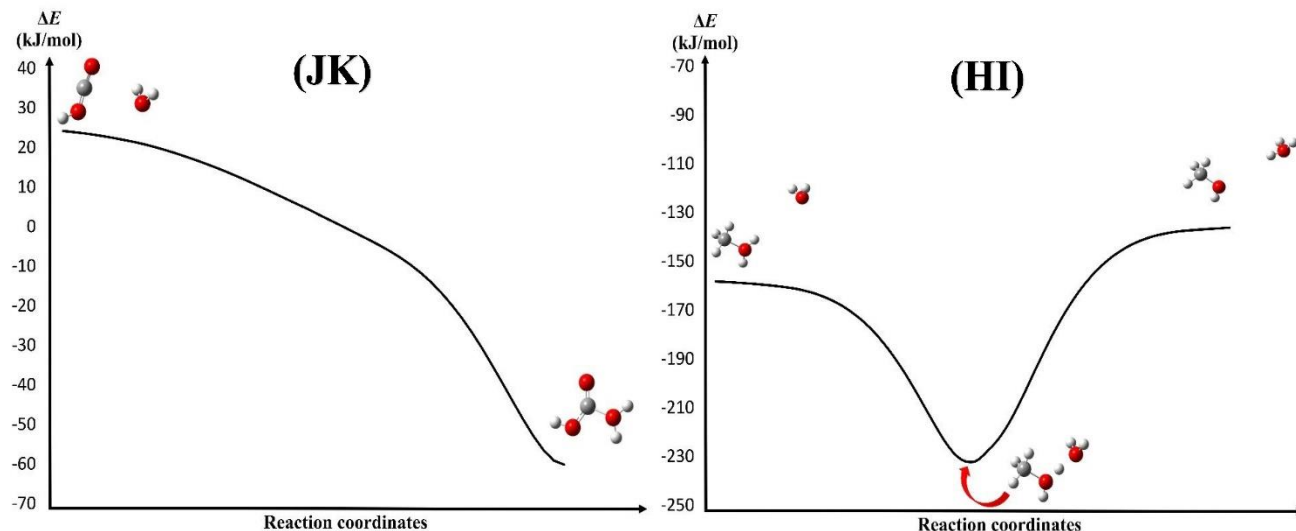


**Figure 20:** Total energy change ( $\Delta E_{\text{tot}}$ ) of the two types of barrierless reactions (**JK**) (Morse potential, hydration) and (**HI**) (Double Morse potential, protonation).

The relative total energy change of the reaction (**HI**) (**Figure 20**, left) has a shape of a parabola with a plateau at each extremity. The beginning of the reaction is at the first plateau, where the water molecule and the protonated methanol form a complex (protonated methanol-water). After this point, the total energy decreases and reach a minimum (first Morse potential), where the proton belongs to both methanol and water. Then, the energy increases to advance to another plateau (second Morse potential), where the products are located. Thus, the product is formed (methanol +  $\text{H}_3\text{O}^+$ ) without going through an energy barrier.

In case of (**JK**) (**Figure 20**, right), the total energy decreases from the reactant energy level ( $\text{H}_3\text{COH}_2^+ + \text{H}_2\text{O}$ ) directly to the energy level of the products ( $\text{H}_3\text{COH} + \text{H}_3\text{O}^+$ ) without going through an energy barrier.

Since the barrierless reaction (**DE**) is the second energetically lowest reaction of the system, it has also been studied through a flexible scan (**Figure 21**).

### 3. Results and discussion

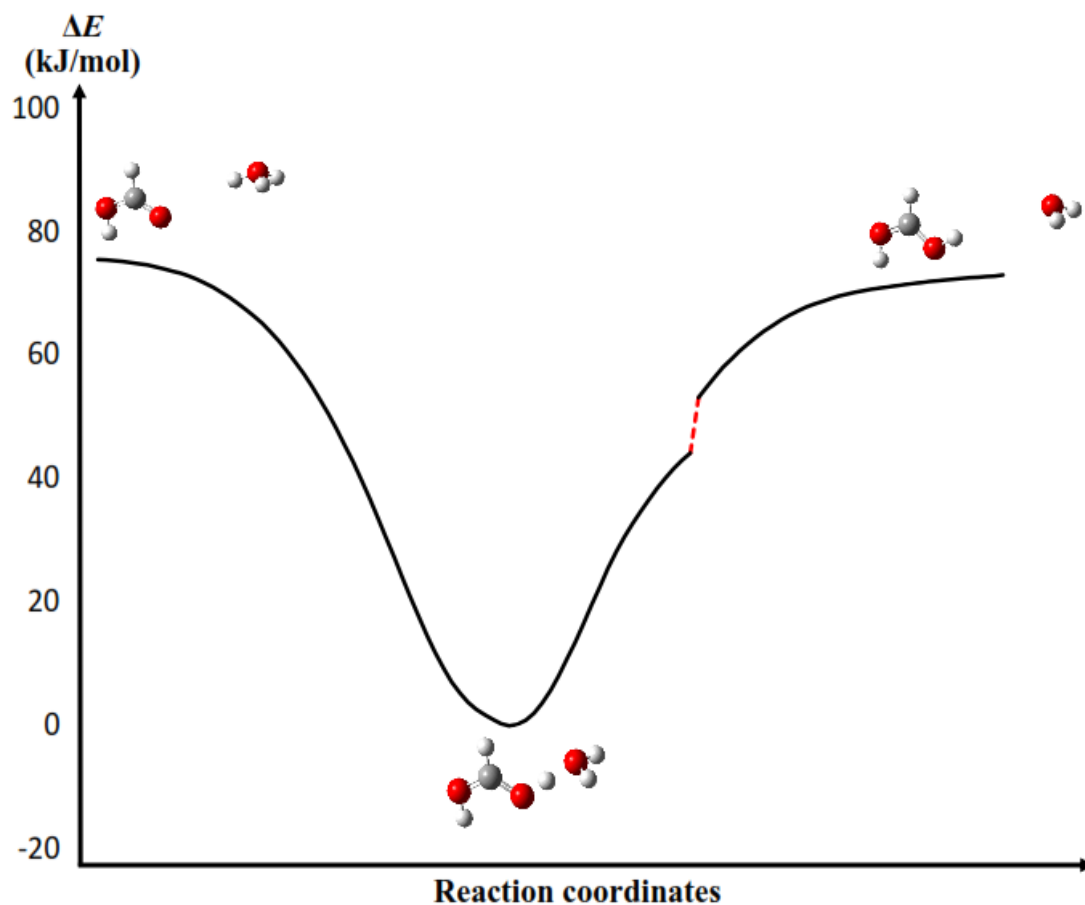


**Figure 21:** Total energy change ( $\Delta E_{\text{tot}}$ ) of the **(DE)** reaction step (double Morse potential).

**(DE)** is a barrierless process, which is similar to **(HI)** discussed above. The reaction decreases to a local minimum where the total energy change is close to 0 kJ/mol, as well as the relative Gibbs energy (see  $\Delta G_{DE}^{\circ}$  at the **Table 9**).

### 3. Results and discussion

**Table 8:** Thermodynamic properties ( $\Delta H_r^o$ ,  $\Delta G_r^o$  in kJ/mol and  $S$  in J/mol\*K) of carbon dioxide – methanol conversion reaction mechanism calculated at the W1U level of theory. The transition states of each elementary reaction steps are named as TS followed with the letter of the reactant and then the product (e.g. **TS<sub>AB</sub>**). The barrierless reactions are noted by giving a letter of the reactant followed by the product (e.g. **AJ**). The structures corresponding to the preferred pathway are highlighted in red.

Code	Particules	$\Delta H_r^o$ kJ/mol	$\Delta G_r^o$ kJ/mol	$S$ J/mol*K
<b>A</b>	<b>CO<sub>2</sub></b>	<b>0.00</b>	<b>0.00</b>	<b>213.78</b>
<b>B</b>	<b>H<sub>2</sub>CO<sub>3</sub></b>	<b>23.96</b>	<b>63.41</b>	<b>270.16</b>
<b>C</b>	HC(OH) <sub>3</sub>	28.15	100.93	288.63
<b>D</b>	HCOOH	2.30	30.80	248.48
<b>E</b>	<b>HCOOH<sub>2</sub><sup>+</sup></b>	<b>-4.47</b>	<b>27.38</b>	<b>250.68</b>
<b>F</b>	<b>H<sub>2</sub>O-H<sub>2</sub>COH<sup>+</sup></b>	<b>-28.17</b>	<b>36.42</b>	<b>271.12</b>
<b>G</b>	<b>H<sub>2</sub>COH<sup>+</sup></b>	<b>25.23</b>	<b>46.46</b>	<b>227.86</b>
<b>H</b>	<b>H<sub>3</sub>COH<sub>2</sub><sup>+</sup></b>	<b>-101.81</b>	<b>-46.78</b>	<b>244.74</b>
<b>I</b>	<b>H<sub>3</sub>COH</b>	<b>-77.06</b>	<b>-24.24</b>	<b>238.71</b>
<b>J</b>	HCO <sub>2</sub> <sup>+</sup>	166.11	162.31	239.96
<b>K</b>	H <sub>3</sub> CO <sub>3</sub> <sup>+</sup>	98.83	138.67	282.28
<b>L</b>	<b>C(OH)<sub>3</sub><sup>+</sup></b>	<b>7.97</b>	<b>50.75</b>	<b>272.44</b>
<b>TS<sub>AB</sub></b>	<b>A → B</b>	<b>270.25</b>	<b>237.28</b>	<b>270.25</b>
<b>TS<sub>BC</sub></b>	<b>B → C</b>	<b>282.42</b>	<b>402.34</b>	<b>282.42</b>
<b>TS<sub>CD</sub></b>	<b>C → D</b>	<b>282.31</b>	<b>255.58</b>	<b>282.31</b>
<b>TS<sub>EF</sub></b>	<b>E → F</b>	<b>263.21</b>	<b>295.83</b>	<b>263.21</b>
<b>TS<sub>GH</sub></b>	<b>G → H</b>	<b>238.87</b>	<b>209.81</b>	<b>238.87</b>
<b>TS<sub>JE</sub></b>	<b>J → E</b>	<b>256.89</b>	<b>383.18</b>	<b>256.89</b>
<b>TS<sub>KL</sub></b>	<b>K → L</b>	<b>271.27</b>	<b>256.78</b>	<b>271.27</b>
<b>TS<sub>LE</sub></b>	<b>L → E</b>	<b>284.66</b>	<b>355.52</b>	<b>284.66</b>
<b>AJ</b>	A-H <sub>3</sub> O <sup>+</sup>	-13.29	17.08	314.03
<b>BK</b>	B-H <sub>3</sub> O <sup>+</sup>	-9.17	65.54	354.05
<b>BL</b>	<b>B-H<sub>3</sub>O<sup>+</sup></b>	<b>-49.12</b>	<b>28.49</b>	<b>344.31</b>
<b>DE</b>	D-H <sub>3</sub> O <sup>+</sup>	-66.50	0.97	319.88
<b>HI</b>	H-H <sub>2</sub> O	-163.16	-71.79	311.58

### 3. Results and discussion

At this point, the protonated formic acid is forming a molecular complex with a water molecule, and the energy increases with the increasing distance between the water molecule and the protonated formic acid. The red dashed part of the graphic represents an internal conformational change, the oxygen atom of the water molecule got an interaction with the second closest hydrogen from the protonated formic acid while the distance between the two molecules was increasing during the flexible scan.

The highest energy barriers of the pathways are  $\Delta G_{\text{TS}_{\text{BC}}}^{\circ}=402.34$  kJ/mol,  $\Delta G_{\text{TS}_{\text{JE}}}^{\circ}=383.18$  kJ/mol,  $\Delta G_{\text{TS}_{\text{LE}}}^{\circ}=355.52$  kJ/mol and  $\Delta G_{\text{TS}_{\text{EF}}}^{\circ}=295.83$  kJ/mol (**Table 9**), and all of the corresponding reaction steps are hydrogenations ( $\text{H}_2$  molecule addition). Surprisingly, the last hydrogenation reaction step ( $\Delta G_{\text{TS}_{\text{GH}}}^{\circ}=209.81$  kJ/mol) is in the range and even lower, than the other processes such as hydrations (*e.g.*  $\Delta G_{\text{TS}_{\text{AB}}}^{\circ}=237.28$  kJ/mol), dehydrations (*e.g.*  $\Delta G_{\text{TS}_{\text{CD}}}^{\circ}=255.58$  kJ/mol) and hydrogen shifts (*e.g.*  $\Delta G_{\text{TS}_{\text{KL}}}^{\circ}=256.78$  kJ/mol).

Exothermic reactions are necessary to be involved in energy storage applications, ( $\Delta H^{\circ}_r < 0$ ). Although the relative enthalpy values of  $\text{HCOOH}_2^+$ ,  $\text{H}_2\text{O}-\text{H}_2\text{COH}^+$  and  $\text{H}_3\text{COH}_2^+$  are negative (**Table 9**), these products are non-isolable, and thus, the only remaining option for energy storage will be methanol ( $\Delta H_{\text{H}_3\text{COH}}^{\circ} = -77.06$  kJ/mol) in the system studied. Comparing this value to the amount of heat of the highest energy barrier ( $\Delta H_{\text{H}_3\text{COH}} = 284.66$  kJ/mol) allow us to determine the theoretical efficiency of methanol formation in the mechanism. It corresponds to the ratio of the stored enthalpy  $|\Delta H_r^{\circ}|$  and the invested enthalpy (the highest activation energy of the reaction path  $\Delta H_{\text{TS}}^{\text{max}}$ ) (**Equation (3)**).

The two preferred pathways of  $\text{CO}_2$  conversion to methanol in gas phase (section 3.1)<sup>91</sup> and aqueous phase<sup>105</sup> have been compared (**Table 10**). It has to be emphasized that the aqueous phase pathway involves some ionic and barrierless reactions, while the gas phase pathway doesn't. In the best aqueous phase pathway, there is only one energy barrier higher than 300 kJ/mol  $\Delta G_{\text{TS}_{\text{LE}}}^{\circ}=355.52$  kJ/mol, unlike in the case of gas phase, where all the barriers are  $>300$  kJ/mol. The rate of the recovered energy from what has to be invested in the uncatalyzed methanol formation from  $\text{CO}_2$  hydrogenation in gas phase and aqueous phase has also been provided, and in the case of the aqueous phase mechanism the efficiency is 27.1%, which is almost two times higher than in the gas phase (14.4%).

### 3. Results and discussion

**Table 9:** The comparison of the preferred carbon dioxide-methanol conversion pathways in gas and aqueous phase.

	<b>Gas phase</b> <sup>91</sup>	<b>Aqueuse phase</b>
Barrierless reactions	No	Yes
Ionic reactions	No	Yes
Number of barriers >300 kJ/mol	All (4)	One
Highest energy barrier (kJ/mol)	400.66	355.52
Efficiency ( $\eta$ )	14.4%	27.1%

According to the results mentioned so far, the hydrogenation reaction barriers are in both of the gas phase and the aqueous phase mechanisms are higher than the average energy level of the rest of the elementary reactions. The challenge would be then to find alternative reactions to reduce the hydrogenation barriers. This can be done by adding the appropriate catalyst to the reaction which will reduce the hydrogenation barriers and alter the number of elementary steps. By considering a homogeneous process, there is no obvious choice for the catalyst to speed up the reaction by lowering the hydrogenation barriers. In the case of a heterogeneous process, metal based catalysts such as Cu/ZnO or nickel could be an adequate choice as they are already tested before<sup>106,107</sup>. However, in a catalytic system, hydrogen molecules (H<sub>2</sub>) are split into hydrogen atoms (H<sup>•</sup>) and to study the process at the molecular level, the reaction mechanism should be altered accordingly.

### 3. Results and discussion

#### 3.3 Catalyzed-like aqueous phase mechanism for CO<sub>2</sub> conversion to methanol

The heterogeneous catalytic process of carbon dioxide hydrogenation will involve a bond breaking step within which hydrogen molecules will split into hydrogen atoms. The possibility of hydrogen bond dissociation occurring in the adsorption process of the H<sub>2</sub> molecule on the surface of a catalyst is discussed in several works in the literature<sup>108,109</sup>. In this way, hydrogen atoms would be adsorbed and ready to react at the surface of the catalyst. Thus, the hydrogen addition reactions will be then replaced by atomic hydrogenations (H<sup>•</sup>). Therefore, it is reasonable to further improve the feasibility of the carbon dioxide transformation process by considering an aqueous phase catalyzed-like mechanism within which atomic hydrogenations occur. By studying a system like this, new insights can be achieved into the catalytic CO<sub>2</sub> conversion which can be applicable in catalyst design and development.

It is also worth to mention water electrolyzers<sup>110,111</sup>, where hydrogen atoms and ions might also be observed in the reaction media. This relatively new technology is designed to create electrolysis cells capable of realizing an electrolytic reduction of CO<sub>2</sub> to other carbon chemicals (CO, HCOOH, CH<sub>3</sub>OH, and CH<sub>4</sub>) using the hydrogen generated from the water electrolysis (**Figure 22**).

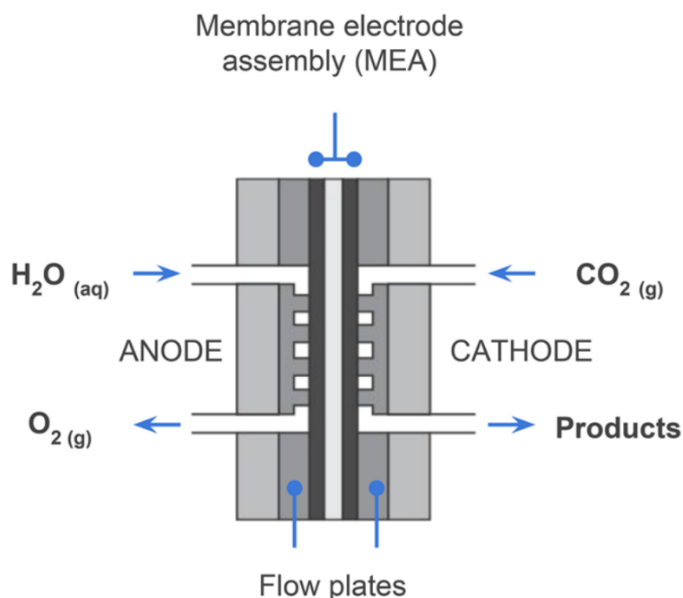


**Figure 22:** Cross-sectional diagram of an electrolytic CO<sub>2</sub> reduction flow cell<sup>110</sup>.

A typical flow cell setup is composed of a cathode where CO<sub>2</sub> is delivered for the reduction, an anode where the electrolysis of water occurs, and a membrane allowing the ionic exchanges.

### 3. Results and discussion

A concrete example has been presented below<sup>112</sup>, showing a H<sub>2</sub>O and CO<sub>2</sub> electrolysis using new alkaline stable anion membranes, where the reduction of CO<sub>2</sub> to formic acid (HCOOH) occur (Figure 23).

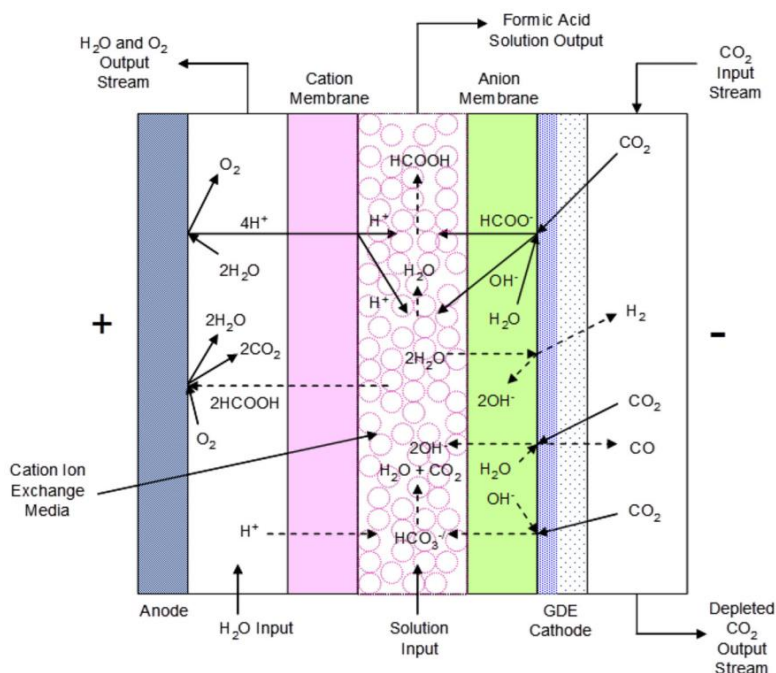


**Figure 23:** CO<sub>2</sub> - formic acid conversion cell configuration showing reactions and ion transport<sup>112</sup>.

The electrochemical reduction of CO<sub>2</sub> occurs at the cathode in the presence of water, generating formate (HCOO<sup>-</sup>) and hydroxide (OH<sup>-</sup>) ions, and at the same time the oxidation of water occurs at the anode, forming oxygen gas and hydrogen ions (hydronium cations H<sub>3</sub>O<sup>+</sup>) in aqueous solutions. Both formate ions and hydroxide ions migrate through the anion exchange membrane into the centre flow compartment, where they react with hydrogen ions produced in the anode compartment to yield water and formic acid. The hydrogenation of CO<sub>2</sub> to methanol can happen similarly, and the reduction could occur by involving ions or radicals.

The hydrogen molecule may be dissociating following two possible reactions:



In an electrochemical redox reaction, the hydrogen molecule may be dissociating to H<sup>+</sup> and :H<sup>-</sup> at the appropriate step, but we chose to explore the radical dissociation only (H<sup>·</sup> + ·H), as it is expected to occur just like in most every thermal catalytic hydrogenation.

### 3. Results and discussion

If radicals are considered instead of hydrogen molecules, the previously discussed aqueous phase mechanism (**Figure 18**) could be redesigned and the effect of a catalyst could be mimicked (**Figure 24**).

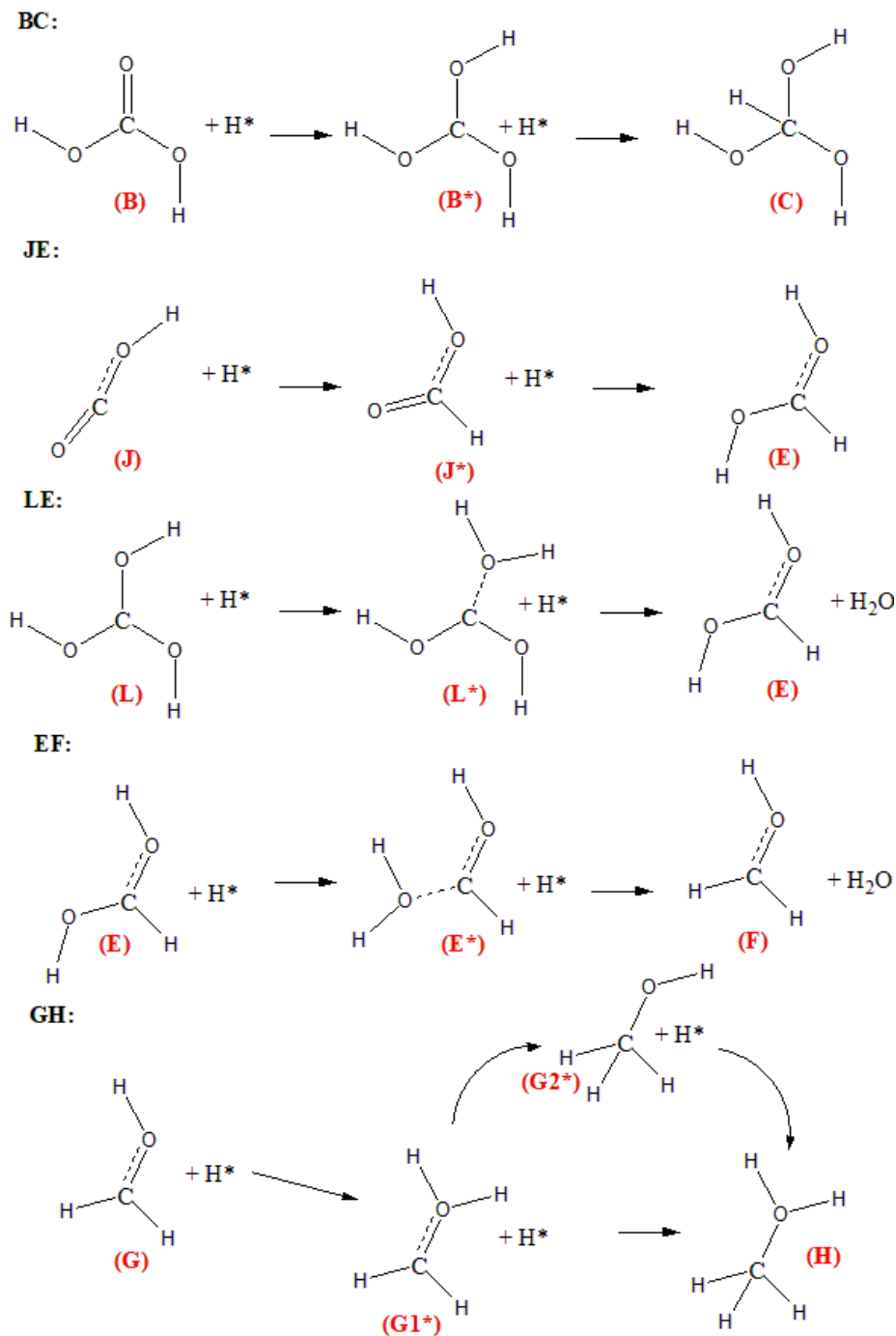


**Figure 24:** Step-by-step water enhanced CO<sub>2</sub> hydrogenation reaction considering hydrogen atoms as reaction partners.

### 3. Results and discussion

The previously described reaction steps (**BC**, **JE**, **LE**, **EF** and **GH**, **Figure 18**) have been replaced by the appropriate hydrogen atom containing steps (**Figure 24**).

A special catalyzed-like CO<sub>2</sub> hydrogenation mechanism to achieve methanol is envisaged and studied. The catalytic effect of a metal surface has been mimicked by considering hydrogen atoms instead of hydrogen molecules as reaction partners (**Figure 25**). The presence of water (and H<sub>3</sub>O<sup>+</sup>) further enhance the reaction by lowering reaction barriers and thus, behave like additional catalyst even though its effect is modest rather than dramatic.

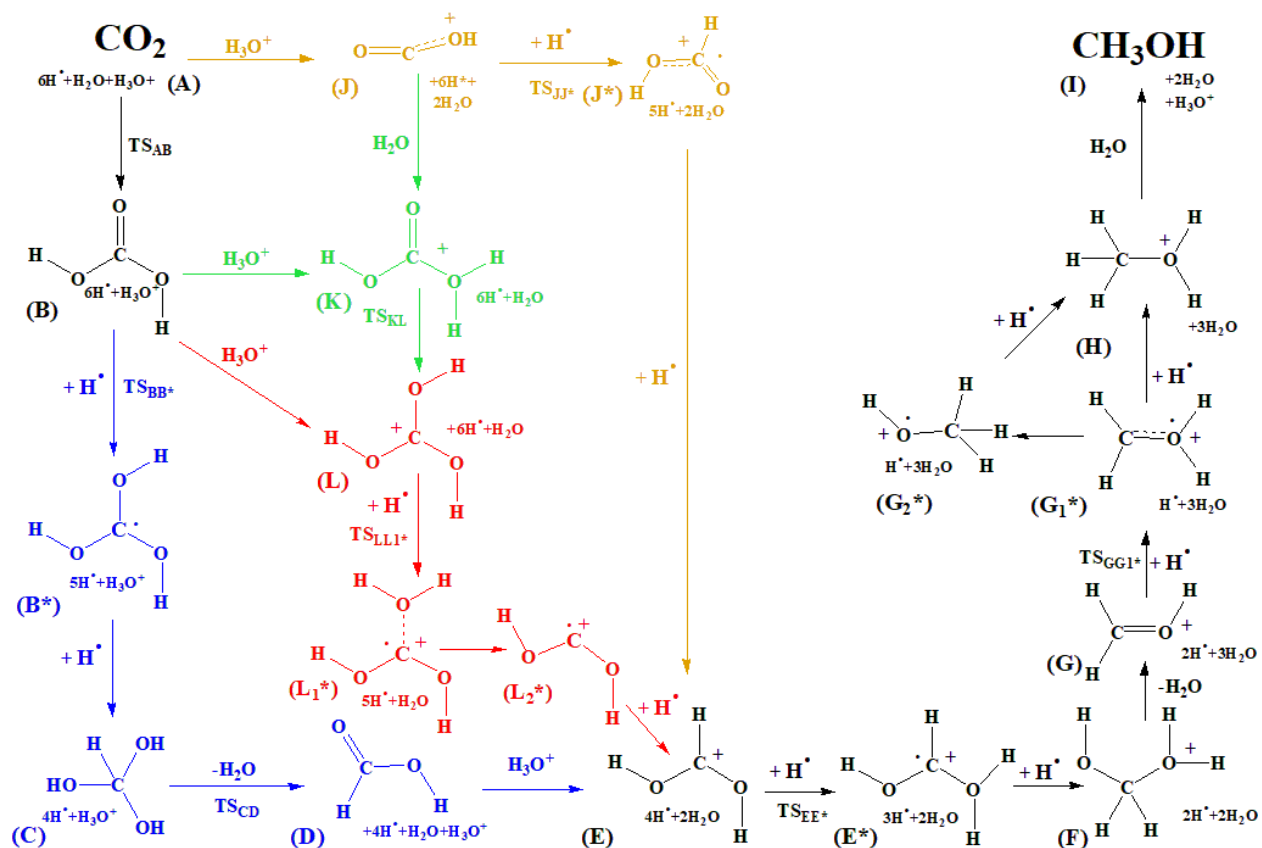


**Figure 25:** Reaction pathways of the envisaged CO<sub>2</sub> – methanol conversion mechanism using atomic hydrogenations. Letters are assigned to every structure, and each transition state is named as TS followed with the letter referring to the reactant and then the product (*e.g.* **TS<sub>AB</sub>**), respectively. The +H<sup>•</sup> refers to a hydrogen atom addition.

As a first step CO<sub>2</sub> (**A**) can either be protonated or hydrated and thus, (**J**) or (**B**) can be formed, respectively. To reach the central element of the mechanism which is the protonated formic

### 3. Results and discussion

acid (**E**), four pathways can be followed going through a two-step atomic hydrogenation in each case:

1. **Hydration-hydrogenation route (ABB\*CDE, Figure 1, blue):** by the hydration of CO<sub>2</sub> (**A**) carbonic acid (**B**) will be formed (three conformations are possible, the one considered here is energetically higher by 3.14 kJ/mol than the most stable conformer). After that, a sequence of two atomic hydrogenations (**TS<sub>BB</sub>\*** and **B\*C**) have to occur to produce methanetriol (**C**). Then, a water elimination (**TS<sub>CD</sub>**), leads to formic acid (**D**) and via a protonation step (**E**) is formed.
2. **Protonation-hydrogenation route (AJJ\*E, Figure 1, brown):** this route consists of three elementary steps which connects CO<sub>2</sub> with the desired protonated formic acid (**E**) **intermediate**. A protonation (**AJ**) followed by two atomic hydrogenations (**TS<sub>JJ</sub>\***, **J\*E**) will lead to (**E**). It has to be noted that this route is a part of the preferred pathway of the mechanism (the reason will be discussed later).
3. **Hydration-protonation route (ABLL<sub>1</sub>\*L<sub>2</sub>\*E, Figure 1, red):** this route is diverted from the hydration-hydrogenation route (*blue*) after (**B**) is formed. The protonation of carbonic acid (**B**) can lead to (**L**). Then, the first atomic hydrogenation occurs (**TS<sub>LL1</sub>\***). After that, a water subtraction (**L<sub>1</sub>\*L<sub>2</sub>\***) followed by the second atomic hydrogenation (**L<sub>2</sub>\*E**) leads to the protonated formic acid (**E**).
4. **Protonation-hydrogenation/hydration-protonation route (A[B/J]KLL<sub>1</sub>\*L<sub>2</sub>\*E, Figure 1, green):** this route starts with either a protonation (**AJ**) which is followed by a hydration (**JK**) or with a hydration (**TS<sub>AB</sub>**) which is followed by a protonation (**BK**) to reach protonated carbonic acid (**K**). Then, (**L**) can be formed via a hydrogen shift (**KL**), which will put this to the track of the *red* (**hydration-protonation**) **route**. From here, (**E**) can be achieved through the reactions (**TS<sub>LL1</sub>\***, **L<sub>1</sub>\*L<sub>2</sub>\***, **L<sub>2</sub>\*E**) as in the case of the **hydration-protonation route**.

All the routes lead to the formation of (**E**), protonated formic acid. After that, another two atomic hydrogenations (**TS<sub>EE</sub>\*** and **E\*F**) will occur and (**F**) will be formed. Then, a water elimination will lead to (**G**), which is protonated formaldehyde. From here, there are two possible ways to reach (**H**), and in both cases, the first step would be the formation of (**G1\***).

### 3. Results and discussion

The shortest way to reach (**H**) is a direct hydrogen atom addition (**G1\*H**). The other way will include the formation of (**G2\***) through a hydrogen shift (**TS<sub>G1\*G2\*</sub>**), and then, through a hydrogen atom addition (**G2\*H**) the desired intermediate (**H**) will be reached. As a final step, a water mediated proton release (**HI**) will lead to the formation of methanol (**I**) and a hydronium ion. The relative thermodynamic properties of the individual steps have been computed as *e.g.*  $\Delta G_{\text{r}}^{\circ} = G_{(\text{X})} - G_{\text{ref}}$ , where  $G_{(\text{X})}$  and  $G_{\text{ref}}$  are the Gibbs free energy of structure X and the reference, respectively (**Figure 26**). The ( $\text{CO}_2 + 6\text{H}^{\bullet} + \text{H}_2\text{O} + \text{H}_3\text{O}^+$ ) are considered as the reference throughout the reaction.

### 3. Results and discussion

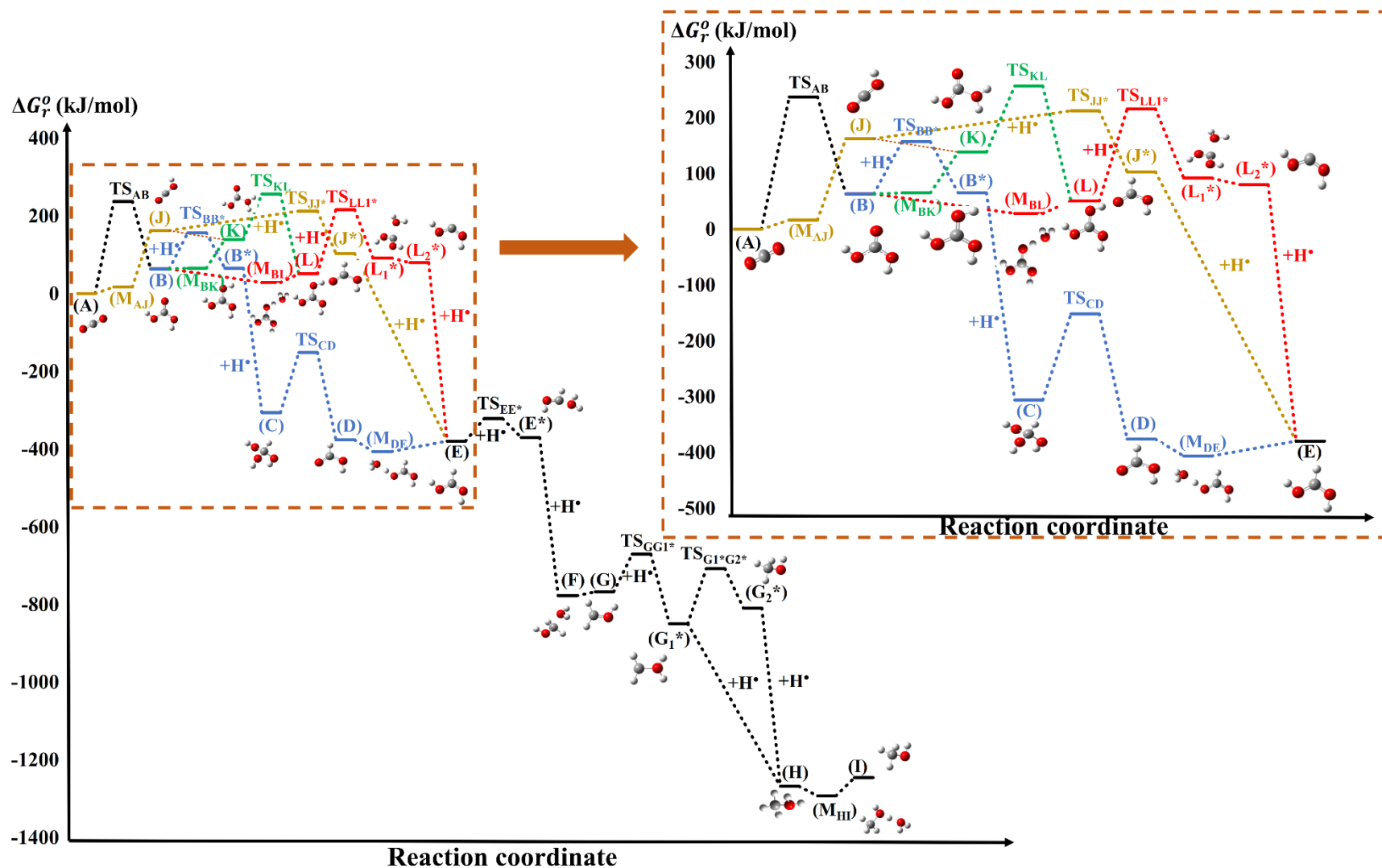


**Figure 26:** Gibbs free energy change ( $\Delta G_r^0$ , kJ/mol) of the water enhanced conversion of  $\text{CO}_2$  to methanol calculated at the W1U level of theory. The transition states are named as TS followed by the reactant and the product, where the hydrogen addition steps are highlighted with the (+H) sign close to the barrier. (B), (K), (E) and (L) could have more than one conformer.

### 3. Results and discussion

The mechanism can be divided into two sections: [A-E] and [E-I] (Figure 26). In the section [A-E] the conversion of CO<sub>2</sub> (A) to protonated formic acid (E) could occur through several different pathways. All the routes start (or can start) with a hydration of CO<sub>2</sub> (A) to get carbonic acid (B) except the **protonation-hydrogenation** (*brown*) pathway. This goes directly from CO<sub>2</sub> (A) through a protonation followed by two atomic hydrogenations to the protonated formic acid (E) with one single barrier ( $\Delta G_{\text{TS}_{\text{JJ}}^*}^0 = 212.67$  kJ/mol). It is the lowest relative energy barrier in the [A-E] section, and this makes it the preferred pathway. Thus, the overall preferred pathway would be then: [A-TS<sub>AJ</sub>-J-TS<sub>JJ</sub>\* -J\*-E-TS<sub>EE</sub>\* -E\*-F-G-TS<sub>GG1</sub>\* -G1\*-H-I].

Through the **hydration-hydrogenation** (Figure 26, *blue*) pathway (E) could be reached within 5 reaction steps. The highest relative barrier height here is 237.28 kJ/mol which corresponds to (TS<sub>AB</sub>). There are two other transition states which are more preferred and their relative Gibbs free energies are significantly lower (TS<sub>BB</sub>\*,  $\Delta G_{\text{TS}_{\text{BB}}^*}^0 = 156.97$  kJ/mol and TS<sub>CD</sub>,  $\Delta G_{\text{TS}_{\text{CD}}}^0 = -151.49$  kJ/mol). This pathway involves also an immediate hydrogen atom addition (B\*C) and a barrierless reaction with an intermediate (MDE) having the lowest relative energy value ( $\Delta G_{\text{DE}}^0 = -406.09$  kJ/mol) in the [A-E] section.

Protonated formic acid (E) can also be reached through 5 reaction steps within the **hydration-protonation** (Figure 26, *red*) pathway. The first step is the same as before (TS<sub>AB</sub>), which is followed by a barrierless processes which includes an intermediate (MBL). Then, two atomic hydrogenations occur, with a barrierless water removal reaction in between (L1\*L2\*). The first atomic hydrogenation goes through (TS<sub>LL1</sub>\*) ( $\Delta G_{\text{TS}_{\text{LL1}}^*}^0 = 216.31$  kJ/mol), while the second (L\*E) is a barrierless step. It is possible to link the **protonation-hydrogenation** (*brown*) and **hydration-protonation** (*red*) pathways through a hydration (JK) followed by a hydrogen shift (TS<sub>KL</sub>,  $\Delta G_{\text{TS}_{\text{KL}}}^0 = 256.78$  kJ/mol) which has the highest relative energy among all the routes. This TS is a part of the *green* reaction channel as well. The [E-I] is one single route where (E) will be converted to methanol (I) after 6 consecutive reaction steps or 7 if the side reaction between (G1\*) and (G2\*) is considered. The relative Gibbs free energy difference between these two molecules ( $\Delta \Delta G_{(\text{G2}^*-\text{G1}^*)}^0$ ) is 40 kJ/mol, but since TS<sub>GG1</sub>\* > TS<sub>G1</sub>\*G2\*, a preferred side reaction route cannot be chosen as both processes could occur. It has to be mentioned that in some cases several conformers can be formed,

### 3. Results and discussion

and several transition states leading to these conformers are possible. In each case, the most appropriate conformer has been chosen and included into the discussion. Among all the consecutive hydrogen atom additions, the second step is always a barrierless radical recombination reaction (Morse potential). Therefore, the second hydrogen atom in each case, is attached to the rest of the molecule without any additional energy needed (**Figure 27**).

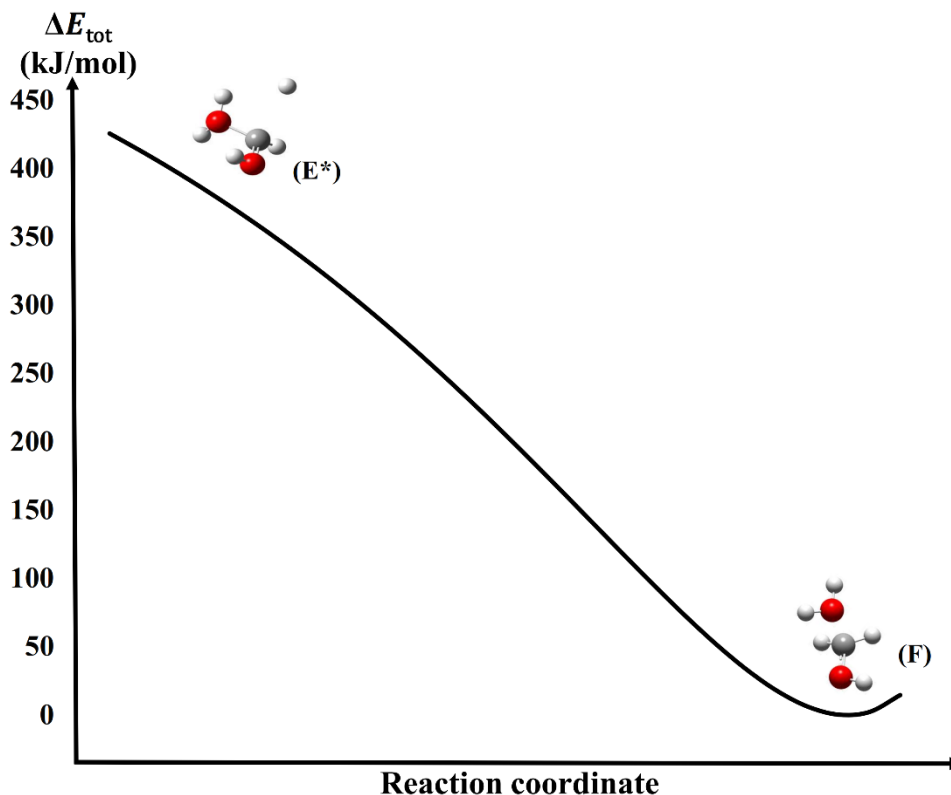


**Figure 27:** Total energy change ( $\Delta E_{\text{tot}}$ ) of the (E\*F) barrierless reaction step (Morse potential).

There are six barrierless atomic hydrogenation steps (radical recombination), (**B\*C**), (**L<sub>2</sub>\*E**), (**J\*E**), (**E\*F**), (**G<sub>1</sub>\*H**) and (**G<sub>2</sub>\*H**). There were also barrierless water addition/subtraction reactions such as (**JK**), (**L<sub>1</sub>\*L<sub>2</sub>\***) and (**FG**). The association of two Morse potentials is another barrierless reaction type involved in the discussed mechanism (**Figure 2**). It goes through a minimum, a molecular complex such as (**M<sub>AJ</sub>**), (**M<sub>BK</sub>**), (**M<sub>BL</sub>**), (**M<sub>DE</sub>**) or (**M<sub>HI</sub>**), instead of going through a transition state. These reactions are always protonations and thus, the intermediate molecular complexes are always formed by the starting structure and an oxonium ion ( $\text{H}_3\text{O}^+$ ). To show the energetic properties of these

### 3. Results and discussion

barrierless reaction steps, (**E\*F**) have been examined in detail (**Figure 27**) and the corresponding total energy change has been computed.

The total energy decreases from the reactant's energy level (**E\***) directly to the energy level of the product (**F**) without going through a barrier. The energy level of the product has been considered as a reference for the calculation of the total energy change.

### 3. Results and discussion

**Table 10:** Thermodynamic properties ( $\Delta H_r^o$ ,  $\Delta G_r^o$  in kJ/mol and  $S$  in J/mol\*K) of the studied water enhanced carbon dioxide – methanol conversion reaction mechanism have been calculated at the WIU level of theory. The complexes formed during barrierless reactions and corresponds to double Morse potentials are noted as M followed by the letter of the reactant and then the product (*e.g.*  $M_{AJ}$ ). The species labelled with an (\*) and highlighted in red are involved in the atomic hydrogenations.

Species		$\Delta H_r^o$ kJ/mol	$\Delta G_r^o$	$S$ J/mol*K
<b>A</b>	CO <sub>2</sub>	0.00	0.00	0.00
<b>B</b>	H <sub>2</sub> CO <sub>3</sub>	23.96	63.41	-132.32
<b>B*</b>	<b>H<sub>2</sub>CO<sub>3</sub>-H</b>	<b>-1.01</b>	<b>65.48</b>	<b>-223.01</b>
<b>C</b>	HC(OH) <sub>3</sub>	-408.42	-306.14	-343.05
<b>D</b>	HCOOH	-434.26	-376.27	-194.51
<b>E</b>	HCOOH <sub>2</sub> <sup>+</sup>	-441.03	-379.69	-205.74
<b>L<sub>1</sub>*</b>	<b>HCOOH<sup>+</sup>-H<sub>2</sub>O</b>	<b>26.50</b>	<b>92.01</b>	<b>-219.70</b>
<b>L<sub>2</sub>*</b>	<b>HOCOH<sup>+</sup></b>	<b>54.20</b>	<b>79.77</b>	<b>-85.74</b>
<b>J</b>	HCO <sub>2</sub> <sup>+</sup>	166.11	162.31	12.74
<b>J*</b>	<b>H<sub>2</sub>CO<sub>2</sub><sup>+</sup></b>	<b>77.18</b>	<b>102.99</b>	<b>-86.54</b>
<b>E*</b>	<b>HCOH<sup>+</sup>-H<sub>2</sub>O</b>	<b>-458.97</b>	<b>-370.40</b>	<b>-297.07</b>
<b>F</b>	H <sub>2</sub> COH <sup>+</sup> -H <sub>2</sub> O	-901.29	-777.71	-414.51
<b>G</b>	H <sub>2</sub> COH <sup>+</sup>	-847.90	-767.68	-269.07
<b>G<sub>1</sub>*</b>	<b>H<sub>2</sub>COH<sup>+</sup>-H</b>	<b>-957.84</b>	<b>-849.56</b>	<b>-363.18</b>
<b>G<sub>2</sub>*</b>	<b>H<sub>3</sub>COH<sup>+</sup></b>	<b>-918.46</b>	<b>-809.17</b>	<b>-366.58</b>
<b>H</b>	H <sub>3</sub> COH <sub>2</sub> <sup>+</sup>	-1411.50	-1267.97	-481.40
<b>I</b>	H <sub>3</sub> COH	-1386.75	-1245.43	-473.98
<b>k</b>	H <sub>3</sub> CO <sub>3</sub> <sup>+</sup>	98.83	138.67	-133.64
<b>L</b>	C(OH) <sub>3</sub> <sup>+</sup>	7.97	50.75	-143.48
<b>TS<sub>AB</sub></b>	<b>A → B</b>	197.86	237.28	-132.23
<b>TS<sub>BB*</sub></b>	<b>B → B*</b>	<b>87.24</b>	<b>156.97</b>	<b>-233.89</b>
<b>TS<sub>CD</sub></b>	<b>C → D</b>	-255.65	-151.49	-349.37
<b>TS<sub>LL*</sub></b>	<b>L → L*</b>	<b>144.20</b>	<b>216.31</b>	<b>-241.86</b>
<b>TS<sub>JJ*</sub></b>	<b>J → J*</b>	<b>188.90</b>	<b>212.67</b>	<b>-79.70</b>
<b>TS<sub>EE*</sub></b>	<b>E → E*</b>	<b>-412.56</b>	<b>-321.32</b>	<b>-306.03</b>
<b>TS<sub>GG<sub>1</sub>*</sub></b>	<b>G → G<sub>1</sub>*</b>	<b>-780.73</b>	<b>-670.72</b>	<b>-369.00</b>
<b>TS<sub>G<sub>1</sub>*G<sub>2</sub>*</sub></b>	<b>G<sub>1</sub>* → G<sub>2</sub>*</b>	<b>-818.20</b>	<b>-707.39</b>	<b>-371.66</b>
<b>TS<sub>KL</sub></b>	<b>K → L</b>	213.66	256.78	-144.65
<b>M<sub>DE</sub></b>	D-H <sub>3</sub> O <sup>+</sup>	-503.06	-406.09	-325.24
<b>M<sub>BL</sub></b>	B-H <sub>3</sub> O <sup>+</sup>	-49.12	28.49	-260.30
<b>M<sub>AJ</sub></b>	A-H <sub>3</sub> O <sup>+</sup>	-13.29	17.08	-101.89
<b>M<sub>HI</sub></b>	H-H <sub>3</sub> O <sup>+</sup>	-1472.85	-1292.99	-603.24
<b>M<sub>BK</sub></b>	B- H <sub>3</sub> O <sup>+</sup>	-9.17	65.54	-250.56

### 3. Results and discussion

After choosing 200 kJ/mol as an arbitrary reference for high energy structures, four transition states have been found which are above this limit,  $\Delta G_{\text{TS}_{\text{AB}}}^{\circ}=237.28$  kJ/mol,  $\Delta G_{\text{TS}_{\text{LL}^*}}^{\circ}=216.31$  kJ/mol,  $\Delta G_{\text{TS}_{\text{JJ}^*}}^{\circ}=212.67$  kJ/mol and  $\Delta G_{\text{TS}_{\text{KL}}}^{\circ}=256.78$  kJ/mol (Table 1). The corresponding reaction steps are a hydration (**TS<sub>AB</sub>**, water molecule addition), two atomic hydrogenations (H atom addition, **TS<sub>LL</sub>\*** and **TS<sub>JJ</sub>\***) and a hydrogen atom shift (**TS<sub>KL</sub>**). It is possible to calculate the energy storage efficiency ( $\eta$ ) of the preferred pathway (**Protonation-hydrogenation, brown**) as follows (Equation 2):

$$\eta = \frac{|\Delta H_{\text{r}}^{\circ}|}{\Delta H_{\text{TS}}^{\text{max}}} = \frac{|\Delta H_{\text{H}_3\text{COH}}^{\circ}|}{\Delta H_{\text{TS}_{\text{JJ}^*}}} \quad (3)$$

This corresponds to the ratio of the stored enthalpy  $|\Delta H_{\text{r}}^{\circ}|$  ( $\Delta H_{\text{H}_3\text{COH}}^{\circ} = -1386.75$  kJ/mol) and the invested enthalpy (the relative enthalpy of the transition state with the highest relative activation energy of the reaction path  $\Delta H_{\text{TS}}^{\text{max}}$  is equal to  $\Delta H_{\text{TS}_{\text{JJ}^*}} = 188.90$  kJ/mol). However, in this way, the theoretical efficiency of methanol formation is 734.1 %, which is not possible, as the efficiency would be >100%. However, in this case, the invested energy is not equal to the maximal barrier height only. The energy demand to break three hydrogen-hydrogen bonds (Bond Dissociation Energy of H<sub>2</sub>, BDE<sub>H<sub>2</sub></sub>) which will provide the 6 hydrogen atoms has to be also taken into account to get the correct efficiency ( $\eta_{\text{corr}}$ ) as follows:

$$\eta_{\text{corr}} = \frac{|\Delta H_{\text{H}_3\text{COH}}^{\circ}|}{\Delta H_{\text{TS}_{\text{JJ}^*}} + 3 \cdot \text{BDE}_{\text{H}_2}} \quad (4)$$

Calculated BDE<sub>H<sub>2</sub></sub> (436.56 kJ/mol) has been used in the correction, but it was also compared to the experimentally determined value and the difference is <1 kJ/mol ( $\Delta \text{BDE}_{\text{H}_2} = 0.56$  kJ/mol<sup>113</sup>), which also verifies the method selection. All in all,  $\eta_{\text{corr}}$  was found to be equal to 92.5%.

The efficiency increased a lot compare to the uncatalyzed gas phase ( $\eta = 14.4\%$ )<sup>91</sup> and water enhanced aqueous phase mechanisms ( $\eta = 27.1\%$ )<sup>105</sup>. Even though, the number of electrons and atoms were kept the same compare to the previous water enhanced case<sup>105</sup>, the difference in efficiency arises from the fact that hydrogen molecules were part of the reactant mixture (CO<sub>2</sub>+H<sub>2</sub>O+H<sub>3</sub>O<sup>+</sup>+3H<sub>2</sub>) previously, while in the current catalyzed-like

### 3. Results and discussion

system, H atoms are considered ( $\text{CO}_2 + \text{H}_2\text{O} + \text{H}_3\text{O}^+ + 6\text{H}^\bullet$ ). It has to be mentioned that the presence of water (and  $\text{H}_3\text{O}^+$ ) will enhance the reaction by lowering reaction barriers. Thus, it acts like a catalyst even though its effect is modest rather than dramatic. The reactant mixture in the catalyzed-like case is less stable compare to the previous system. However, if the reaction occurs at the surface of a metal catalyst, the hydrogen atoms would be bonded to the catalyst along with the rest of the molecules. Thus, the whole system would be more stable, and the barriers could decrease even more.

### 3. Results and discussion

#### 3.4 Comparison between the uncatalyzed and the catalyzed-like water enhanced mechanism

The two preferred pathways of the CO<sub>2</sub> conversion to methanol in the uncatalyzed and catalyzed-like mechanisms have been compared (**Table 12**).

**Table 11:** Comparison of the preferred carbon dioxide-methanol conversion pathways of the uncatalyzed and catalyzed-like aqueous phase mechanisms.

	<b>Aqueous phase (uncatalyzed)</b>	<b>Aqueous phase (catalyzed-like)</b>
Reactant mixture	CO <sub>2</sub> + 3H <sub>2</sub> + H <sub>2</sub> O + H <sub>3</sub> O <sup>+</sup>	CO <sub>2</sub> + 6H <sup>•</sup> + H <sub>2</sub> O + H <sub>3</sub> O <sup>+</sup>
Barrierless reactions	Yes	Yes
Ionic reactions	Yes	Yes
Hydrogen atom addition reactions	No	Yes
Highest energy barrier (kJ/mol)	355.52	212.67
Efficiency ( $\eta$ )	27.1%	92.5 %

It has to be emphasized that the mechanisms do not have the same initial reactant mixtures as it was mentioned above. Both mechanisms involve barrierless and ionic reaction steps, but hydrogen atom additions obviously occur only in the catalyzed-like case. In the catalyzed-like pathway, there is only one transition state with a relative barrier higher than 200 kJ/mol ( $\Delta G_{TS_{JJ}^*}^0 = 212.67$  kJ/mol). Unlike in the other case, where all the barriers are above >200 kJ/mol. In the case of the uncatalyzed mechanism the efficiency is 27.1%, which is far lower than what can be achieved with the catalyzed-like mechanism (92.5 %).

A significant decrease of the energy barriers was observed in the overall process compared to the uncatalyzed water enhanced mechanism. A large increase has also been achieved in the energy storage efficiency. The catalyzed-like mechanism is 3.4 times more efficient (92.5%) than the corresponding uncatalyzed process (27.1%). The results are an important step further to understand carbon dioxide hydrogenation and to design new catalysts with better performance.

## 4 Summary

*“All institutes must renew themselves, from time to time, as the price of survival”*

### **Anonymous**

*We must emphasize that all institutes really mean ALL INSTITUTES since every institutes that were operationally acceptable in the previous phase of global civilization will become obsolete and therefore useless in the upcoming new phase of the global civilization. By ALL INSTITUTES we mean education, energy production, material production, food production, medicine, scientific research and development to mention only a few. Finally, this universal law implies that an institute that renewed itself payed the price of survival and continue to be active at the nearby future, consequently, an institute that didn't renew itself didn't pay the price of survival, condemn itself to die.*

#### 4. Summary

The high capacity storage of the renewable electrical energy can be completed with the Substitute Natural Gas (SNG) alternative. The SNG alternative is the chemical bounding of hydrogen obtained from electrolysis using renewable electricity and the carbon dioxide which can be obtained from several sources. This will for sure contribute to the reduction of the emissions into the atmosphere. However, the conversion of CO<sub>2</sub> to methanol is a rather complicated multistep process. The reduction of carbon dioxide has several reaction steps and intermediate products. Newly developed uncatalyzed and catalyzed-like mechanisms have been envisaged and studied thermodynamically in gas phase and aqueous phase using computational chemistry tools. The Gibbs free energy change of the preferred pathways of the uncatalyzed and catalyzed-like mechanisms have been described (**Figure 28**).

By comparing the uncatalyzed gas phase and aqueous phase processes the following conclusions can be drawn:

- In both cases, the highest energy barriers are hydrogenations.
- The highest energy barriers in the preferred pathways of the two mechanisms are equal to  $\Delta G_{(\text{Gas})} = 400.66 \text{ kJ/mol}$  and  $\Delta G_{(\text{Aqueous})} = 355.52 \text{ kJ/mol}$ .
- Considering the efficiencies of these mechanisms, the aqueous phase mechanism is almost two times more efficient than the gas phase ( $\eta_{(\text{Aqueous})} = 27.1\%$  vs  $\eta_{(\text{Gas})} = 14.4\%$ ).

#### 4. Summary

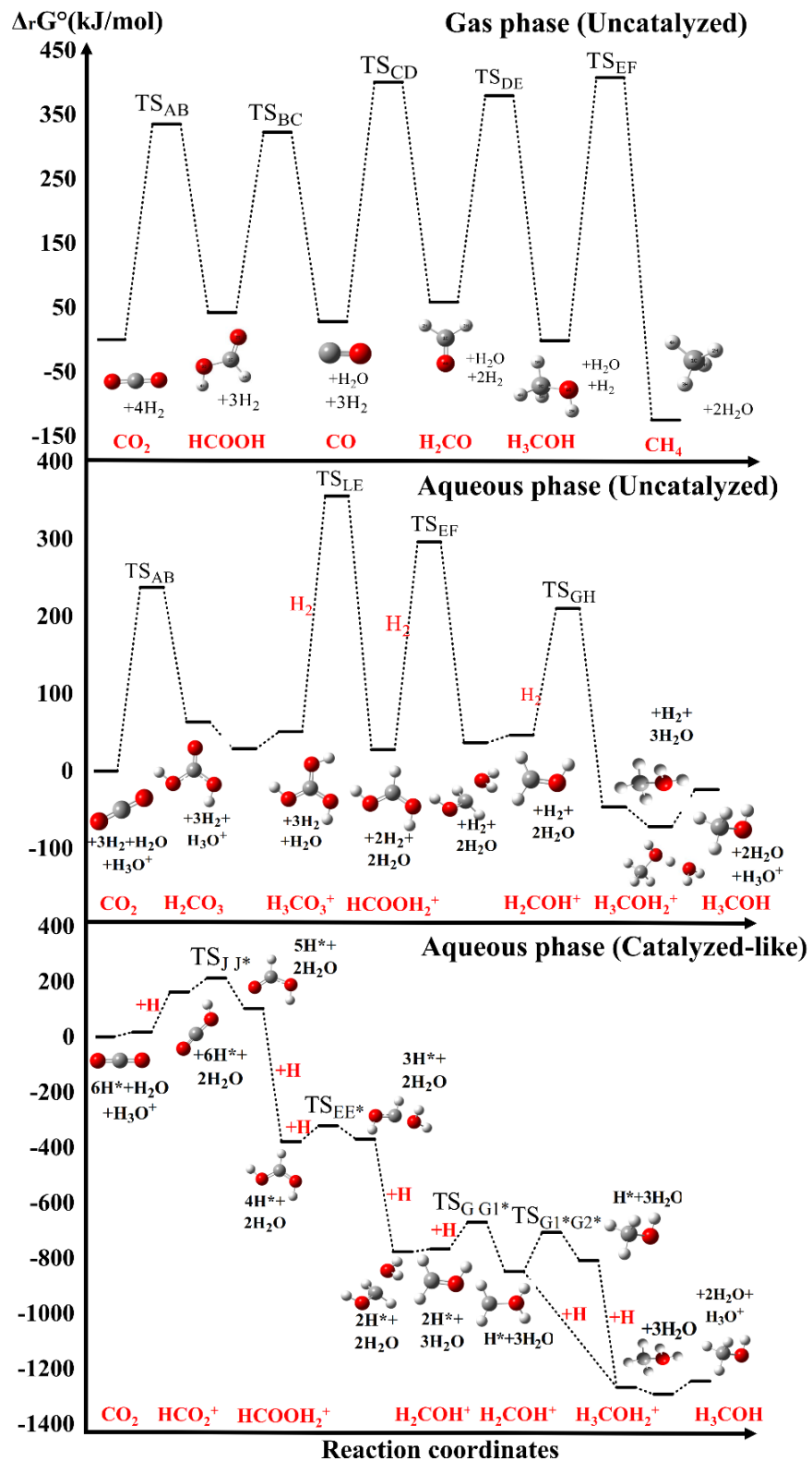


**Figure 28:** Gibbs free energy change of the preferred pathways of the gas phase and aqueous phase uncatalyzed mechanism, and catalyzed-like process.

#### 4. Summary

We notice that in the gas phase mechanism (**Figure 28**, top) the reaction barriers are the highest between the three PESs. In the preferred pathway of the aqueous phase mechanism (**Figure 28**, middle) the energy barriers are already lower.

The efficiencies can be increased by decreasing the energy barriers (hydrogenations). This can be achieved by involving hydrogen atoms instead of hydrogen molecules, which can be realized by using a catalyst or an electrocatalytic systems.

Since the uncatalyzed aqueous phase mechanism has a better efficiency it was used as a starting point. Hydrogen molecules have been replaced by hydrogen atoms and a catalyzed-like mechanism have been designed (**Figure 28**, bottom).

After analyzing the catalyzed-like mechanism, further improvement and a significant decrease of the energy barriers was observed in the overall process and the corresponding energy barriers are significantly lowered. In the preferred pathway, the highest barrier is only equal to  $\Delta G_{(H^*)} = 212.67$  kJ/mol which compared to the uncatalyzed mechanism, is almost twice smaller. Thus, a considerable increase has been achieved in the efficiency. The catalyzed-like mechanism is 3.4 times more efficient than the gas phase non-catalyzed process ( $\eta_{(H^*)} = 92.5\%$ ).

## 5 New scientific results

*“Books are like mirrors: if a fool looks in, you cannot expect a genius to look out.”*

**J.K. Rowling**

## 5. New scientific results

### 1<sup>st</sup> Thesis

Several uncatalyzed reaction routes of CO<sub>2</sub> to methanol conversion have been designed and studied in gas phase where **9** intermediate molecular complexes were involved (**Figure 16**). The thermochemical properties have been computed and the potential energy surfaces (PES) have been drawn (**Figure 17**). Among the several possible pathways, the most favourable ones have been selected and discussed. We have shown that the uncatalyzed gas phase CO<sub>2</sub> hydrogenation is thermodynamically unavailable considering its rate determining step  $\Delta G_{(\text{Gas})}=400.66$  kJ/mol.

### 2<sup>nd</sup> Thesis

In the newly designed uncatalyzed aqueous phase CO<sub>2</sub> reduction mechanism (**Figure 18**), the energy barriers are significantly lower than in the gas phase (about 100kJ/mol lower). The most favorable route has been found within the aqueous phase catalyzed-like hydrogenation mechanism. There is only one barrier above 300 kJ/mol in the uncatalyzed version of the aqueous phase mechanism ( $\Delta G_{(\text{Aqueous})}= 355.52$  kJ/mol).

### 3<sup>rd</sup> Thesis

Further improvement and a significant decrease of the energy barriers was observed in the catalyzed-like mechanism (**Figure 25**), where the highest barrier is only equal to  $\Delta G_{(\text{H}\cdot)}= 212.67$  kJ/mol. Based on the energetics of the studied mechanisms and the calculated efficiencies, it can be concluded that the atomic hydrogenation mechanism is a key process for CO<sub>2</sub> reduction, because of its relatively low energy barriers and high efficiency ( $\eta_{(\text{H}\cdot)} = 92.5$  %). This mechanism can be achieved by using appropriately selected/selected/designated catalysts or electrocatalytic systems.

### 4<sup>th</sup> Thesis

We have introduced the concept of energy storage efficiency. This allows us to compare the most favourable pathways of the conversion of CO<sub>2</sub> to methanol in each case. The aqueous phase processes have a better efficiency over the gas phase mechanism. The efficiency is almost doubled in the non-catalyzed case:  $\eta_{(\text{Aqueous})} = 27.1\%$  vs  $\eta_{(\text{Gas})} = 14.4\%$ . Mimicking the catalytic process in aqueous phase leads to an enormous increase and it is 3.4 times more efficient than the gas phase non-catalyzed process ( $\eta_{(\text{H}^*)} = 92.5$  %).

## 5. New scientific results

### 5<sup>th</sup> Thesis

The W1 composite method has been selected for all calculations and its applicability to describe the thermochemistry of the studied processes (and other similar reactions) has been verified. The method has been tested and compared to experimental values. The average deviation observed from the experimental results is equal to **1.61 kJ/mol = 0.39 kcal/mol**.

## 6 Scientific publications

*“Life is a train that stops at no stations; you either jump aboard or stand on the platform and watch as it passes”*

**Yasmina Khadra**



Contents lists available at ScienceDirect

Journal of Cleaner Production

journal homepage: [www.elsevier.com/locate/jclepro](http://www.elsevier.com/locate/jclepro)

## Renewable energy and raw materials – The thermodynamic support

Rachid Hadjadj, Csaba Deák, Árpád Bence Palotás, Péter Mizsey\*, Béla Viskolcz

University of Miskolc, Miskolc-Egyetemváros, H-3515, Miskolc, Hungary



## ARTICLE INFO

## Article history:

Received 22 January 2019

Received in revised form

22 August 2019

Accepted 28 August 2019

Available online 4 September 2019

Handling editor: Prof. Jiri Jaromir Klemes

## Keywords:

Carbon dioxide hydrogenation

Methane

Methanol

Thermodynamic study

Energy storage

## ABSTRACT

The energy and raw material supplies are crucial issues in our societies. The possible solution of these issues can be coupled with the storage alternatives of renewable energy. The chemical way of energy storage can be quite different but we follow the Supplement of Natural Gas concept since this delivers a high storage capacity solution. The chemical way of energy storage is based on the carbon dioxide hydrogenation. It is in agreement with the theory of the circular economy so that the carbon emission is reduced with the concept of Carbon Capture and Utilization (CCU).

In this work the reaction system of the carbon dioxide hydrogenation is studied thermodynamically applying the tool of quantum chemistry. The aim of the study is to support the carbon dioxide transformation alternatives of industrial scale, that is, the CCU. It is determined that the methane production has the highest thermodynamic efficiency where the methanol production is the second in the ranking. These thermodynamic efficiencies are 14.4% for methanol and 44.4% for methane. Both alternatives have, however, advantages since the methane can be introduced directly into the natural gas network and the methanol has the highest volumetric energy content. Both molecules can be transformed into different kind of raw materials, see e.g. methanol economy. At the selection, however, other, practical points of view should be also considered where industrial experiences and circumstances are to be also taken into account.

Having recognized the need to deal with the reduction and utilization of carbon dioxide emission (CCU), the University of Miskolc established the "Environmental Carbon Dioxide Partnership". It has several industrial partners having significant carbon dioxide emission and therefore experience in this issue. The experts of the partnership help to solve emission problems and the carbon dioxide utilization, based on the theoretical and practical results and experiences of the Partnership. This thermodynamic investigation supports the development of the Partnership to carry out the most efficient CCU method.

© 2019 Elsevier Ltd. All rights reserved.

## 1. Introduction

The harmful effect of the carbon dioxide emitted into the atmosphere is a well-known issue (Vo et al., 2019). To answer the challenges of environmental protection, University of Miskolc, Hungary, established a network called "Environmental Carbon dioxide Partnership" aiming to contribute to

- the global warming problem (Chandler, 2018),
- storage of renewable energies (Banerjee et al., 2019),
- production of materials on renewable basis (Islam et al., 2018).

To complete these goals the carbon dioxide can be the key

molecule, the so-called platform molecule that is used for the solution of these challenges. The carbon dioxide can be chemically converted into different molecules for the sake of energy storage like formic acid, formic aldehyde, methanol or methane (Leonzio, 2018). These molecules can be used not only for the storage and production of energy but to produce other chemicals on renewable basis (Markewitz et al., 2012).

The three goals of the Partnership are associated with the energy and energy production. Energy, the basic element that every nation need, is now a debated subject pushing the scientific world to look for its sustainable forms considering its declining resources combined with the increasing demand as well as the environmental impact (Matthews et al., 2018).

It is important to note that the large capacity energy storage is badly needed for the extensive use of renewable electricity. The reason is that the renewable electricity production highly depends

\* Corresponding author.

E-mail address: [kemizsey@uni-miskolc.hu](mailto:kemizsey@uni-miskolc.hu) (P. Mizsey).

## 6. Scientific publications

Chemical Physics Letters 746 (2020) 137298



Contents lists available at ScienceDirect

Chemical Physics Letters

journal homepage: [www.elsevier.com/locate/cplett](http://www.elsevier.com/locate/cplett)



Research paper

### Water enhanced mechanism for CO<sub>2</sub> – Methanol conversion

Rachid Hadjadj<sup>a</sup>, Imre G. Csizmadia<sup>a,c</sup>, Péter Mizsey<sup>a</sup>, Svend Knak Jensen<sup>d</sup>, Béla Viskolcz<sup>a</sup>, Béla Fiser<sup>a,b,\*</sup>



<sup>a</sup> Institute of Chemistry, University of Miskolc, 3515 Miskolc-Egyetemváros, Hungary

<sup>b</sup> Ferenc Rákóczi II. Transcarpathian Hungarian Institute, 90200 Beregszász, Transcarpathia, Ukraine

<sup>c</sup> Department of Chemistry, University of Toronto, Toronto, M5S 1A1 Ontario, Canada

<sup>d</sup> Department of Chemistry, Langelandsgade 140, Aarhus University, DK-8000 Aarhus C, Denmark

#### HIGHLIGHTS

- CO<sub>2</sub>–CH<sub>3</sub>OH conversion in aqueous phase has been envisaged: (CO<sub>2</sub> + 3H<sub>2</sub> + H<sub>2</sub>O + H<sub>3</sub>O<sup>+</sup>).
- The reaction has been investigated by using the high level W1U composite method.
- Hydrogenations are the least favourable steps in the reaction.
- The energy storage efficiency of the studied mechanism is 27.1%.
- Catalysts can be designed to decrease the energy barrier and increase efficiency.

#### ARTICLE INFO

##### Keywords:

Carbon dioxide hydrogenation  
Climate change  
Computational study  
Energy storage

#### ABSTRACT

Carbon dioxide can be converted into fine chemicals such as methanol and thus, the produced renewable energy can be stored in chemical bonds through reductions. To achieve this, a water enhanced mechanism of CO<sub>2</sub> hydrogenation leading to methanol has been designed by applying 1:3 (CO<sub>2</sub> + 3H<sub>2</sub>) extended with a water molecule and a hydronium. The thermodynamic properties of the intermediate species and transition states have been calculated by using the W1U composite method. The energy efficiency of the studied mechanism is 27.1%. By understanding the mechanism, special purpose catalysts can be designed to accelerate carbon dioxide conversion.

#### 1. Introduction

It is widely known that carbon dioxide (CO<sub>2</sub>) release in nature has a detrimental effect, and research in environmental protection is a challenge nowadays [1]. Since the industrial revolution, CO<sub>2</sub> emissions did not stop increasing [2], which could be one of the possible factors behind global warming and the acidification of the oceans [3]. These adverse processes should be prevented by either inhibiting the release or developing large scale carbon dioxide capturing procedures. Most of the solutions proposed till now are mainly Carbon Capture and Storage (CCS) methods, which are not definitive solutions to eradicate the excess of CO<sub>2</sub> from the atmosphere [4]. Some ocean scientists think that ocean storage of CO<sub>2</sub> might be a good idea. In this case, the gas would be injected and trapped into the deep ocean [5], but will it stay there forever? Will it not be able to diffuse? From a chemical point of view, the best solution would be the total transformation of carbon dioxide

into added value products [6], and in this way the produced renewable energy can also be stored [7]. Renewable energy production is not stable, and highly depends on the weather and other factors, and the energy consumption fluctuates as well, which means that the energy storage is unavoidable [8]. The common solution to both of these problems is to use renewable energy to convert carbon dioxide chemically into different molecules such as formic acid, formaldehyde, methanol or methane for the sake of energy storage [9]. These molecules can be used not only for the storage and production of energy, but to produce other chemicals in a renewable basis [10]. Energy will be stored in chemical bonds by recycling of carbon dioxide via hydrogenative reductions, and the hydrogen would be obtained from electrolysis using renewable electrical energy [11], which ideally will contribute to the decrease of CO<sub>2</sub> emission [12]. Carbon dioxide can be collected from several sources such as the industrial or biochemical processes [13], and the hydrogen has also many possible sources such

\* Corresponding author.

E-mail address: [kemfiser@uni-miskolc.hu](mailto:kemfiser@uni-miskolc.hu) (B. Fiser).

<https://doi.org/10.1016/j.cplett.2020.137298>

Received 11 January 2020; Received in revised form 18 February 2020; Accepted 1 March 2020

Available online 02 March 2020

0009-2614/ © 2020 Elsevier B.V. All rights reserved.

## Journal publications

1. Rachid Hadjadj, Csaba Deák, Árpád Bence Palotás, Péter Mizsey, Béla Viskolcz, Renewable energy and raw materials – The thermodynamic support, *Journal of Cleaner Production*, doi:10.1016/j.jclepro.2019.118221. (**Q1; IF = 6.395**)
2. Rachid Hadjadj, Imre G.Csizmadia, Péter Mizsey, Svend Knak Jensen, Béla Viskolcz, Béla Fiser, Water enhanced mechanism for CO<sub>2</sub> – Methanol conversion, *Chemical Physics Letters*, doi:10.1016/j.cplett.2020.137298. (**Q2; IF = 2.291**)
3. Rachid Hadjadj, Imre G.Csizmadia, Péter Mizsey, Béla Viskolcz and Béla Fiser, Catalysed-like mechanism for CO<sub>2</sub> conversion to methanol, under review, *Physical chemistry chemical physics*, **2020**.

## Oral and Poster presentations

1. 9<sup>th</sup> Visegrad Symposium on Structural Systems Biology, Water catalysed reduction of CO<sub>2</sub> to methanol in Aqueous-phase, Szilvásvárad, Hungary, **2019**, *Poster*.
2. 1<sup>st</sup> Science Unlimited Conference – Eötvös Symposium, Uncatalyzed molecular network for CO<sub>2</sub> hydrogenation to methanol end methane, Miskolc, Hungary **2019**, *Oral presentation*.
3. 25<sup>th</sup> International Symposium on Gas Kinetics and Related Phenomena, Detailed molecular network of CO<sub>2</sub> hydrogenation **2018**, Lille, France, *Poster*.
4. Conversion of CO<sub>2</sub> to CH<sub>3</sub>OH - A mechanistic study, XXIII. Bolyai Conference, **2018**, Budapest, Hungary, *Poster*.
5. 7<sup>th</sup> Visegrad Symposium on Structural Systems Biology, Systematic theoretical investigation for high energy C<sub>2</sub>H<sub>8</sub>O<sub>4</sub> molecules, Nove Hradý, Czech Republic, **2017**, *Poster*.

## 7 References

*“When the snows fall and the white winds blow, the lone wolf dies but the pack survives.”*

**George R.R. Martin**

## 7. References

- <sup>1</sup> M. Stork, J. de Beer, N. Lintmeijer, and B. den Ouden, 1 (2018).
- <sup>2</sup> BP, Full Report – BP Statistical Review of World Energy (2019).
- <sup>3</sup> H.D. Matthews, K. Zickfeld, R. Knutti, and M.R. Allen, *Environ. Res. Lett.* **13**, 010201 (2018).
- <sup>4</sup> P. Ibarra-Gonzalez and B.G. Rong, *Chinese J. Chem. Eng.* **27**, 1523 (2019).
- <sup>5</sup> I. Dincer and C. Acar, *Int. J. Hydrogen Energy* **40**, 11094 (2014).
- <sup>6</sup> K.K. Rajan, in 2018 Int. Conf. Control. Power, Commun. Comput. Technol. ICCPCCT 2018 (Institute of Electrical and Electronics Engineers Inc., 2018), pp. 107–113.
- <sup>7</sup> S. Weitemeyer, D. Kleinhaus, T. Vogt, and C. Agert, *Renew. Energy* **75**, 14 (2015).
- <sup>8</sup> G.A. Olah, G.K.S. Prakash, and A. Goepfert, *J. Am. Chem. Soc.* **133**, 12881 (2011).
- <sup>9</sup> G.A. Olah, A. Goepfert, and G.K.S. Prakash, *Beyond Oil and Gas: The Methanol Economy* (WILEY-VCH, 2006).
- <sup>10</sup> A.J. Pain, J.B. Martin, and C.R. Young, *Limnol. Oceanogr.* (2019).
- <sup>11</sup> F.M. Baena-Moreno, M. Rodríguez-Galán, F. Vega, B. Alonso-Fariñas, L.F. Vilches Arenas, and B. Navarrete, *Energy Sources, Part A Recover. Util. Environ. Eff.* **41**, 1403 (2019).
- <sup>12</sup> D.H. Vo, H.M. Nguyen, A.T. Vo, and M. McAleer, *Econom. Inst. Res. Pap.* (2019).
- <sup>13</sup> W. Chandler, *Energy and Environment in the Transition Economies* (Routledge, 2018).
- <sup>14</sup> J.-P. Gattuso and L. Hansson, *Ocean Acidification* (Oxford University Press, 2011).
- <sup>15</sup> A. Raza, R. Gholami, R. Rezaee, V. Rasouli, and M. Rabiei, *Petroleum* **5**, 335 (2019).
- <sup>16</sup> P. Larkin, W. Leiss, and D. Krewski, *Int. J. Risk Assess. Manag.* **22**, 254 (2019).
- <sup>17</sup> E.E. Adams and K. Caldeira, *Elements* **4**, 319 (2008).
- <sup>18</sup> M.T. Islam, N. Huda, A.B. Abdullah, and R. Saidur, *Renew. Sustain. Energy Rev.* **91**, 987 (2018).
- <sup>19</sup> G. Centi, E.A. Quadrelli, and S. Perathoner, *Energy Environ. Sci.* **6**, 1711 (2013).
- <sup>20</sup> J. Banerjee, K. Dutta, and D. Rana, in (Springer, Cham, 2019), pp. 51–104.

## 7. References

- <sup>21</sup> G. Leonzio, *J. CO2 Util.* **27**, 326 (2018).
- <sup>22</sup> X.-M. Hu and K. Daasbjerg, *Nature* **575**, 598 (2019).
- <sup>23</sup> C. Steinlechner and H. Junge, *Angew. Chemie Int. Ed.* **57**, 44 (2018).
- <sup>24</sup> A. Xia, X. Zhu, and Q. Liao, in *Fuel Cells Hydrog. Prod.* (Springer New York, New York, NY, 2019), pp. 833–863.
- <sup>25</sup> F. Samimi, N. Hamed, and M.R. Rahimpour, *J. Environ. Chem. Eng.* **7**, 102813 (2019).
- <sup>26</sup> D. Sheldon, *Johnson Matthey Technol. Rev.* **61**, 172 (2017).
- <sup>27</sup> M. Huš, V.D.B.C. Dasireddy, N. Strah Štefančič, and B. Likozar, *Appl. Catal. B Environ.* **207**, 267 (2017).
- <sup>28</sup> F. (Ferenc) Ruff and I.G. Csizmadia, *Organic Reactions : Equilibria, Kinetics, and Mechanism* (Elsevier, Amsterdam ;New York, 1994).
- <sup>29</sup> M. Huš, V.D.B.C. Dasireddy, N. Strah Štefančič, and B. Likozar, *Appl. Catal. B Environ.* **207**, 267 (2017).
- <sup>30</sup> C. Tisseraud, C. Comminges, T. Belin, H. Ahouari, A. Soualah, Y. Pouilloux, and A. Le Valant, *J. Catal.* **330**, 533 (2015).
- <sup>31</sup> R. Grabowski, J. Słoczyński, M. Śliwa, D. Mucha, R.P. Socha, M. Lachowska, and J. Skrzypek, *ACS Catal.* **1**, 266 (2011).
- <sup>32</sup> S.A. Kondrat, P.J. Smith, L. Lu, J.K. Bartley, S.H. Taylor, M.S. Spencer, G.J. Kelly, C.W. Park, C.J. Kiely, and G.J. Hutchings, *Catal. Today* (2018).
- <sup>33</sup> P. Gao, L. Zhong, X. Li, H. Wang, H. Yang, C. Zhang, S. Wang, W. Wei, and Y. Sun, (2017).
- <sup>34</sup> S. YANG, J. HE, N. ZHANG, X. SUI, L. ZHANG, and Z. YANG, *J. Fuel Chem. Technol.* **46**, 179 (2018).
- <sup>35</sup> P. Gao, L. Zhong, L. Zhang, H. Wang, N. Zhao, W. Wei, and Y. Sun, *Catal. Sci. Technol.* **5**, 4365 (2015).
- <sup>36</sup> J. Toyir, R. Miloua, N.E. Elkadri, M. Nawdali, H. Toufik, F. Miloua, and M. Saito, *Phys.*

## 7. References

Procedia **00**, 0 (2008).

- <sup>37</sup> N. Austin, J. Ye, and G. Mpourmpakis, *Catal. Sci. Technol.* **7**, 2245 (2017).
- <sup>38</sup> S. Kattel, B. Yan, Y. Yang, J.G. Chen, and P. Liu, *J. Am. Chem. Soc.* **138**, 12440 (2016).
- <sup>39</sup> P. Xu, K. Ye, M. Du, J. Liu, K. Cheng, J. Yin, G. Wang, and D. Cao, *RSC Adv.* **5**, 36656 (2015).
- <sup>40</sup> B. An, J. Zhang, K. Cheng, P. Ji, C. Wang, and W. Lin, *J. Am. Chem. Soc.* **139**, 3834 (2017).
- <sup>41</sup> Y. Hartadi, D. Widmann, and R.J. Behm, *Phys. Chem. Chem. Phys.* **18**, 10781 (2016).
- <sup>42</sup> H. Bahruji, M. Bowker, G. Hutchings, N. Dimitratos, P. Wells, E. Gibson, W. Jones, C. Brookes, D. Morgan, and G. Lalev, *J. Catal.* **343**, 133 (2016).
- <sup>43</sup> H. Bahruji, R.D. Armstrong, J. Ruiz Esquiús, W. Jones, M. Bowker, and G.J. Hutchings, *Ind. Eng. Chem. Res.* *acs.iecr.8b00230* (2018).
- <sup>44</sup> J. Díez-Ramírez, P. Sánchez, A. Rodríguez-Gómez, J.L. Valverde, and F. Dorado, *Ind. Eng. Chem. Res.* **55**, 3556 (2016).
- <sup>45</sup> J. Díez-Ramírez, J.A. Díaz, P. Sánchez, and F. Dorado, *J. CO2 Util.* **22**, 71 (2017).
- <sup>46</sup> J. Qu, X. Zhou, F. Xu, X.-Q. Gong, and S.C.E. Tsang, *J. Phys. Chem. C* **118**, 24452 (2014).
- <sup>47</sup> A. García-Trenco, E.R. White, A. Regoutz, D.J. Payne, M.S.P. Shaffer, and C.K. Williams, *ACS Catal.* **7**, 1186 (2017).
- <sup>48</sup> I. Sharafutdinov, C.F. Elkjær, H.W. Pereira de Carvalho, D. Gardini, G.L. Chiarello, C.D. Damsgaard, J.B. Wagner, J.-D. Grunwaldt, S. Dahl, and I. Chorkendorff, *J. Catal.* **320**, 77 (2014).
- <sup>49</sup> Y. Chen, S. Choi, and L.T. Thompson, *J. Catal.* **343**, 147 (2016).
- <sup>50</sup> A. García-Trenco, A. Regoutz, E.R. White, D.J. Payne, M.S.P. Shaffer, and C.K. Williams, *Appl. Catal. B Environ.* **220**, 9 (2018).
- <sup>51</sup> D. Sheldon, *Johnson Matthey Technol. Rev.* **61**, 172 (2017).
- <sup>52</sup> M. Born and J.R. Oppenheimer, *Ann. Phys.* **84**, 457 (1927).
- <sup>53</sup> A. Leach, *Molecular Modelling : Principles and Applications*, 2nd ed. (Prentice Hall, Harlow England ;;New York, 2001).

## 7. References

- <sup>54</sup> D. Hartree, Math. Proc. Cambridge Philos. Soc. **24**, 89 (1928).
- <sup>55</sup> Roothaan C.C.J., **23**, 69 (1951).
- <sup>56</sup> C. Møller and M.S. Plesset, **46**, 618 (1934).
- <sup>57</sup> M.J. Frisch, M. Head-Gordon, and J.A. Pople, Chem. Phys. Lett. **166**, 275 (1990).
- <sup>58</sup> J.A. Pople, M. Head-Gordon, and K. Raghavachari, J. Chem. Phys. **87**, 5968 (1987).
- <sup>59</sup> R.J. Bartlett and G.D. Purvis, Int. J. Quantum Chem. **14**, 561 (1978).
- <sup>60</sup> G.D. Purvis and R.J. Bartlett, J. Chem. Phys. **76**, 1910 (1982).
- <sup>61</sup> W. Kohn, A.D. Becke, and R.G. Parr, J. Phys. Chem. **100**, 12974 (1996).
- <sup>62</sup> B.G. Johnson, P.M.W. Gill, and J.A. Pople, J. Chem. Phys. **98**, 5612 (1993).
- <sup>63</sup> A.D. Becke, J. Chem. Phys. **98**, 5648 (1993).
- <sup>64</sup> P. Review, Phys. Rev. A **38**, 3098 (1988).
- <sup>65</sup> C. Lee, C. Hill, and N. Carolina, **37**, (1988).
- <sup>66</sup> D. Samuel, J. Hepatol. **56**, 4 (2012).
- <sup>67</sup> A.D. Becke, J. Chem. Phys. **140**, (2014).
- <sup>68</sup> E.R. Davidson and D. Feller, Chem. Rev. **86**, 681 (1986).
- <sup>69</sup> R. Ditchfield, W.J. Hehre, and J.A. Pople, J. Chem. Phys. **54**, 724 (1971).
- <sup>70</sup> R. Ditchfield, W.J. Hehre, and J.A. Pople, J. Chem. Phys. **54**, 724 (1971).
- <sup>71</sup> V.A. Rassolov, M.A. Ratner, J.A. Pople, P.C. Redfern, and L.A. Curtiss, J. Comput. Chem. **22**, 976 (2001).
- <sup>72</sup> T.H. Dunning, J. Chem. Phys. **90**, 1007 (1989).
- <sup>73</sup> J.A. Pople, M. Head-Gordon, D.J. Fox, K. Raghavachari, and L.A. Curtiss, J. Chem. Phys. **90**, 5622 (1989).
- <sup>74</sup> J.W. Ochterski, G.A. Petersson, and J.A. Montgomery, J. Chem. Phys. **104**, 2598 (1996).

## 7. References

- <sup>75</sup> E.C. Barnes, G.A. Petersson, J.A. Montgomery, M.J. Frisch, and J.M.L. Martin, *J. Chem. Theory Comput.* **5**, 2687 (2009).
- <sup>76</sup> P. Pulay, G. Fogarasi, F. Pang, and J.E. Boggs, *J. Am. Chem. Soc.* **101**, 2550 (1979).
- <sup>77</sup> M.P. Andersson and P. Uvdal, *J. Phys. Chem. A* **109**, 2937 (2005).
- <sup>78</sup> R.E. Skyner, J.L. McDonagh, C.R. Groom, T. Van Mourik, and J.B.O. Mitchell, *Phys. Chem. Chem. Phys.* **17**, 6174 (2015).
- <sup>79</sup> B. Mennucci and R. Cammi, *Continuum Solvation Models in Chemical Physics: From Theory to Applications* (Wiley Online Library, n.d.).
- <sup>80</sup> M. J. Frisch, G. W. Trucks, H. B. Schlegel, G. E. Scuseria, M. A. Robb, J. R. Cheeseman, G. Scalmani, V. Barone, G. A. Petersson, H. Nakatsuji, X. Li, M. Caricato, A. Marenich, J. Bloino, B. G. Janesko, R. Gomperts, B. Mennucci, H. P. Hratchian, J. V. Ortiz, A. F. Izmaylov, J. L. Sonnenberg, D. Williams-Young, F. Ding, F. Lipparini, F. Egidi, J. Goings, B. Peng, A. Petrone, T. Henderson, D. Ranasinghe, V. G. Zakrzewski, J. Gao, N. Rega, G. Zheng, W. Liang, M. Hada, M. Ehara, K. Toyota, R. Fukuda, J. Hasegawa, M. Ishida, T. Nakajima, Y. Honda, O. Kitao, H. Nakai, T. Vreven, K. Throssell, J. A. Montgomery, Jr., J. E. Peralta, F. Ogliaro, M. Bearpark, J. J. Heyd, E. Brothers, K. N. Kudin, V. N. Staroverov, T. Keith, R. Kobayashi, J. Normand, K. Raghavachari, A. Rendell, J. C. Burant, S. S. Iyengar, J. Tomasi, M. Cossi, J. M. Millam, M. Klene, C. Adamo, R. Cammi, J. W. Ochterski, R. L. Martin, K. Morokuma, O. Farkas, J. B. Foresman, and D. J. Fox, *Gaussian 09, Revision E.01*, Gaussian Inc. 2013.
- <sup>81</sup> D. Feller, *J. Chem. Phys.* **96**, 6104 (1992).
- <sup>82</sup> T. Helgaker, W. Klopper, H. Koch, and J. Noga, *J. Chem. Phys.* **106**, 9639 (1998).
- <sup>83</sup> J. Pottel and N. Moitessier, *J. Chem. Inf. Model.* **57**, 454 (2017).
- <sup>84</sup> C. Benecke, T. Gruer, A. Kerber, R. Laue, and T. Wieland, *Fresenius J Anal Chem* **359**, 23 (1997).
- <sup>85</sup> R. Gugisch, A. Kerber, A. Kohnert, R. Laue, M. Meringer, C. Rucker, and A. Wassermann, (2009).
- <sup>86</sup> J.M.L. Martin and G. de Oliveira, *J. Chem. Phys.* **111**, 1843 (1999).

## 7. References

- <sup>87</sup> L. Deng, T. Ziegler, and L. Fan, *J. Chem. Phys.* **99**, 3823 (1993).
- <sup>88</sup> K. Kim and K.D. Jordan, *J. Phys. Chem.* **98**, 10089 (1994).
- <sup>89</sup> P.J. Stephens, F.J. Devlin, C.F. Chabalowski, and M.J. Frisch, *J. Phys. Chem.* **98**, 11623 (1994).
- <sup>90</sup> S. Parthiban and J.M.L. Martin, *J. Chem. Phys.* **114**, 6014 (2001).
- <sup>91</sup> R. Hadjadj, C. Deák, Á.B. Palotás, P. Mizsey, and B. Viskolcz, *J. Clean. Prod.* **241**, 118221 (2019).
- <sup>92</sup> J. Tomasi, B. Mennucci, and R. Cammi, *Chem. Rev.* **105**, 2999 (2005).
- <sup>93</sup> M. Cossi, N. Rega, G. Scalmani, and V. Barone, *J. Comput. Chem.* **24**, 669 (2003).
- <sup>94</sup> V. Barone and M. Cossi, *J. Phys. Chem. A* **102**, 1995 (1998).
- <sup>95</sup> X. Li and M.J. Frisch, *J. Chem. Theory Comput.* **2**, 835 (2006).
- <sup>96</sup> E. Papajak, J. Zheng, X. Xu, H.R. Leverentz, and D.G. Truhlar, *J. Chem. Theory Comput.* **7**, 3027 (2011).
- <sup>97</sup> R.J. Bartlett and G.D. Purvis, *Int. J. Quantum Chem.* **14**, 561 (1978).
- <sup>98</sup> M. McGlashan, *Thermodynamic Properties of Individual Substances* (Hemisphere Pub. Corp, New York :, 2004).
- <sup>99</sup> E.U. Franck, *Berichte Der Bunsengesellschaft Für Phys. Chemie* **94**, 93 (1990).
- <sup>100</sup> B. Ruscic, J.E. Boggs, A. Burcat, A.G. Császár, J. Demaison, R. Janoschek, J.M.L. Martin, M.L. Morton, M.J. Rossi, J.F. Stanton, P.G. Szalay, P.R. Westmoreland, F. Zabel, and T. Bérces, *J. Phys. Chem. Ref. Data* **34**, 573 (2005).
- <sup>101</sup> B. Ruscic, R.E. Pinzon, M.L. Morton, N.K. Srinivasan, M.-C. Su, A. James W. Sutherland, and J. V. Michael, (2006).
- <sup>102</sup> E.W. Lemmon, M.O. McLinden, and D.G. Friend, *NIST Chemistry WebBook, NIST Standard Reference Database* (2017).
- <sup>103</sup> A.J.C. Varandas, *Annu. Rev. Phys. Chem.* **69**, 177 (2018).
- <sup>104</sup> A.F.G. Neto, F.C. Marques, A.T. Amador, A.D.S. Ferreira, and A.M.J.C. Neto, *Renew. Energy*

## 7. References

**130**, 495 (2019).

<sup>105</sup> R. Hadjadj, I.G. Csizmadia, P. Mizsey, S.K. Jensen, B. Viskolcz, and B. Fiser, *Chem. Phys. Lett.* **746**, 137298 (2020).

<sup>106</sup> S.G. Jadhav, P.D. Vaidya, B.M. Bhanage, and J.B. Joshi, *Chem. Eng. Res. Des.* **92**, 2557 (2014).

<sup>107</sup> X. Jiang, X. Nie, X. Guo, C. Song, and J.G. Chen, *Chem. Rev. acs. chemrev.9b00723* (2020).

<sup>108</sup> G. Righi, R. Magri, and A. Selloni, *J. Phys. Chem. C* **123**, 9875 (2019).

<sup>109</sup> T. Panczyk, P. Szabelski, and W. Rudzinski, *J. Phys. Chem. B* **109**, 10986 (2005).

<sup>110</sup> D.M. Weekes, D.A. Salvatore, A. Reyes, A. Huang, and C.P. Berlinguette, *Acc. Chem. Res.* **51**, 910 (2018).

<sup>111</sup> Y. Zheng, J. Wang, B. Yu, W. Zhang, J. Chen, J. Qiao, and J. Zhang, *Chem. Soc. Rev.* **46**, 1427 (2017).

<sup>112</sup> J.J. Kaczur, H. Yang, Z. Liu, S.D. Sajjad, and R.I. Masel, *Front. Chem.* **6**, 1 (2018).

<sup>113</sup> B. deB, *Bond Dissociation Energies in Simple Molecules* (n.d.).